

1 **Transverse energy analysis of**
2 **relativistic heavy ion collisions**
3 **through the use of identified particles**
4 **spectra**

5 A Thesis Presented for the
6 Master of Science
7 Degree
8 The University of Tennessee, Knoxville

9 Biswas Sharma

10 May 2018

11

© by Biswas Sharma, 2018

12

All Rights Reserved.

13 Table of Contents

14	1 Introduction	1
15	1.1 A Brief History of the Universe	1
16	1.2 Production of Historical Matter	1
17	1.3 Motivation of This Thesis	2
18	1.4 Organization of The Thesis	2
19	2 Theoretical Background	3
20	2.1 Quantum Chromodynamics	3
21	2.2 Phase Transitions	4
22	2.3 Quark-Gluon Plasma	5
23	3 Relativistic Heavy Ion Collisions	7
24	3.1 RHIC and LHC	7
25	3.2 Collision Energy and Geometry	9
26	3.3 Kinematic Variables	11
27	3.4 QGP Evolution	13
28	3.5 Detection of Collision Products	13
29	3.6 Detection of QGP Signatures	15
30	3.6.1 Bjorken Energy Density	15
31	3.6.2 Elliptic Flow	16
32	3.6.3 Dilepton Production	16
33	3.6.4 Direct photons	17
34	3.6.5 Strangeness Enhancement	18

35	3.6.6 Jet Quenching	19
36	3.7 The Beam Energy Scan Program	19
37	4 Measurement of Transverse Energy	22
38	4.1 Definition of Transverse Energy	22
39	4.2 E_T Measurement with Calorimeters	23
40	4.2.1 Calorimeter	23
41	4.2.2 E_T from PHENIX	23
42	4.3 E_T Measurement with Tracking Detectors	24
43	4.3.1 Tracking and Particle Identification	24
44	4.3.2 Calculation of $\frac{dE_T}{d\eta}$ from p_T spectra	25
45	4.3.3 Tracking Detectors in STAR	26
46	5 Data Analysis	28
47	5.0.1 STAR p_T spectra	28
48	5.1 Extrapolation of Spectra	29
49	5.1.1 Boltzmann-Gibbs Blast Wave	30
50	5.1.2 Fitting Spectra to BGBW	30
51	5.2 Calculations from the Spectral Fits	31
52	5.2.1 Calculation of $\frac{dE_T}{dy}$, $\frac{dE_T}{d\eta}$, $\frac{dN_{ch}}{dy}$, and $\frac{dN_{ch}}{d\eta}$	31
53	5.2.2 Corrections for Unidentified Particles and Estimation of Total E_T . .	31
54	5.2.3 Lambdas Centralitiy Adjustments and E_T Interpolations	32
55	5.3 Uncertainties	32
56	6 Results	33
57	7 Conclusion	39
58	8 Future Work	40
59	8.1 Goodness of Fit	40
60	8.2 Bjorken Energy Density Estimate	40
61	8.3 Asymmetric beams	41

⁶²	Bibliography	42
⁶³	Appendices	75

⁶⁴ List of Tables

⁶⁵	3.1 Colliding species and associated collision energies at RHIC [24]	10
⁶⁶	5.1 Isospin states of different identified particles.	31

List of Figures

68	2.1	Schematic of the QCD phase diagram [8].	6
69	3.1	Initial layout of the RHIC.[26].	8
70	3.2	An illustration of a mid-central collision of two nuclei traveling in the z	
71		direction. The X-axis is parallel to the line joining the centers of the two	
72		nuclei at the time of collision. [13].	11
73	3.3	An illustration of a collision consisting of participants (solid red) and	
74		spectators (open blue) within the colliding nuclei labeled A and B. t_c denotes	
75		the time of maximum overlap of the two nuclei. The apparent narrowing of	
76		the volumes of the nuclei in the z-direction is due to Lorentz contraction. [37]	12
77	3.4	Evolution of the QGP represented in a lightcone diagram. τ_0 denotes the	
78		formation time of the QGP. T_c is the critical temperature of the transition	
79		from the QGP to the hadron gas phase. T_{ch} and T_{fo} stand for the temperatures	
80		at, respectively, chemical freeze-out and thermal freeze-out. [13]	14
81	3.5	Minimum-bias Au+Au ($\sqrt{s_{NN}} = 200\text{GeV}$) elliptic flow spectra for identified	
82		particles: (a) v_2 vs p_T and (b) v_2 vs KE_T . [4]	17
83	3.6	Minimum-bias Au+Au ($\sqrt{s_{NN}} = 200\text{GeV}$) elliptic flow spectra for identified	
84		particles: (a) $\frac{v_2}{n_q}$ vs $\frac{p_T}{n_q}$ and (b) $\frac{v_2}{n_q}$ vs $\frac{KE_T}{n_q}$. [4]	18
85	3.7	Feynman diagram representing the production of a lepton pair from a quark	
86		and an antiquark. [39]	19
87	3.8	Feynman diagram representing the production of photons from quarks and	
88		gluons. (a) and (b) represent annihilation processes, whereas (c) and (d)	
89		represent Compton processes.[39]	20

90	3.9	Illustration of jet quenching. Two jets are produced from each of the hard	
91		scatterings occuring at the locations of the solid dots. Jets originating closer	
92		to the initial surface are more probable to propagate outside the medium, as	
93		shown. Jets opposite to them interact with the medium, losing their energy	
94		and resulting in bow front shock waves.[36]	21
95	4.1	Energy loss distribution in the STAR TPC for primary and secondary	
96		particles. [18].	27
97	5.1	Transverse momentum spectra for π^+ , π^- , K^+ , K^- , p , and \bar{p} at midrapidity	
98		($ y < 0.1$) from 39 GeV Au+Au collisions at RHIC. The fitting curves	
99		on the 0-5% central collision spectra for pions, kaons, and protons/anti-	
100		protons represent, respectively, the Bose-Einstein, m_T -exponential, and	
101		double-exponential functions. [2].	29
102	5.2	Red curve shows the Boltzmann-Gibbs blast wave functional fit on the PRE-	
103		LIMINARY transverse momentum spectrum for lambda particles identified	
104		by the STAR detector for 19.6 GeV Au+Au collisions (10-15% central).	
105		Parameters extracted from the chi-square goodness-of-fit test, as well as other	
106		statistics, are shown in the box on the top right.	31
107	6.1	Parallel coordinates plot for 270 different spectra relating 6 different identified	
108		particles (color-coded) to their respective collision centrality classes, good-fit	
109		parameters, and the transverse energy calculated using said parameters. . . .	33
110	6.2	$(dE_T/d\eta)/0.5N_{part}$ at midrapidity as a function of $\sqrt{s_{NN}}$ for different central-	
111		ities.	34
112	6.3	$(dE_T/d\eta)/(dN_{ch}/d\eta)$ at midrapidity as a function of $\sqrt{s_{NN}}$ for different	
113		centralities.	34
114	6.4	$(dE_T/d\eta)/0.5N_{part}$ at midrapidity as a function of N_{part} for different centralities.	35
115	6.5	$(dE_T/d\eta)/(dN_{ch}/d\eta)$ at midrapidity as a function of N_{part} for different	
116		centralities.	35
117	6.6	$(dE_T/dy)/0.5N_{part}$ at midrapidity as a function of $\sqrt{s_{NN}}$ for different centralities.	36

118	6.7	$(dE_T/dy)/(dN_{ch}/dy)$ at midrapidity as a function of $\sqrt{s_{NN}}$ for different	
119		centralities.	36
120	6.8	$(dE_T/dy)/0.5N_{part}$ at midrapidity as a function of N_{part} for different centralities.	37
121	6.9	$(dE_T/dy)/(dN_{ch}/dy)$ at midrapidity as a function of N_{part} for different	
122		centralities.	37
123	6.10	$\frac{dE_T}{d\eta}/0.5N_{part}$ for 0-5% central collisions at midrapidity as a function of $\sqrt{s_{NN}}$.	
124		The PHENIX data are from [3]. The error bars represent the total statistical	
125		and systematic uncertainties.	38

Chapter 1

Introduction

The Big Bang model is based on observational evidence, such as the cosmic microwave background radiation and the cosmological expansion, and suggests that at the beginning the universe must have been at a state of really high density and temperature. As the universe expanded, it went through several stages of cooling characterized by the formation of matters with different compositions. The matter we mostly observe today exists at temperatures and densities much lower compared to those in the early universe.

The Large Hadron Collider (LHC) at CERN and the Relativistic Heavy Ion Collider (RHIC) at the Brookhaven National Laboratory have the ability to collide heavy nuclei, such as those of gold and uranium, at nearly the speed of light, reaching temperatures of trillions of degrees Celcius. These laboratories have provided evidence of the formation of an exotic state of matter, called the quark-gluon plasma (QGP). It only exists for a brief amount of time after such collisions and instantly freezes out into a plethora of new particles, which carry the signatures we can use to deduct QGP properties. Its properties suggest that it should be similar to the matter that existed within microseconds of the genesis of the universe. It behaves like an almost perfect fluid with no resistance and exhibits other interesting properties.

One of the methods to probe the properties of this matter is by analyzing the conversion of the beam-direction energy at the time of collision into transverse energy after the collision. This analysis is generally done by using data from the calorimeters placed around the

147 collision site. In this thesis, I use the data collected by the tracking detectors, instead
148 of the conventional calorimeters, to perform the transverse energy analysis.

149 This thesis is structured as follows. Chapter 2 touches on the theoretial background
150 associated with the concept of the quark-gluon plasma. In Chapter 3, I attempt to
151 summarize the experimental concepts pertaining to heavy-ion collisions, and the production
152 and detection of QGP. Chapter 4 consists of the formalism of the measurement of transverse
153 energy using calorimeters as well as tracking detectors. It also gives an example of what has
154 been done using calorimeters. Chapter 4 describes the data used to perform the analysis in
155 this thesis and notes down the details of the analysis. In Chapter 5, I present the results
156 and compare them to the ones in literature obtained using a different method. Chapter 6
157 concludes the thesis by summarizing it and shedding light on some of its implications.

Chapter 2

Theoretical Background

2.1 Quantum Chromodynamics

The strong force is one of the four fundamental interactions in physics. At large scale, it is responsible for binding the nucleons together to give the nucleus its structure. At the smaller scale, it binds the fundamental units of subnuclear matter, the quarks, together to form the nucleons. The force carriers of the interaction are the mesons at the former scale and the gluons at the latter. The scales of the different interactions and their relative strengths are summarized in table ??..... The electrodynamic interaction between charged particles such as protons and electrons is described by quantum electrodynamics (QED) as mediated by photons; the strong interaction, albeit more complicated, is explained under the framework of quantum chromodynamics (QCD). [21, 32] ??? The quarks and gluons of QCD are collectively known as partons. The gluons are the gauge bosons of the Yang-Mills theory.

The Yang-Mills theory is a non-Abelian gauge theory. It has a Lagrangian that is described by several parameters, some of which are redundant and need to be gauged. This is done by a mathematical treatment as prescribed under a gauge theory. [?] The gauge theory associated with the Yang-Mills theory is based on the $SU(N)$ group. It is non-Abelian as represented by the transformations being non-commutative. QCD is a gauge theory that describes the application of the $SU(3)$ symmetry transformations on the triplet (what does the tripleness imply?????????) of quarks, namely red, blue, and green (with the

179 nomenclature having no physical dependence on the three primary colors). The Electroweak
 180 interaction, on the other hand, can be formalized under the gauge group $SU(2) \times U(1)$.
 181 Together, they form the $SU(3) \times SU(2) \times (U1)$ gauge theory called the standard model.

182 One of the aspects in which QCD is different from QED is the confinement of partons.
 183 In QED, the fundamental particles are bound together by the Coulomb potential, which
 184 diminishes with distance between the charge-carrying particles, as demonstrated by the
 185 relation 2.1:

$$V_C \propto \frac{1}{r} \quad (2.1)$$

186 where V_C is the Coulomb potential, and r is the spatial separation between the particles.
 187 This means that bound QED particles can be isolated by increasing their spatial separation.
 188 The QCD potential, on the other hand, has an extra linear term in it:

$$V_{QCD} = -\frac{4}{3} \frac{\alpha_S}{r} + kr \quad (2.2)$$

189 where α_S is the QCD fine-structure constant and k is the strength of the color interaction (1
 190 GeV/fm). This means that the potential increases linearly with distance at large distances,
 191 and so an infinite amount of energy is required to separate quarks. Hence, we never observe
 192 isolated quarks and they are said to be confined, not just bound, to form composite structures
 193 called hadrons.[29] Composition of a quark and an anti-quark forms a meson and that of
 194 three quarks forms a baryon. In addition to having a color charge, a quark also carries a
 195 flavor. There are six different quarks based on the flavors they carry: up, down, top, bottom,
 196 beauty, and strange.

197 2.2 Phase Transitions

198 In everyday life, we observe matter existing in four distinct phases: solid, liquid, gas, and
 199 plasma. Changes in physical conditions can lead to a transition from one of these phases
 200 to another, exemplified by the commonly observed conversion of ice to water. Distinctions
 201 among the various phases can be represented in a chart called the phase diagram.

202 The phase diagram consists of thermodynamic observables such as temperature and
 203 density on its axes. Curves in the phase diagram represent boundries of physical conditions
 204 at which two or more phases of matter can coexist in equilibrium. Crossing a boundary
 205 represents an abrupt transition from one phase to another; this abruptness is mathematically
 206 characterized by the discontinuity in the change of the derivative of the free energy – a
 207 thermodynamic variable – with respect to the physical quantities in the axes. There can also
 208 be regions in the diagram representing the ranges of physical conditions in which a smooth
 209 phase transition can take place.

210 One of the main focuses of current experimental and theoretical nuclear physics research
 211 is the study of the phase diagram of strongly interacting matter at a range of temperatures
 212 and baryon chemical potentials. In experiments involving the collisions of heavy ions at
 213 high and low energies, different regions of the phase diagram can be probed by varying the
 214 collision energy [3]. For instance, the high-baryon chemical potential regime corresponds
 215 to lower beam energies and higher temperatures correspond to higher beam energies. The
 216 results of these experiments and model calculations can be used to study the nature of
 217 transitions in the QCD phase diagram.

218 A schematic representing the QCD phase diagram on the temperature (T) and quark
 219 chemical potential (μ) plane is shown in Figure 2.1 [8]. A second-order transition is
 220 predicted at low baryon chemical potentials (close to baryon-antibaryon symmetry) and
 221 high temperatures reminiscent of the early universe. Methods to study this region of the
 222 phase space will be explored in this thesis. At low temperatures and high chemical potentials,
 223 loose predictions have been made regarding the existence of exotic phases of high density
 224 matter, and programs, such as the Compressed Baryonic Matter experiment at the Facility
 225 for Antiproton and Ion Research in Germany, are being designed to study this region of the
 226 phase diagram.

227 **2.3 Quark-Gluon Plasma**

228 The confinement of quarks into the hadronic phase of QCD matter, as described in section
 229 2.1, has its limitations. At very high densities, when the wave function of a single hadron

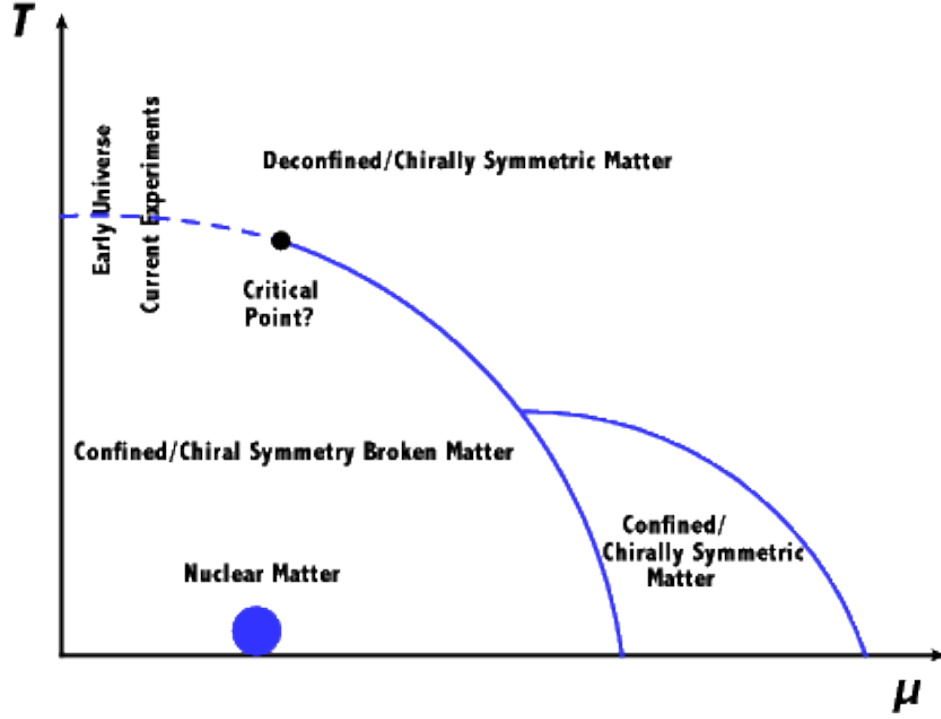


Figure 2.1: Schematic of the QCD phase diagram [8].

230 encompasses the spatial regions covered by multiple such hadrons, it is impossible to classify
 231 which pair or triplet of quarks belongs to which meson or baryon. As long as a particular
 232 quark is close enough to the other quarks in the volume, it is deconfined in such a way that it
 233 can freely move anywhere in the volume. [29] QCD predicts such phase transition, at energy
 234 densities above $0.2\text{-}1 \text{ GeV}/\text{fm}^3$ [1] and around a critical temperature of about 200 MeV [23],
 235 of strongly interacting matter to a phase with quarks and gluons in thermal and chemical
 236 equilibrium representing the relevant degrees of freedom and behaving like an almost perfect
 237 quantum fluid [11]. This deconfined state of quarks and gluons is termed the quark-gluon
 238 plasma (QGP) in analogy to the quantum electrodynamical plasma phase of matter.

Chapter 3

Relativistic Heavy Ion Collisions

The experimental evidences of the theoretically appealing existence of QGP come from the collisions of large nuclei. The signatures of such evidence are described in section 3.6. Physicists started noting down such evidences since as far back as 1984, when nuclei were accelerated and collided with stationary targets.[17] They were able to agree on a conclusive discovery of this matter during the 2000s, after colliding accelerated nuclei with other such nuclei or smaller species (protons, deuterons) at unprecedented energies and with improved detection schemes.[34] With further increase in collision energies and enhancement in detector technology, modern accelerator facilities have not only added such evidences but also provided estimates of some of the properties as well as the dynamics of the evolution of the QGP. The following sections describe two such facilities, the physics of the collisions and what happens after the collisions.

3.1 RHIC and LHC

The Relativistic Heavy Ion Collider (RHIC) is located in Upton, New York in the premises of the Brookhaven National Laboratory (BNL). Its construction started in 1991 and was completed in 1999. Figure 3.1 shows the layout, at the time of construction, of the collider along with the Alternating Gradient Synchrotron (AGS) complex and the locations of the original four detectors: Solenoidal Tracker At RHIC (STAR), Pioneering High Energy Nuclear Interaction eXperiment (PHENIX), PHOBOS and BRAHMS (Broad RAnge

Hadron Magnetic Spectrometers). PHOBOS and BRAHMS were decommissioned after the completion of their science objectives, but STAR and PHENIX are still functional. The AGS was part of BNL before the construction of the RHIC, and its capabilities were augmented with the construction of the AGS Booster in 1991.

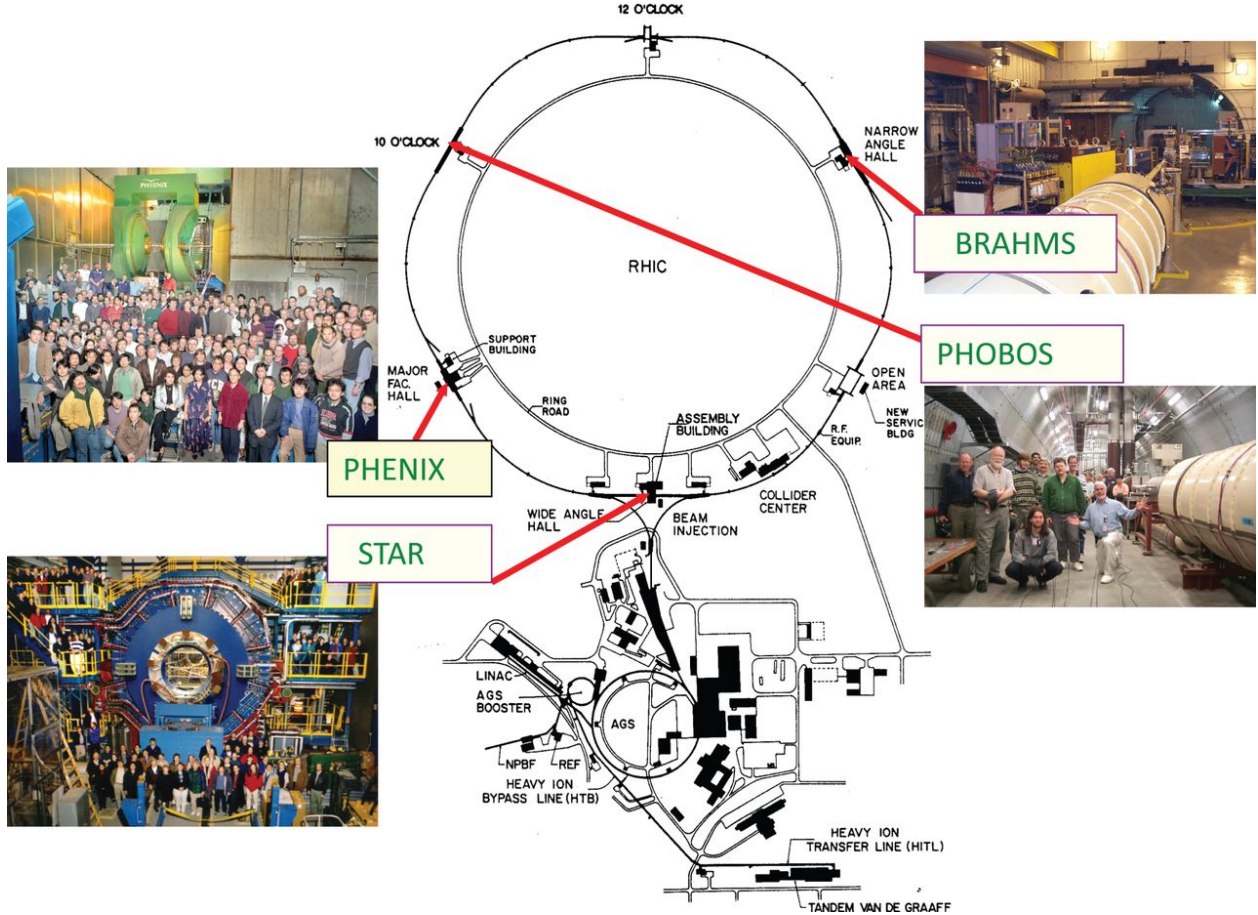


Figure 3.1: Initial layout of the RHIC.[26].

262

Heavy ion beams in the RHIC are created in a series of steps before collision. In case of gold ions, a pulsed sputter source produces negatively charged ions, which are stripped of some of their electrons with a foil on the positive end of the high-voltage Tandem Van de Graff. The ions are now positively charged and are accelerated to 1MeV/u toward the negative terminal of the Tandem, upon exiting which some more stripping takes place. The bending magnets then selectively deliver +32 charge states of the ions to the Booster Synchrotron, which accelerates them to 95MeV/u and strips them to +77 charge state before injecting them to the AGS. The AGS accelerates them to 10.8 GeV/u and strips them of

the remaining two electrons at the exit. The gold ions are then injected through the AGS-to-RHIC Beam Transfer Line to the two RHIC rings. These rings carry beams moving in opposite directions and intersect at six symmetric locations in the 3.8 km circumference. The original four detectors are located in four of these six locations where the beams undergo head-on collisions.

The Large Hadron Collider (LHC) is located underground (between 45m and 170m) beneath the France-Switzerland border near the city of Geneva. The two rings of the collider were constructed between 1998 and 2008 by the European Organization for Nuclear Research (CERN) in the 26.7 km circular tunnel originally housing CERN's Large Electron-Positron collider. Analogous to the RHIC, the LHC gets its beams prepared by a series of machines in the CERN accelerator complex. The collisions occur at the locations of the four big LHC experiments: Compact Muon Solenoid (CMS), A Toroidal LHC ApparatuS (ATLAS), Large Hadron Collider beauty (LHCb) experiment, and A Large Ion Collider Experiment (ALICE). ALICE is dedicated to the study of heavy-ion collisions. [15]

3.2 Collision Energy and Geometry

What happens in the aftermath of a collision depends on how much energy is available at the time of the collision as well as the geometry of the collision. The experimenter controls the collision energy, so it's known before the collision. The geometry of the collision is deduced from the constraints imposed by the static (eg. rest mass) and dynamic (eg. trajectory) properties of the detected products.

In collision experiments, it is convenient to use a reference frame in which the net momentum of the pair of colliding species is zero. This frame is called the center-of-mass frame. In this frame, the total energy of the species in the two beams is a function of the number of nucleons and the center-of-mass energy per nucleon. In case of symmetric collisions, i.e, collisions involving identical species in the two beams, the collision energy is reported as the center-of-mass energy per nucleon pair, $\sqrt{s_{NN}}$. The magnitude of this quantity constrains the species that can be produced from any collision.

298 The RHIC has the unique capability of colliding species at a range of energies spanning
 299 almost two orders of magnitude. Table 3.1 lists the collision energies produced so far at
 300 RHIC for various collision systems. The LHC, on the other hand, boasts the highest amount
 301 of collision energy for any collider on earth. It collided species (p+p, p+A, Pb+Pb) at a
 302 center of mass energy upto 2.76 TeV per nucleon pair at the end of 2010. At the end of
 303 2015, 5.02 TeV Pb-Pb collisions were successfully completed. [16]

Collision system	$\sqrt{s_{NN}}(GeV)$
p+p	200, 500
d+Au	200
Cu+Cu	62, 200
Au+Au	9, 20, 62, 130, 200

Table 3.1: Colliding species and associated collision energies at RHIC [24]

304 In general, any collision between two nuclei is not perfectly head-on. Some collisions are
 305 close to being head-on and are called central collisions. Some are far from being head-on and
 306 are called peripheral collisions. The amount by which a collision is central is quantitatively
 307 represented by a variable called centrality. By convention, 0% is the centrality of a perfectly
 308 head-on collision and 100% is that of the least head-on, i.e., the most peripheral collision. In
 309 practice, each collision event is deducted to belong to a specific centrality bin, for instance,
 310 0-5%. Figure 3.2 illustrates the aftermath of a mid-central collision, i.e, a collision in which
 311 about half of the volume of each of the nuclei intersects the other.

312 The collision of two nuclei can be modeled as a set of collisions of the constituents
 313 that make up the nuclei. The constituents that take part in the collisions and are called
 314 participants. The rest of the constituents are known as spectators. Figure 3.3 illustrates the
 315 distribution of participants and spectators in two colliding nuclei. Expectedly, the number
 316 of participants is more in more central collisions.

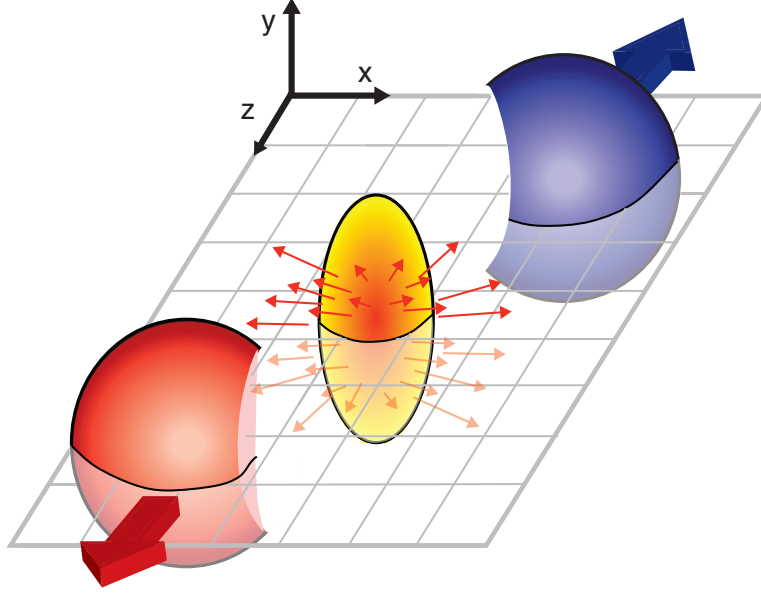


Figure 3.2: An illustration of a mid-central collision of two nuclei traveling in the z direction. The X -axis is parallel to the line joining the centers of the two nuclei at the time of collision. [13].

3.3 Kinematic Variables

The description of the collision physics and the interpretation of its results are aided by the construction of variables that undergo simple transformations under a change of reference frame. Two such variables, rapidity and pseudorapidity, are described in this section.

The rapidity, y , of a particle is defined as:

$$y \equiv \frac{1}{2} \ln \frac{p_0 + p_z}{p_0 - p_z} \quad (3.1)$$

$$= \frac{1}{2} \ln \frac{E + p_z}{E - p_z}, \quad (3.2)$$

where p_0 and p_z are the components of its contravariant four-momentum $p = (p_0, p_x, p_y, p_z)$ with $p_0 = \frac{E}{c}$, E being the relativistic energy of the particle and c , the speed of light, being equal to 1 in natural units.

The rapidity of a particle is used as a relativistic description of its velocity. Unlike the canonical velocity of a particle, its rapidity transforms simply additively under a Lorentz

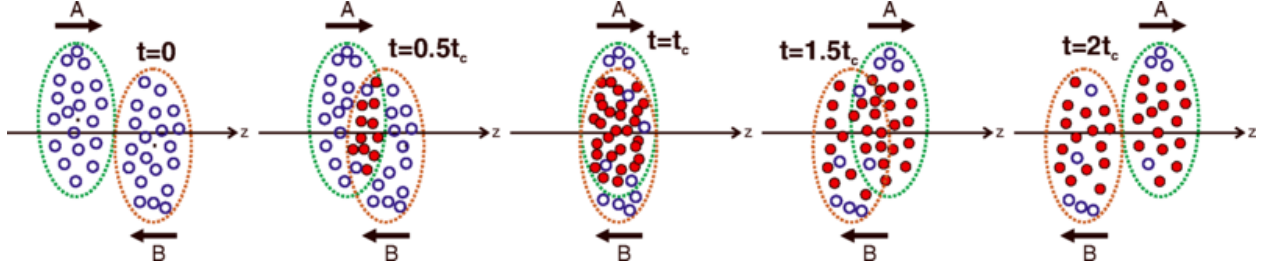


Figure 3.3: An illustration of a collision consisting of participants (solid red) and spectators (open blue) within the colliding nuclei labeled A and B. t_c denotes the time of maximum overlap of the two nuclei. The apparent narrowing of the volumes of the nuclei in the z -direction is due to Lorentz contraction. [37]

327 boost of the frame of reference. For example, suppose a particle has a rapidity y in
 328 a laboratory frame. Let y' denote its rapidity as measured in a frame that is Lorentz
 329 boosted with a velocity β in the z -direction with respect to the laboratory frame. Then the
 330 relationship between the rapidities in the two different frames is simply

$$y' = y - y_\beta \quad (3.3)$$

331 Here,

$$y_\beta = \frac{1}{2} \ln \frac{1 + \beta}{1 - \beta} \quad (3.4)$$

332 is the rapidity the particle would have in the laboratory frame if it were moving with a
 333 velocity β in the z -direction with respect to the laboratory frame, as can be verified from
 334 equation 3.1 with $p_0 = \gamma m$ and $p_z = \gamma \beta m$, γ being the Lorentz factor $\frac{1}{\sqrt{1-\beta^2}}$. [39]

335 The convenience provided by this construct comes with a cost. As evident from equation
 336 3.1, the calculation of the rapidity of a particle requires the measurement of two different
 337 observables associated with it, such as the energy and the z -direction momentum. However,
 338 experimental constraints may sometimes only facilitate the measurement of the direction of
 339 the detected particle with respect to the beam axis. What's more convenient in such a case
 340 is the use of another variable construct called pseudorapidity, η , defined as:

$$\eta \equiv -\ln \tan \frac{\theta}{2}, \quad (3.5)$$

where θ is the angle the particle's momentum vector, \mathbf{p} , makes with the z -direction. The above equation can also be written in terms of the momentum as:

$$\eta = \frac{1}{2} \ln \frac{|\mathbf{p}| + p_z}{|\mathbf{p}| - p_z} \quad (3.6)$$

From equations 3.1 and 3.6, it is evident that $\eta \approx y$ when $|\mathbf{p}| \approx p_0$, i.e., when the momentum is large. The transformation of the particle distribution from the y -space to the η -space is discussed in section 4.3.2.

3.4 QGP Evolution

The evolution of the QGP is shown in a lightcone diagram in figure 3.4. The initial state of the colliding nuclei is not well known and is the topic of research for upcoming experiments. During the collision, the participants scatter off of each other while the spectators don't and keep traveling almost unperturbed in their original direction. The immediate aftermath of a central collision of heavy ions at RHIC and LHC energies is the formation of a hot fireball. This fireball evolves in time to form a liquid-like medium of quarks and gluons. This medium attains a local equilibrium and remains in such a state, depending on the collision energy, for about 1-10 fm/c. This equilibrium is broken as the liquid QGP evolves by expanding and cooling to attain a density and temperature at which the deconfinement of quarks and gluons is lost and they undergo a chemical freeze-out to form a hadron gas. Collisions between the constituents of this gas become scant as it evolves with further expansion and cooling, and the hadrons undergo a thermal freeze-out to attain their final energies and momenta.

3.5 Detection of Collision Products

Detectors are placed around the collision site to perform measurements on the final state particles emitting from the thermal freeze-out of the medium. These measurements typically include the estimation of the location and time of production of the final states, the type of particle, and the momentum and energy it carries.

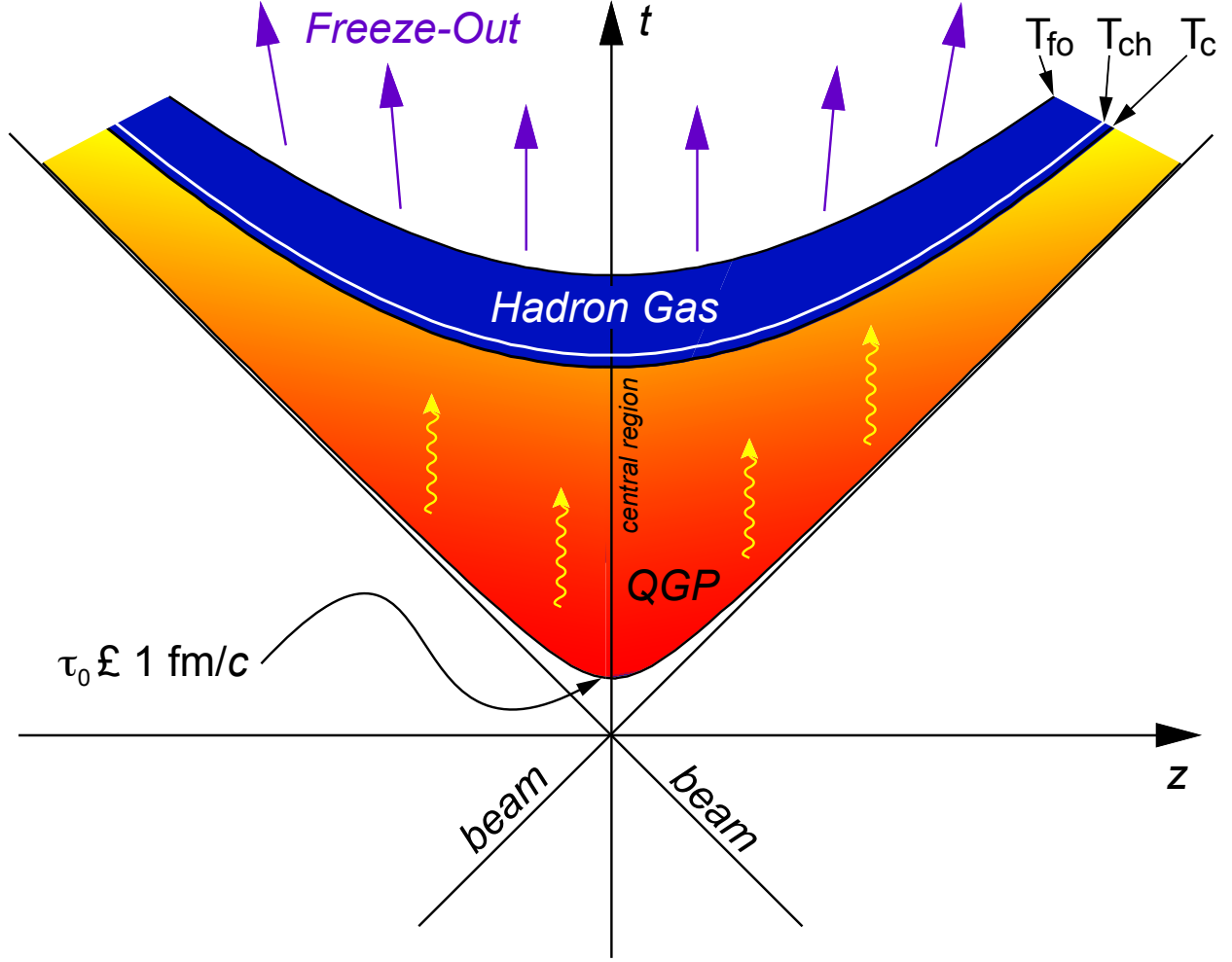


Figure 3.4: Evolution of the QGP represented in a lightcone diagram. τ_0 denotes the formation time of the QGP. T_c is the critical temperature of the transition from the QGP to the hadron gas phase. T_{ch} and T_{fo} stand for the temperatures at, respectively, chemical freeze-out and thermal freeze-out. [13]

364 Generally, a tracking detector surrounds the collision site, and there are calorimeters
 365 followed by particle identifiers around it. A magnetic field is applied parallel to the beam
 366 direction around the collision site. Due to this orientation of the magnetic field, the spectators
 367 traveling parallel to it move undeflected and the final state charged particles with components
 368 of velocity transverse to the beam axis get deflected around the beam axis with angular
 369 frequency given by

$$\omega = \frac{qB}{m}, \quad (3.7)$$

where q is the electric charge of the particle, m is its mass and B is the applied magnetic field. Two kinds of detectors most relevant to this thesis, tracking detectors and calorimeters, are described in chapter 4.

3.6 Detection of QGP Signatures

The existence and properties of the QGP in the aftermath of high-energy heavy-ion collisions can be probed using different techniques relevant to several theoretical characteristics of the phase. No such signature can alone be used to claim the production of the QGP, and some of the probes, which should be interpreted together, are described below.

3.6.1 Bjorken Energy Density

In 1983, J.D. Bjorken[10] prescribed a formula to use the final state particles to estimate the initial energy density, ϵ_0 , in a nucleus-nucleus collision. With slight changes in the original formula, the energy density is given by:

$$\epsilon_0 = \frac{1}{\tau_0 A_T} \langle \frac{dET}{dy} \rangle, \quad (3.8)$$

where τ_0 is the proper time at the moment of QGP equilibration, A_T is the transverse area of the intersection of the two nuclei, and $\langle \frac{dET}{dy} \rangle$ is the mean transverse energy per unit rapidity. τ_0 is model-dependent and is normally of the order of $1 fm$. A_T depends on the centrality of the collision. $\langle \frac{dET}{dy} \rangle$ is found from the measurement of the transverse energy carried by the final state particles from the collision and is the central theme of this thesis. Details about it are in the following chapters. The estimate of the initial energy density from Bjorken formula can be compared with the QCD prediction of the critical energy density[1] to check if the results from a collision imply the achievement of the critical physical condition required for the phase transition.[20]

3.6.2 Elliptic Flow

For yet unknown reasons, the evolution of the medium produced after relativistic heavy ion collisions can be well described under the framework of relativistic hydrodynamics. [30, 35] This description indicates the presence of a collective flow, and hence a liquid-like and thermalized nature, of the constituents that make up the system. The momentum distribution of the final state particles emitting out of the collectively flowing system can be decomposed into its azimuthal Fourier components. The second harmonic coefficient, $\nu_2(y, p_T)$, of this decomposition characterizes what is known as the elliptic flow.[19] The magnitude of the elliptic flow from a non-central collision represents the anisotropy in azimuthal momentum space of the thermalized post-collision system.[33] The elliptic flow of the medium, as a function of the momentum or the kinetic energy in the transverse direction, points towards quarks, rather than hadrons, being the relevant degrees of freedom in the QGP. Figure 3.5 shows ν_2 plotted against the transverse momentum and the transverse kinetic energy for identified particles. The spectra scale consistently at lower values of both p_T and KE_T . However, they branch out at higher values: $p_T \gtrsim 2\text{GeV}/c$ and $KE_T \gtrsim 1\text{GeV}$. Figure 3.6, on the other hand, is similar to figure 3.5, with the exception that both the axes have quantities that are normalized by the number of quarks, n_q . In this case, the KE_T spectra strongly exhibits (p_T does so less strongly) a scaling which is more comprehensively consistent with the number of quarks than in case of figure 3.5. This universal quark-number scaling can be interpreted as the degrees of freedom of the system being quark-like.[4]

3.6.3 Dilepton Production

When the color degree of freedom is liberated in the post-collision system, a quark can interact with an antiquark to produce a virtual photon which decays into a lepton and an antilepton. This pair of leptons is devoid of a color charge and can interact with the particles in the fireball only electromagnetically. This leads to them having a significantly larger mean-free path as compared to colored probes, and the number of collision they undergo before reaching a detector is negligible. However, the thermodynamic state of the fireball affects the momenta of the quarks and the antiquarks, which in turn affect the momenta and

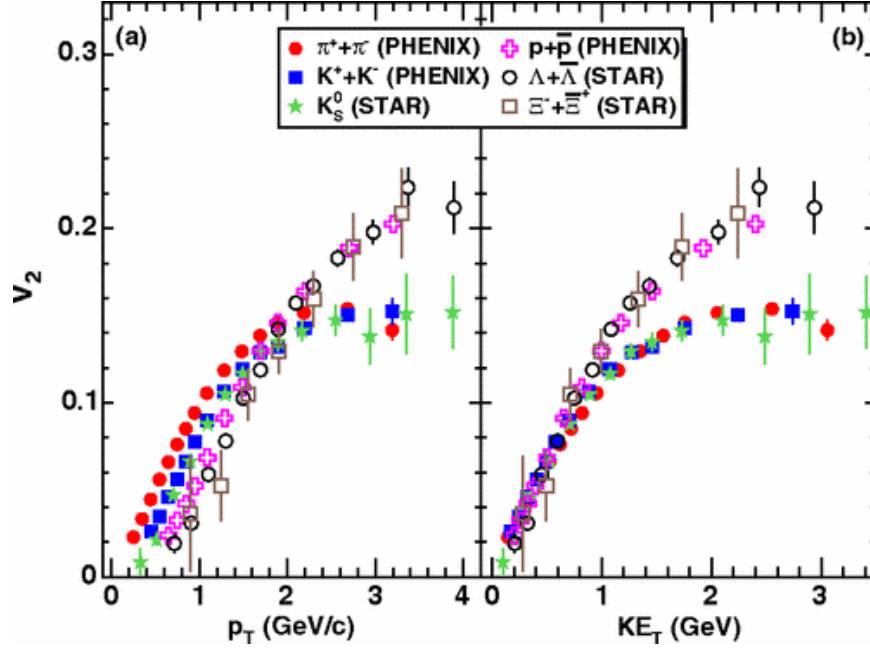


Figure 3.5: Minimum-bias Au+Au ($\sqrt{s_{NN}} = 200 \text{ GeV}$) elliptic flow spectra for identified particles: (a) v_2 vs p_T and (b) v_2 vs KE_T . [4]

the production rates of the lepton pairs. Specifically, the temperature of the QGP can be estimated using the dilepton spectra. The caveat of doing so is that the QGP is not the only possible source of dileptons. Hence, the contributions from other sources, mainly the Drell-Yan process, must be figured out before using the dilepton spectra as a QGP diagnostic. [39]

3.6.4 Direct photons

In the QGP, a quark and an antiquark can annihilate to produce a photon and a gluon. It is also possible for the pair to annihilate and produce two photons, but the probability of this process is smaller than the former by about two orders of magnitude. Furthermore, a quark (or an antiquark) can interact with a gluon to produce an antiquark (or a quark) and a photon, a process analogous to Compton scattering in QED. Just like the leptons described in the previous section, the photons produced in the QGP can only interact with the medium electromagnetically. Therefore, they undergo minimal scattering before being detected, and hence can be used to probe the thermodynamical state of the medium at the time of their creation. [39] Photons can also be produced after hadronization as a result of

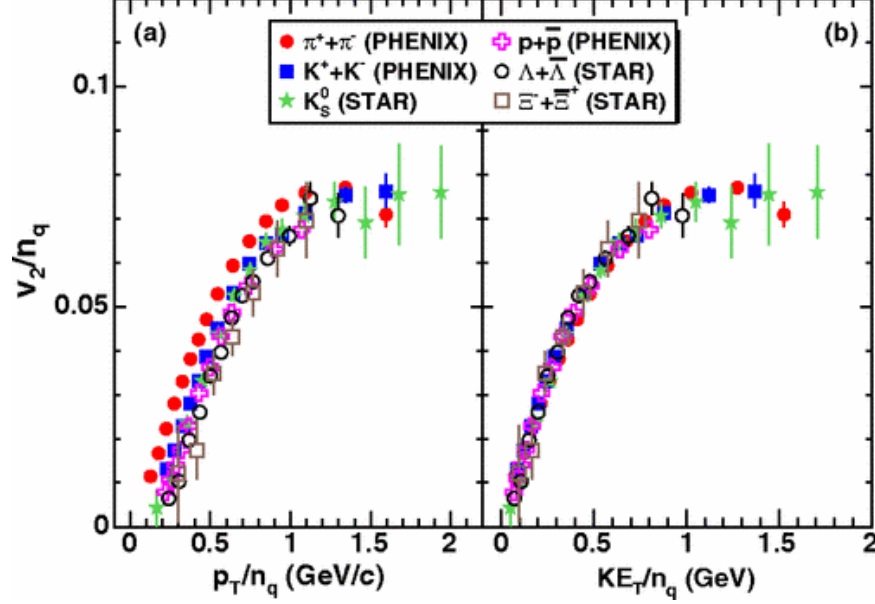


Figure 3.6: Minimum-bias Au+Au ($\sqrt{s_{NN}} = 200 \text{ GeV}$) elliptic flow spectra for identified particles: (a) $\frac{v_2}{n_q}$ vs $\frac{p_T}{n_q}$ and (b) $\frac{v_2}{n_q}$ vs $\frac{KE_T}{n_q}$. [4]

the scattering of the hadrons within the evolved medium. However, the nature of the p_T distribution is different in this case, and this difference helps distinguish these photons from the direct photons produced by partonic interactions. [38]

3.6.5 Strangeness Enhancement

The interacting nuclei carry no net strangeness before colliding, and so a post-collision observation of strange and multi-strange particles can be a signal for an antecedent existence of deconfined quarks and gluons [14]. Strangeness can also be produced in hadron-hadron collisions. However, it is enhanced in nucleus-nucleus collisions in which a large number of hadrons are produced and are in chemical equilibrium at very high temperatures. Consider the ratio of the production of the strange kaons to that of the non-strange pions, which are the most abundant hadrons produced from nucleus-nucleus collisions. Kaon yield increases more rapidly than does pion yield as the temperature increases. This can be shown mathematically by treating the system as a hadron gas in thermal and chemical equilibrium that follows the Bose-Einstein distribution, but it is beyond the scope of this thesis. [39]

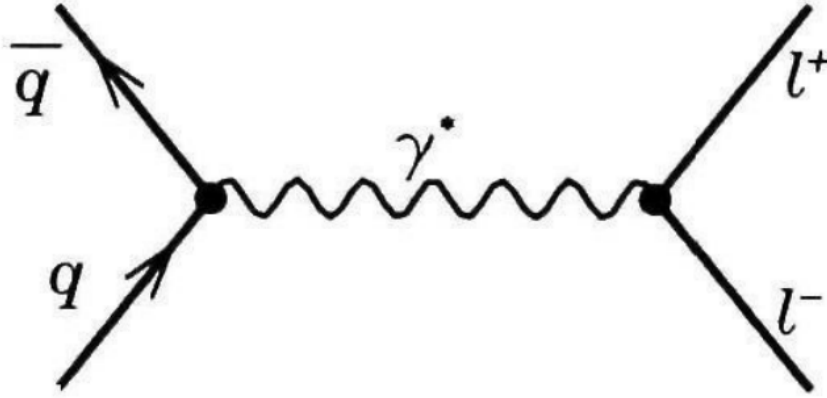


Figure 3.7: Feynman diagram representing the production of a lepton pair from a quark and an antiquark. [39]

3.6.6 Jet Quenching

A scattering event in which the participants transfer a large amount of their original momenta is called hard scattering. The products of the scattering, carrying high transverse momenta in opposite directions, are called jets. In heavy-ion collisions, most of the hard scatterings are the results of two partons from the opposite nuclei scattering off of each other. These partons can lose their momenta by strongly interacting with a medium made of deconfined quarks and gluons. Therefore, the properties of the jets, as carried by the final state hadrons, should be different for collisions that produce the QGP as compared to those that don't, and hence they can be used as signatures and probes of QGP. Figure 3.9 illustrates the quenching of jets that have to travel long distances in the medium. Formalisms developed to study jet quenching due to radiative and collisional energy losses are detailed in [28].

3.7 The Beam Energy Scan Program

The RHIC, in 2010, started a multi-phase Beam Energy Scan (BES) program to study the QCD phase diagram. The collider has two different detectors that are currently operational, STAR and PHENIX, which facilitate the cross-checking of results. Between 2010 and 2011, under the exploratory phase I of the BES program, 7.7, 11.5 (not completed in PHENIX), 19.6, 27, and 39 GeV collisions were completed using pairs of Au nuclei. Together with the data formerly collected by the RHIC at higher collision energies, BES phase I data can

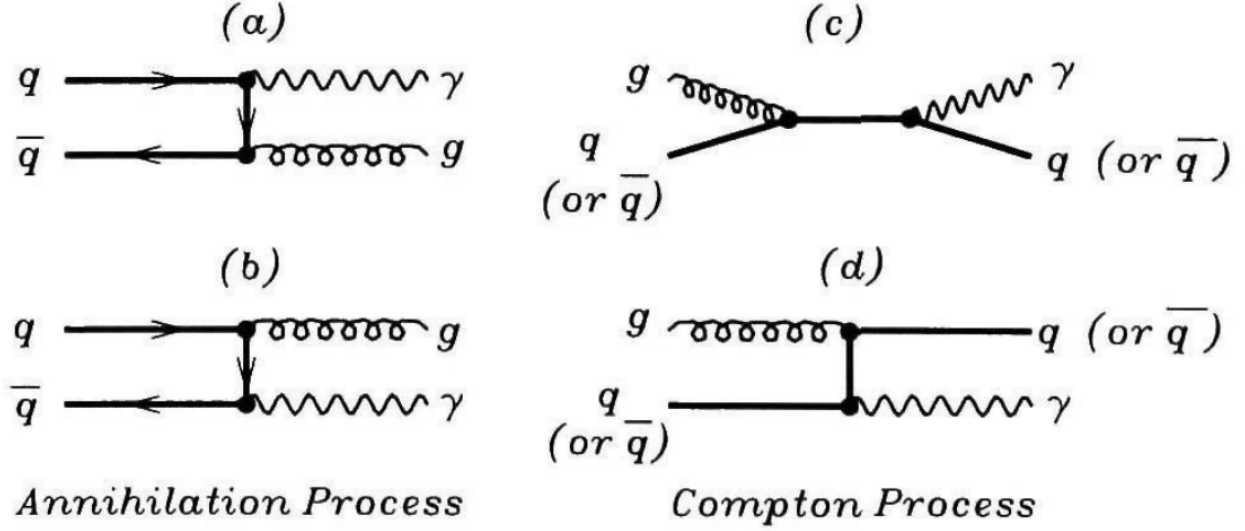


Figure 3.8: Feynman diagram representing the production of photons from quarks and gluons. (a) and (b) represent annihilation processes, whereas (c) and (d) represent Compton processes.[39]

scan the interval from 450 MeV to 20 MeV in μ_B space [25, 22]. One of the things that can be studied with the data associated with this region of the phase space is statedly the possibility of a “turn-off of new phenomena already established at higher RHIC energies” (<https://drupal.star.bnl.gov/STAR/starnotes/public/sn0493>). Results corresponding to the high- μ_B region might provide evidence of a first order phase transition, and possibly the critical point [22].

The manifestation of such phenomena would be in terms of the fluctuations in the properties of the post-collision system. One can, for instance, study the scaling of the transverse energy after the collision with the longitudinal energy at the time of the collision, $\sqrt{s_{NN}}$. This can be done in multiple ways for a detector like STAR or PHENIX that is made up of sub-systems such as the TOF detectors, TPCs/Time Expansion Chambers, as well as calorimeters. The next chapter gives an example of the measurement of transverse energy using BES data from PHENIX calorimeters. Also, the next chapter and the ones after it contain the procedures and the results of the analysis of the BES data from STAR using the identified particles spectra.

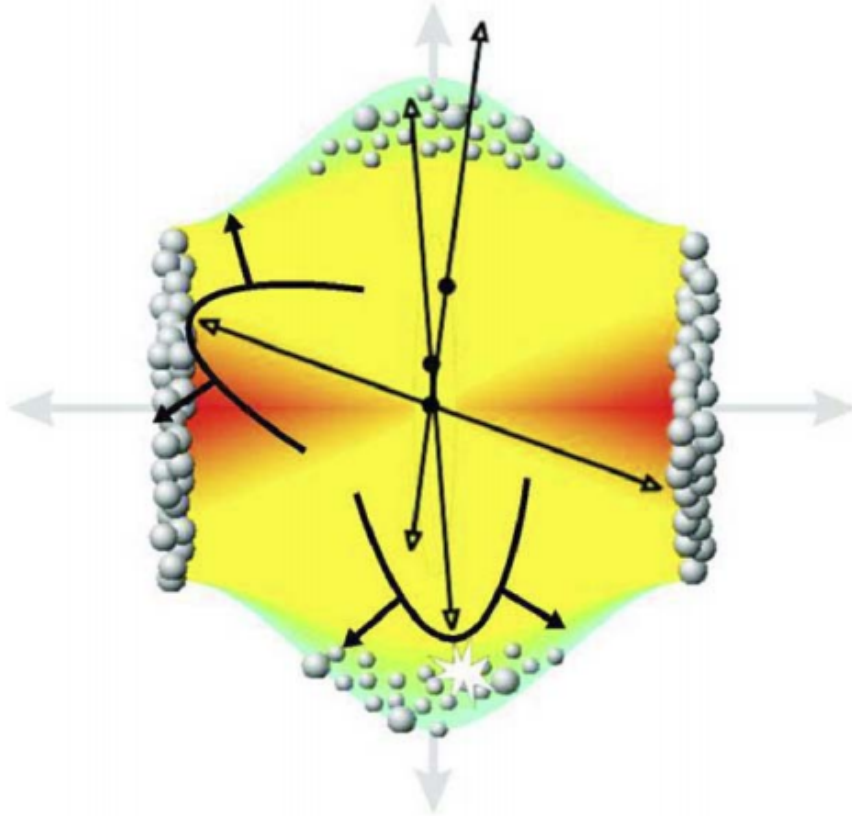


Figure 3.9: Illustration of jet quenching. Two jets are produced from each of the hard scatterings occurring at the locations of the solid dots. Jets originating closer to the initial surface are more probable to propagate outside the medium, as shown. Jets opposite to them interact with the medium, losing their energy and resulting in bow front shock waves.[36]

Chapter 4

Measurement of Transverse Energy

This chapter introduces the definitions of transverse energy, ways to measure it using different detectors, and particular examples for the detectors at the RHIC.

4.1 Definition of Transverse Energy

In theory, E_T from a collision can be defined as the sum of the transverse masses, m_T , of all the particles produced in the collision, i.e.,

$$E_T \equiv \sum_i m_{T,i} \quad (4.1)$$

with

$$m_T \equiv \sqrt{p_T^2 + m^2} \quad (4.2)$$

where m is the rest mass of the particle and p_T is its transverse momentum. Using this definition to calculate the E_T requires perfect identification of all the particles. It has not been possible to do so in experiments, and so a more feasible, operational definition of E_T is fabricated. A commonly accepted definition in case of the feasibility of calorimetric measurements is [5, 11]:

$$E_T = \sum_i E_i \sin \theta_i, \quad (4.3)$$

494

$$\frac{dE_T}{d\eta} = \sin\theta \frac{dE}{d\eta}, \quad (4.4)$$

495 where the index i runs over all the particles going into a fixed solid angle for each event,
 496 θ is the polar angle, i.e, the angle with respect to the beam axis, η is the pseudorapidity
 497 defined as

$$\eta \equiv -\ln \tan \frac{\theta}{2}, \quad (4.5)$$

498 and E_i is the energy deposited in the calorimeter by the i^{th} particle. E_i is considered to be,
 499 by convention [6], the following

$$E_i = \begin{cases} E_i^{tot} - m_0 & \text{for baryons} \\ E_i^{tot} + m_0 & \text{for anti-baryons} \\ E_i^{tot} & \text{otherwise} \end{cases} \quad (4.6)$$

500 where E_i^{tot} is the total energy of the i^{th} particle defined canonically as

$$E^{tot} \equiv \sqrt{p^2 + m_0^2} \quad (4.7)$$

501 and m_0 is the particle's rest mass. In order to account for the portion of the emitted
 502 transverse energy not detected or overestimated by the calorimeters, corrections are made
 503 based on GEANT simulations.

504 **4.2 E_T Measurement with Calorimeters**

505 **4.2.1 Calorimeter**

506 **4.2.2 E_T from PHENIX**

507 Adare et al. [3] use calorimetry in PHENIX to analyze the transverse energy corresponding
 508 to several different pairs of species colliding at a range of energies. They use the raw
 509 transverse energy measured by the EMCal, E_{TEMC} , to obtain the total hadronic E_T by

510 making corrections in three different steps. They first scale the data by a constant factor
 511 calculated to account for the fiducial acceptance in azimuth and pseudorapidity. The second
 512 factor is calculated to adjust for the effects of the calorimeter towers that are disabled. The
 513 third factor, k , is computed as follows

$$k = k_{response} \times k_{inflow} \times k_{losses} \quad (4.8)$$

514 where $k_{response}$ corresponds to hadronic particles only depositing a fraction of their total
 515 energy while passing through the EMCal, k_{inflow} is attributable to the energy deposited
 516 by particles coming from outside the EMCal's fiducial aperture, and k_{losses} accounts for
 517 the energy not registered in the EMCal due to energy thresholds, edge effects, and more
 518 importantly due to the particles that make it into the fiducial aperture but decay into
 519 products outside the aperture.

520 4.3 E_T Measurement with Tracking Detectors

521 Transverse energy analysis can be done using tracking detectors as well if they are able
 522 to produce measurements of other physical quantities that implicitly contain information
 523 about the transverse energy. Specifically, the charged particle multiplicity distributions with
 524 respect to the transverse momenta can be used to calculate the particle's transverse energy
 525 pseudorapidity density. In fact, since the corrections related to the tracking detectors are
 526 very different from those related to the calorimeters, results from the two different methods
 527 can be used to test the assumptions involved in each.

528 4.3.1 Tracking and Particle Identification

529 The tracking detectors in experiments such as the STAR (Solenoidal Tracker At RHIC)
 530 experiment and ALICE (A Large Ion Collider Experiment) at CERN include Time Projection
 531 Chambers (TPCs) and Time-of-Flight (TOF) detectors that can give us the p_T spectra, yields
 532 and particle ratios of the identified charged hadrons [27, 2]. The TPCs provide measurements
 533 of particle trajectories – that can be used to determine the momenta for low-momentum

534 particles – and of their specific energy loss,

$$\frac{dE}{dx}, \quad (4.9)$$

535 which can be used with the trajectories to make particle identifications (PID) using the
 536 Bethe-Bloch formula [9]. TOF detectors, on the other hand, cover the high-momentum part
 537 of the measurements. In ALICE, the combination of the measurements of the TPC with those
 538 of the Inner Tracking System (ITS) effectively adds the tracking length, thereby improving
 539 the resolution of the measured p_T spectrum. Details about the PID and momentum
 540 determination capabilities of the detectors in ALICE can be found in [12].

541 The p_T spectra, available as the counts $\frac{d^2N}{dydp_T}$ with respect to p_T , can be used to calculate
 542 $\frac{dE_T}{d\eta}$ as formulated in the following section.

543 4.3.2 Calculation of $\frac{dE_T}{d\eta}$ from p_T spectra

544 In relativistic heavy ion collisions, rapidity (y) is defined as follows:

$$y \equiv \frac{1}{2} \ln \frac{E + p_z}{E - p_z}, \quad (4.10)$$

where E is given by equation 4.7 and p_z is the component of the momentum parallel to the beam axis. Pseudorapidity, η , is just y with $m_0 = 0$:

$$\begin{aligned} \eta &= \frac{1}{2} \ln \frac{p + p_z}{p - p_z} \\ &= \frac{1}{2} \ln \frac{1 + \cos \theta}{1 - \cos \theta} \\ &= \frac{1}{2} \ln \frac{2 \cos^2 \frac{\theta}{2}}{2 \sin^2 \frac{\theta}{2}} \end{aligned}$$

$$\therefore \eta = - \ln \left| \tan \frac{\theta}{2} \right| \quad (4.11)$$

545 Note that the absolute value is not necessary for $0 \leq \theta \leq \pi$. Then, taking the exponential
 546 of both sides of the above equation and using Euler's formula, we get:

$$\sin \theta = \frac{1}{\cosh \eta}. \quad (4.12)$$

Hence,

$$\begin{aligned} p &= \frac{p_T}{\sin \theta} \\ &= p_T \cosh \eta, \end{aligned}$$

547 and so we have

$$E_T = E \sin \theta = \frac{\sqrt{p_T^2 \cosh^2 \eta + m_0^2}}{\cosh \eta} \quad (4.13)$$

548 The Jacobian for the transformation from y -space to η -space is derived, by differentiating
 549 y with respect to η (obtained from equations 4.10 and 4.11), to be:

$$\frac{\partial y}{\partial \eta} = \frac{p_T \cosh \eta}{\sqrt{m_0^2 + p_T^2 \cosh^2 \eta}} \quad (4.14)$$

550 From equations 4.13 and 4.14, we can see that the product of E_T with the Jacobian is
 551 equal to p_T . That leads to a formulation of $\frac{dE_T}{d\eta}$ as a function of only η and p_T :

$$\frac{dE_T}{d\eta} = \frac{1}{2a} \int_0^{10 \text{ GeV}/c} \int_{-a}^a p_T \frac{d^2 N}{dy dp_T} d\eta dp_T \quad (4.15)$$

552 where a and $-a$ are the bounds for η .

553 4.3.3 Tracking Detectors in STAR

554 In the STAR experiment, the TPC is the primary tracking detector. It is 4.2 m long and it
 555 cylindrically enshrouds the accelerator beam pipe from its outside, with an inner diameter
 556 of 1 m and an outer diameter of 4 m [24]. It covers a pseudorapidity range of $|y| < 1.8$
 557 in all of azimuth in terms of acceptance of charged particles. It can identify particles with

558 momenta over 100 MeV/c up to about 1 GeV/c as well as measure their momenta from
 559 100 MeV/c to 30 GeV/c [7]. Figure 4.1 shows the PID capability of the STAR TPC for
 560 very high-multiplicity events [18]. Separation of pions from protons is demonstrated up to a
 561 little more than 1 GeV/c. At higher momenta, separating particles is more difficult because
 562 their energy loss has lower dependence on the rest mass [7]. The TOF system in STAR,
 563 with a time resolution of $\lesssim 100$ ps, aids PID at higher momenta. However, at intermediate
 564 p_T , between ≈ 2.0 and 4.0 GeV/c, the TPC by itself cannot distinguish between pions and
 565 protons and the TOF by itself cannot separate pions from kaons. This problem is resolved
 566 by utilizing the fact that the dependence of the particle velocity on p_T – in case of the TPC
 567 – is different from that of the energy loss on p_T in case of the TPC; combining the results
 from the two, hence, makes PID feasible in this p_T range. [31]

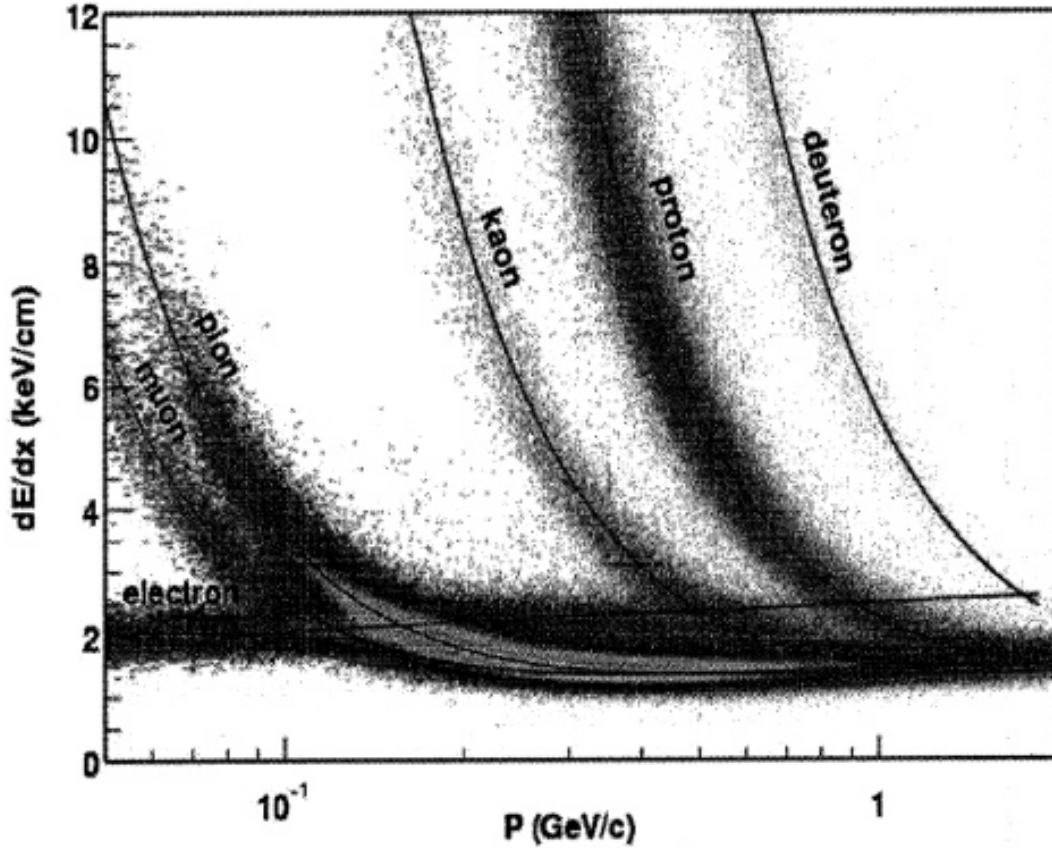


Figure 4.1: Energy loss distribution in the STAR TPC for primary and secondary particles.
 [18].

Chapter 5

Data Analysis

The analysis of the data involved extrapolating the available spectra and using the results from the fits to calculate the transverse energy for all the available spectra and the particle multiplicity corresponding to charged particles. Details follow.

5.0.1 STAR p_T spectra

This thesis details the method of transverse energy analysis through the use of p_T spectra from the STAR BES data. As described in section 4.3.3, the TPCs and TOF detectors in STAR can identify particles as well as their trajectories and ultimately their multiplicity distributions with respect to the momenta. Adamczyk et al. [2] report the results for the p_T spectra for six different identified hadrons, π^+ , π^- , K^+ , K^- , p , and \bar{p} , from the STAR experiment. The spectra come from Au+Au collisions – at $\sqrt{s_{NN}} = 7.7$, 11.5, and 39 GeV in the year 2010 and at $\sqrt{s_{NN}} = 19.6$ and 27 GeV in 2011 – under the BES Program. Figure 5.1 [2] shows the spectra corresponding to 39 GeV collisions categorized into seven different collision centralitiy classes. These spectra, and their counterparts for the rest of the energies, were used to calculate an estimate of the total transverse energy per event per particle species. This result was then used to estimate the total transverse energy due to all the collision products.

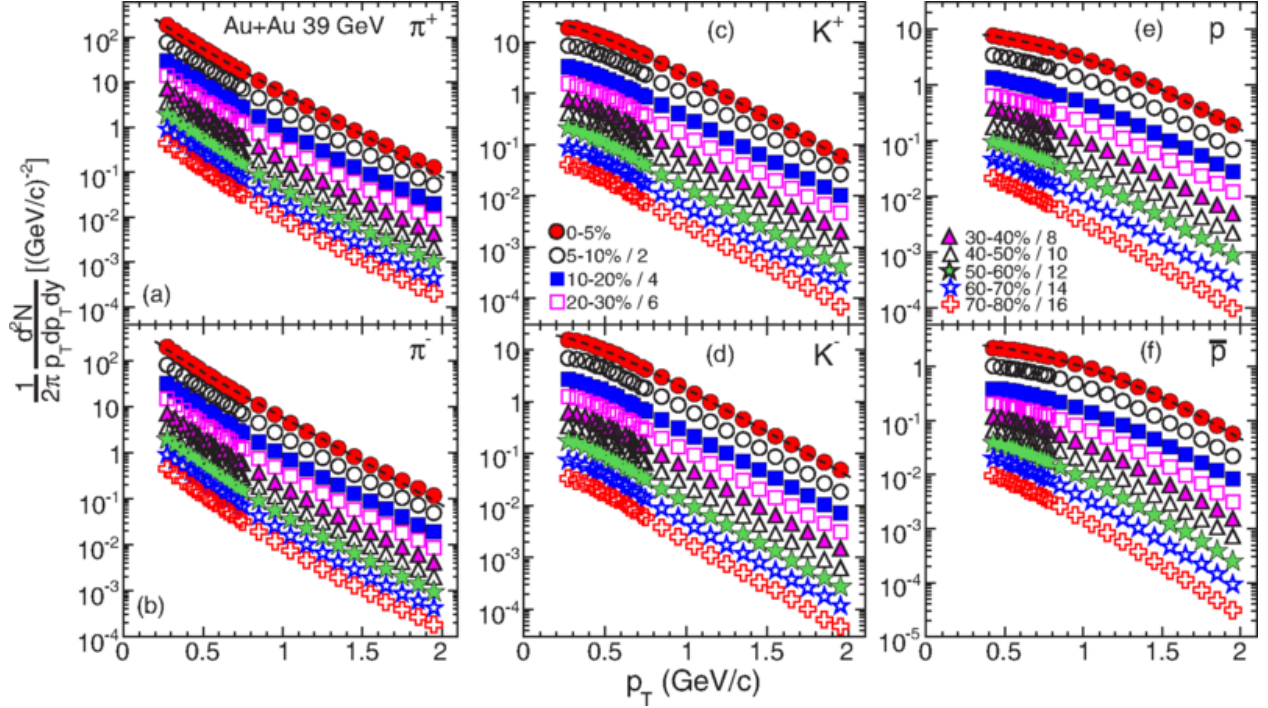


Figure 5.1: Transverse momentum spectra for π^+ , π^- , K^+ , K^- , p , and \bar{p} at midrapidity ($|y| < 0.1$) from 39 GeV Au+Au collisions at RHIC. The fitting curves on the 0-5% central collision spectra for pions, kaons, and protons/anti-protons represent, respectively, the Bose-Einstein, m_T -exponential, and double-exponential functions. [2].

The corrections applied by Adamczyk et al. [2] to the raw data to obtain the spectra and the reported systematic uncertainties in their results are discussed below (under construction)

5.1 Extrapolation of Spectra

The available spectra were limited to a range of transverse momenta ranging from around 0.25 GeV/c to around 2 GeV/c (for pions). To account for the transverse energy corresponding to the momenta for which there was no available data, an extrapolation had to be used. The model used for the extrapolation and the associated statistics are discussed below.

5.1.1 Boltzmann-Gibbs Blast Wave

The blast wave is a common model used in the analysis of the particle spectra.[????] The specific model used in this thesis is the Boltzmann-Gibbs blast wave (BGBW) as represented in equation ?? . It has the parameters mass, temperature, beta, v, and n. I assume that any anomalies in the magnitude of the normalization parameter do not affect the results significantly insomuch as they don't lead to:

- (a) unreasonable relative errors in the extrapolated values of the transverse energy,
- (b) any of the spectral fits having the extrapolated transverse energy more than that calculated from just the available spectra, and
- (c) for the 200 GeV collision samples, at least, the extrapolation at higher p_T being more than that at lower p_T .

$$BGBW \tag{5.1}$$

5.1.2 Fitting Spectra to BGBW

Figure 5.2 presents an example of a Boltzmann-Gibbs Blast Wave (BGBW) fit on one of the individual particle spectra with the goodness-of-fit as well as other statistics and the associated errors. A parallel-coordinates plot is presented in the next chapter in fig. 6.1, which shows the measured centralities, two of the good-fit parameters, and the calculated transverse energies for 270 different particles (lambdas not included).

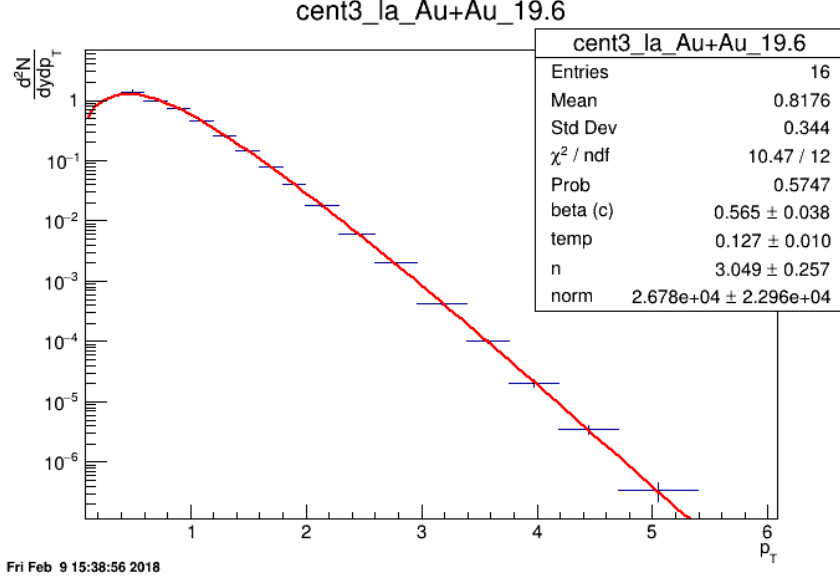


Figure 5.2: Red curve shows the Boltzmann-Gibbs blast wave functional fit on the PRELIMINARY transverse momentum spectrum for lambda particles identified by the STAR detector for 19.6 GeV Au+Au collisions (10-15% central). Parameters extracted from the chi-square goodness-of-fit test, as well as other statistics, are shown in the box on the top right.

5.2 Calculations from the Spectral Fits

5.2.1 Calculation of $\frac{dE_T}{dy}$, $\frac{dE_T}{d\eta}$, $\frac{dN_{ch}}{dy}$, and $\frac{dN_{ch}}{d\eta}$

5.2.2 Corrections for Unidentified Particles and Estimation of Total E_T

It is reasonable to assume that, at high energies, there should be roughly the same multiplicity of all the isospin states of a final state particle. Table 5.1 lists the isospin states associated with the pion, the kaon, the proton, and the lambda particles.

Particle	Isospin multiplets
pion	π^+, π^0, π^-
kaon	K^+, K^0, K^-, \bar{K}^0
proton	p, n
lambda	Λ

Table 5.1: Isospin states of different identified particles.

619text content.....

$$E_T = 3E_T^\pi + 4E_T^K + 4E_T^p + 2E_T^\Lambda \quad (5.2)$$

620text content.....

621 **5.2.3 Lambdas Centralitiy Adjustments and E_T Interpolations**

622 The centrality bins corresponding to the lambdas spectra were slightly different from those
623 corresponding to the rest of the particles.....

624 **5.3 Uncertainties**

625 100% correlated point-to-point and uncorrelated between particles..... ?

Chapter 6

Results

Present results and comparisons to Adare et al....

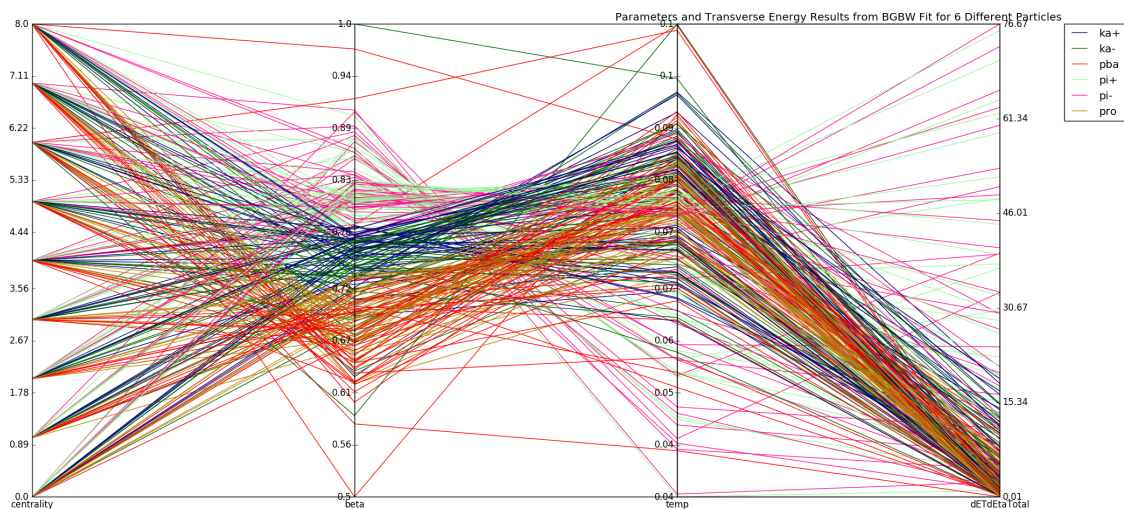


Figure 6.1: Parallel coordinates plot for 270 different spectra relating 6 different identified particles (color-coded) to their respective collision centrality classes, good-fit parameters, and the transverse energy calculated using said parameters.

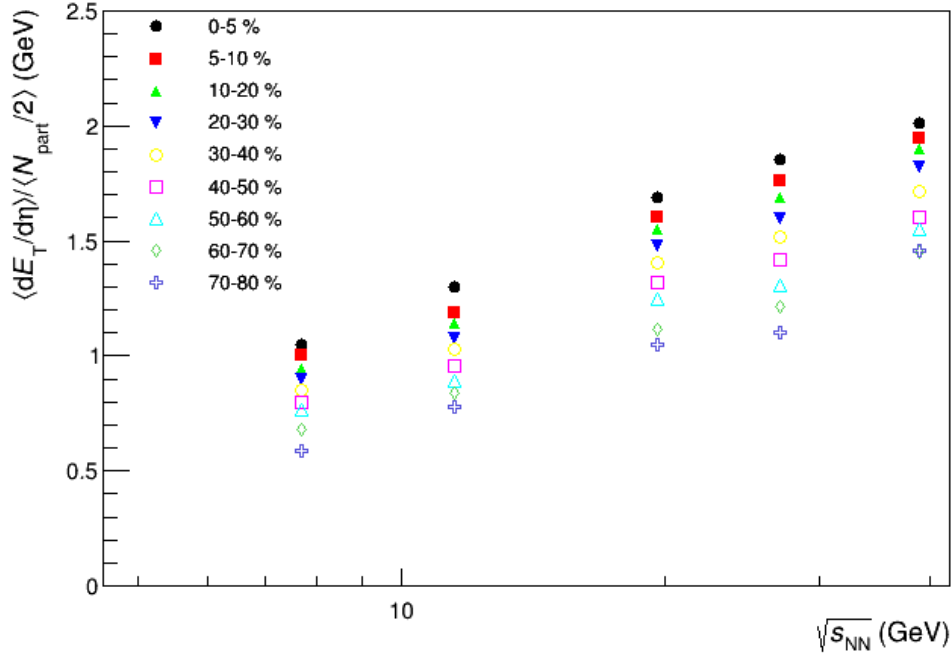


Figure 6.2: $(dE_T/d\eta)/0.5N_{part}$ at midrapidity as a function of $\sqrt{s_{NN}}$ for different centralities.

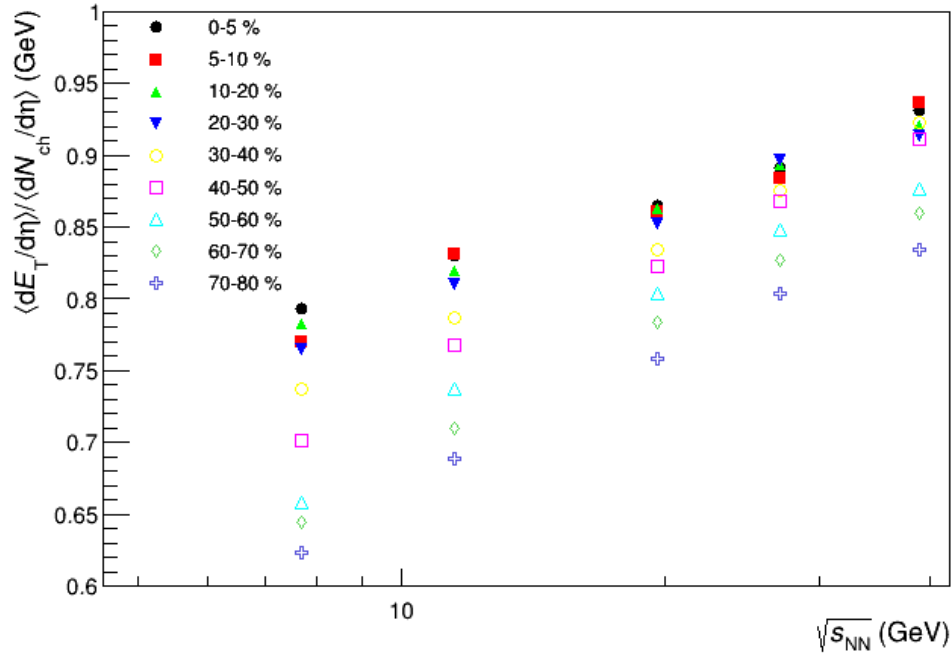


Figure 6.3: $(dE_T/d\eta)/(dN_{ch}/d\eta)$ at midrapidity as a function of $\sqrt{s_{NN}}$ for different centralities.

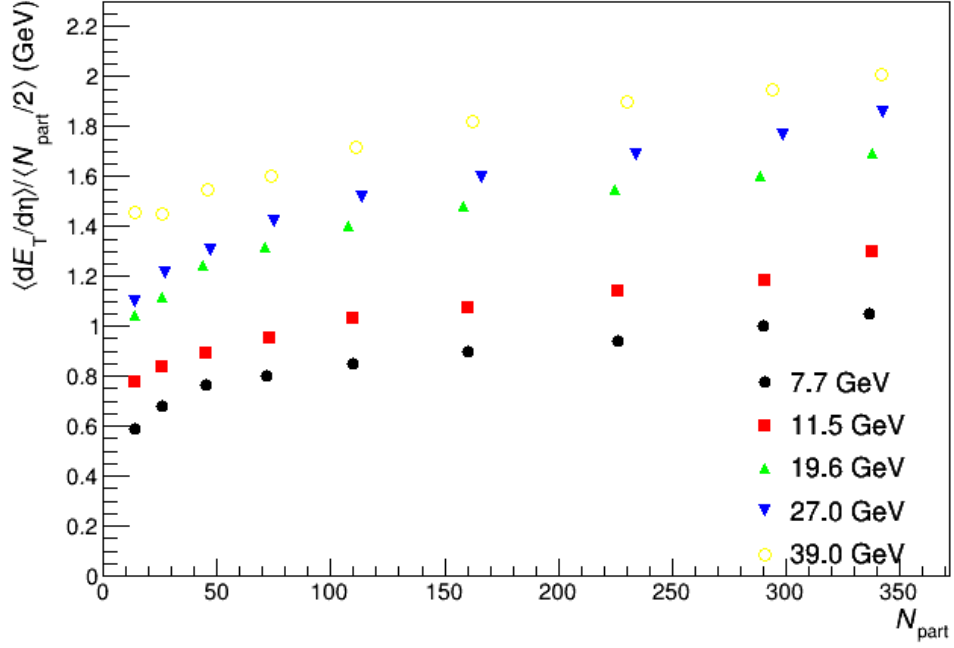


Figure 6.4: $(dE_T/d\eta)/0.5N_{part}$ at midrapidity as a function of N_{part} for different centralities.

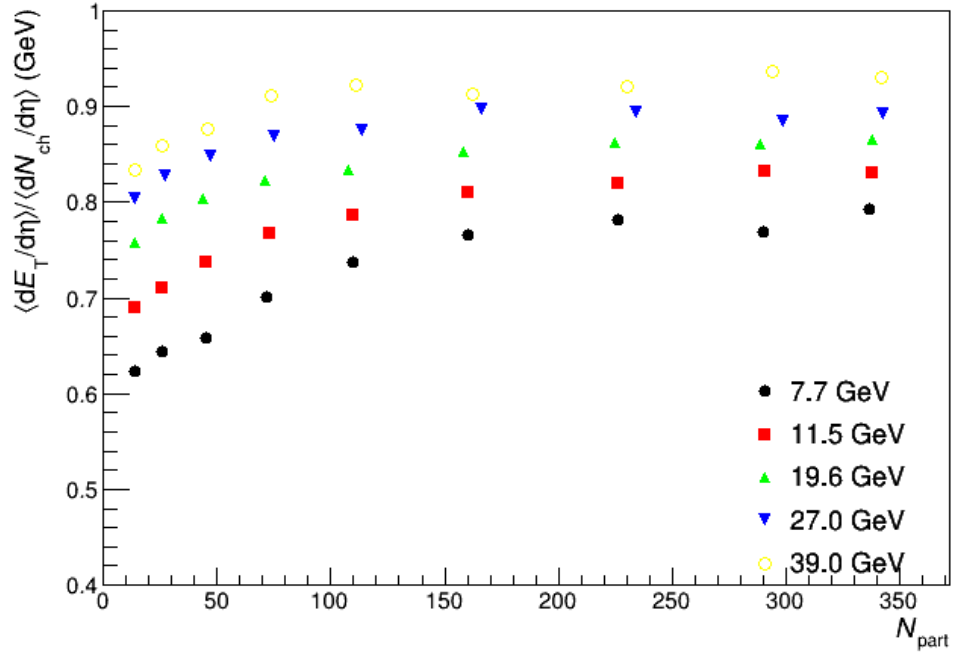


Figure 6.5: $(dE_T/d\eta)/(dN_{ch}/d\eta)$ at midrapidity as a function of N_{part} for different centralities.

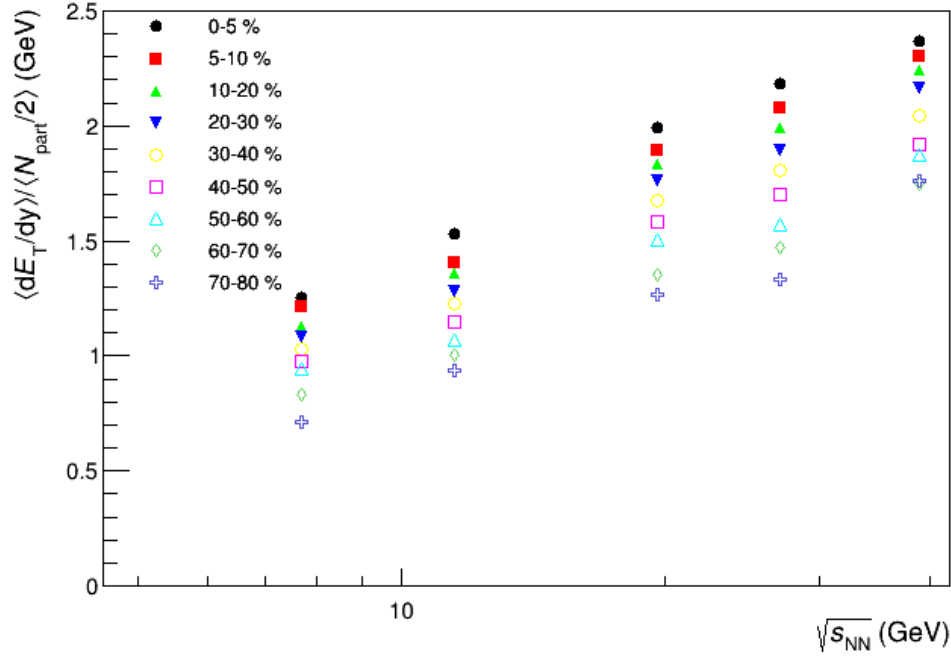


Figure 6.6: $\langle dE_T/dy \rangle / 0.5N_{part}$ at midrapidity as a function of $\sqrt{s_{NN}}$ for different centralities.

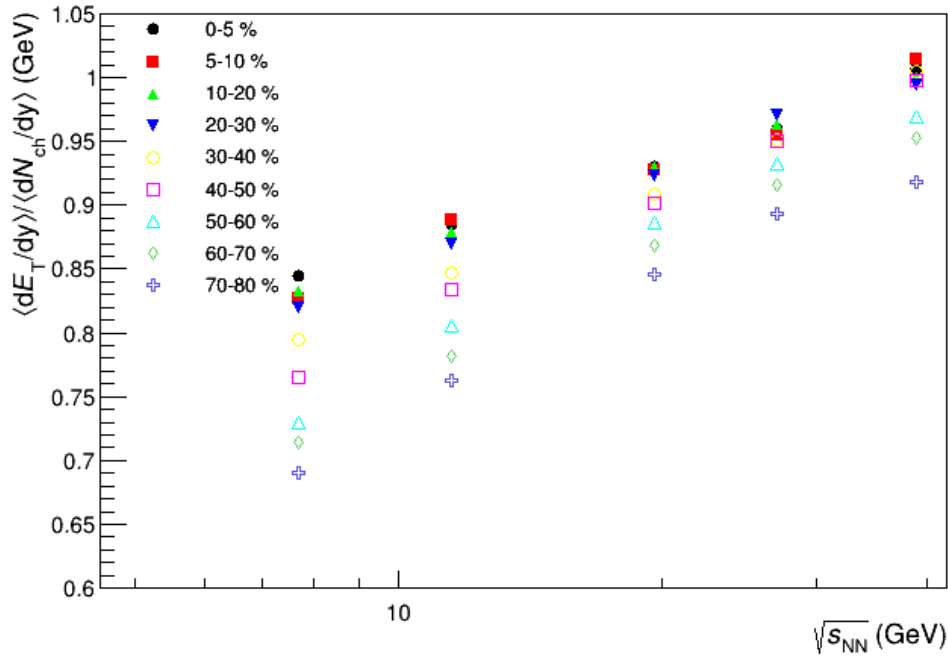


Figure 6.7: $\langle dE_T/dy \rangle / \langle dN_{ch}/dy \rangle$ at midrapidity as a function of $\sqrt{s_{NN}}$ for different centralities.

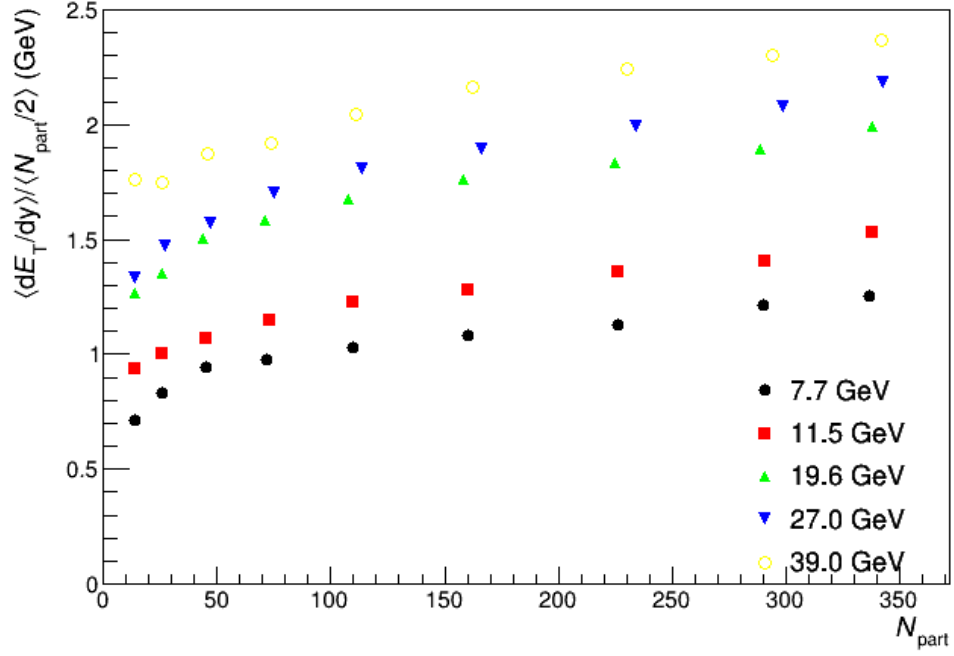


Figure 6.8: $\langle dE_T/dy \rangle / 0.5N_{part}$ at midrapidity as a function of N_{part} for different centralities.

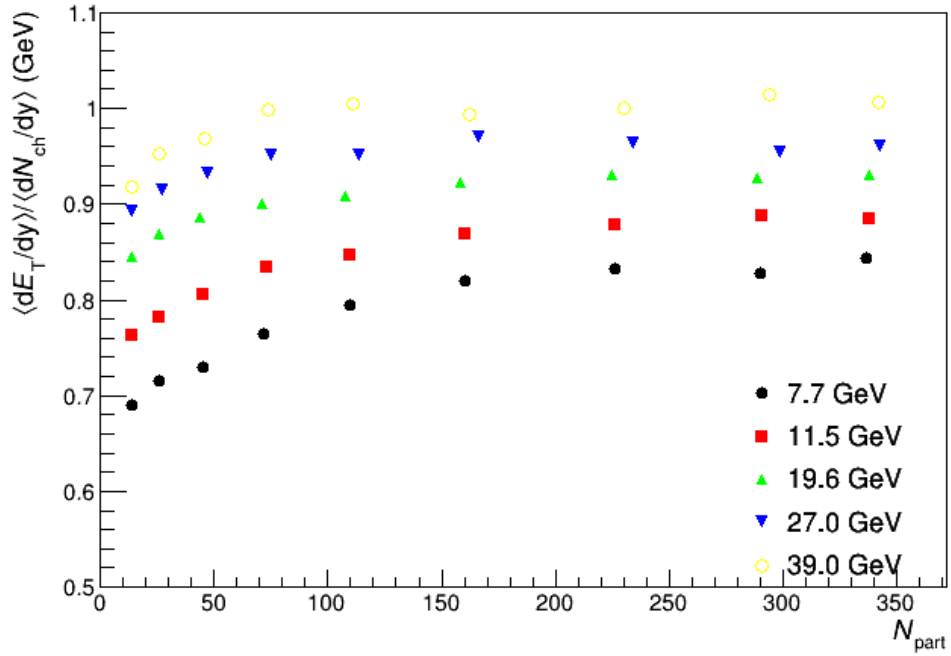


Figure 6.9: $\langle dE_T/dy \rangle / \langle dN_{ch}/dy \rangle$ at midrapidity as a function of N_{part} for different centralities.

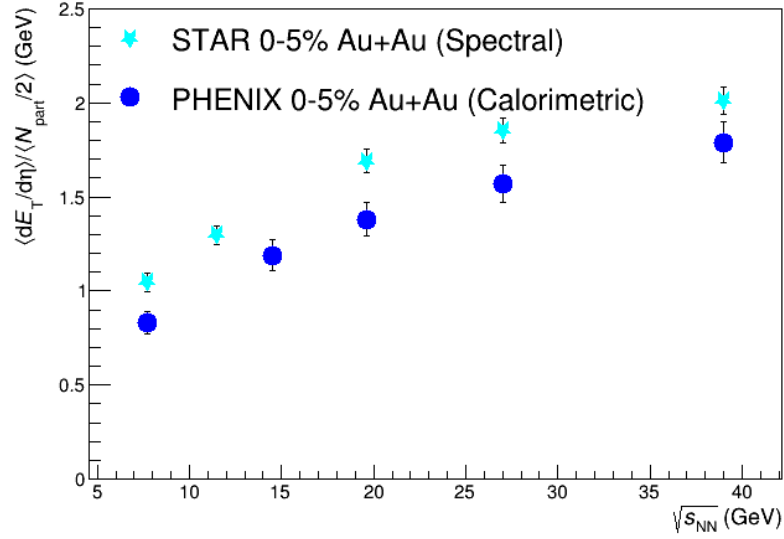


Figure 6.10: $\frac{dE_T}{d\eta} / 0.5N_{part}$ for 0-5% central collisions at midrapidity as a function of $\sqrt{s_{NN}}$. The PHENIX data are from [3]. The error bars represent the total statistical and systematic uncertainties.

629 **Chapter 7**

630 **Conclusion**

631 Summary and implications

Chapter 8

Future Work

8.1 Goodness of Fit

A maximum likelihood? fit method can be adopted to compare the results with those using the chi-squared fits.

8.2 Bjorken Energy Density Estimate

Apart from the transverse energy, the calculation of the initial energy density, ϵ , as given by the Bjorken formula in eq. 3.8, requires the estimate of other physical quantities. Adare et al.[3] use the Glauber model to determine A_T , the area of the intersection of the two nuclei in the transverse plane. Since the results in this thesis are cross-checked with those in [3], it would be reasonable to use the same model in the future work pertaining to this thesis. τ_0 , the proper time at the moment of QGP equilibration, also depends on the model of the collision. However, the product of ϵ and τ_0 is often used instead of just ϵ to study how the energy density scales with the collision energy and the number of participants.

646 **8.3 Asymmetric beams**

647 The codes in the repository can be used to analyze more data. In fact, since there is more
648 data available on collisions of asymmetric systems such as d+Au?, we can expect it to be a
649 test to tell if the assumptions? used in this analysis scale to such domains?

Bibliography

651 [1] Adam, J., Adamova, D., Aggarwal, M. M., Aglieri Rinella, G., Agnello, M., Agrawal,
 652 N., Ahammed, Z., Ahmad, S., Ahn, S. U., Aiola, S., Akindinov, A., Alam, S. N., Silva
 653 De Albuquerque, D., Aleksandrov, D., Alessandro, B., Alexandre, D., Alfaro Molina,
 654 J. R., Alici, A., Alkin, A., Millan Almaraz, J. R., Alme, J., Alt, T., Altinpinar, S.,
 655 Altsybeev, I., Alves Garcia Prado, C., Andrei, C., Andronic, A., Anguelov, V., Anticic,
 656 T., Antinori, F., Antonioli, P., Aphecetche, L. B., Appelshaeuser, H., Arcelli, S., Arnaldi,
 657 R., Arnold, O. W., Arsene, I. C., Arslandok, M., Audurier, B., Augustinus, A., Averbek,
 658 R. P., Azmi, M. D., Badala, A., Baek, Y. W., Bagnasco, S., Bailhache, R. M., Bala,
 659 R., Balasubramanian, S., Baldisseri, A., Baral, R. C., Barbano, A. M., Barbera, R.,
 660 Barile, F., Barnafoldi, G. G., Barnby, L. S., Ramillien Barret, V., Bartalini, P., Barth,
 661 K., Bartke, J. G., Bartsch, E., Basile, M., Bastid, N., Basu, S., Bathen, B., Batigne,
 662 G., Batista Camejo, A., Batyunya, B., Batzing, P. C., Bearden, I. G., Beck, H., Bedda,
 663 C., Behera, N. K., Belikov, I., Bellini, F., Bello Martinez, H., Bellwied, R., Belmont Iii,
 664 R. J., Belmont Moreno, E., Belyaev, V., Bencedi, G., Beole, S., Berceanu, I., Bercuci, A.,
 665 Berdnikov, Y., Berenyi, D., Bertens, R. A., Berzano, D., Betev, L., Bhasin, A., Bhat, I. R.,
 666 Bhati, A. K., Bhattacharjee, B., Bhom, J., Bianchi, L., Bianchi, N., Bianchin, C., Bielcik,
 667 J., Bielcikova, J., Bilandzic, A., Biro, G., Biswas, R., Biswas, S., Bjelogrljic, S., Blair, J. T.,
 668 Blau, D., Blume, C., Bock, F., Bogdanov, A., Boggild, H., Boldizar, L., Bombara, M.,
 669 Book, J. H., Borel, H., Borissov, A., Borri, M., Bossu, F., Botta, E., Bourjau, C., Braun-
 670 Munzinger, P., Bregant, M., Breitner, T. G., Broker, T. A., Browning, T. A., Broz, M.,
 671 Brucken, E. J., Bruna, E., Bruno, G. E., Budnikov, D., Buesching, H., Bufalino, S., Buncic,
 672 P., Busch, O., Buthelezi, E. Z., Bashir Butt, J., Buxton, J. T., Cabala, J., Caffarri, D.,
 673 Cai, X., Caines, H. L., Calero Diaz, L., Caliva, A., Calvo Villar, E., Camerini, P., Carena,
 674 F., Carena, W., Carnesecchi, F., Castillo Castellanos, J. E., Castro, A. J., Casula, E.
 675 A. R., Ceballos Sanchez, C., Cepila, J., Cerello, P., Cerkala, J., Chang, B., Chapeland,
 676 S., Chartier, M., Charvet, J.-L. F., Chattopadhyay, S., Chattopadhyay, S., Chauvin, A.,
 677 Chelnokov, V., Cherney, M. G., Cheshkov, C. V., Cheynis, B., Chibante Barroso, V. M.,
 678 Dobrigkeit Chinellato, D., Cho, S., Chochula, P., Choi, K., Chojnacki, M., Choudhury, S.,
 679 Christakoglou, P., Christensen, C. H., Christiansen, P., Chujo, T., Chung, S.-U., Cicalo,
 680 C., Cifarelli, L., Cindolo, F., Cleymans, J. W. A., Colamaria, F. F., Colella, D., Collu, A.,

681 Colocci, M., Conesa Balbastre, G., Conesa Del Valle, Z., Connors, M. E., Contreras Nuno,
 682 J. G., Cormier, T. M., Corrales Morales, Y., Cortes Maldonado, I., Cortese, P., Cosentino,
 683 M. R., Costa, F., Crochet, P., Cruz Albino, R., Cuautle Flores, E., Cunqueiro Mendez,
 684 L., Dahms, T., Dainese, A., Danisch, M. C., Danu, A., Das, D., Das, I., Das, S., Dash,
 685 A. K., Dash, S., De, S., De Caro, A., De Cataldo, G., De Conti, C., De Cuveland, J.,
 686 De Falco, A., De Gruttola, D., De Marco, N., De Pasquale, S., Deisting, A., Deloff,
 687 A., Denes, E. S., Deplano, C., Dhankher, P., Di Bari, D., Di Mauro, A., Di Nezza,
 688 P., Diaz Corchero, M. A., Dietel, T., Dillenseger, P., Divia, R., Djuvsland, O., Dobrin,
 689 A. F., Domenicis Gimenez, D., Donigus, B., Dordic, O., Drozhzhova, T., Dubey, A. K.,
 690 Dubla, A., Ducroux, L., Dupieux, P., Ehlers Iii, R. J., Elia, D., Endress, E., Engel, H.,
 691 Epple, E., Erasmus, B. E., Erdemir, I., Erhardt, F., Espagnon, B., Estienne, M. D.,
 692 Esumi, S., Eum, J., Evans, D., Evdokimov, S., Eyyubova, G., Fabbietti, L., Fabris, D.,
 693 Faivre, J., Fantoni, A., Fasel, M., Feldkamp, L., Feliciello, A., Feofilov, G., Ferencei, J.,
 694 Fernandez Tellez, A., Gonzalez Ferreiro, E., Ferretti, A., Festanti, A., Feuillard, V. J. G.,
 695 Figiel, J., Araujo Silva Figueredo, M., Filchagin, S., Finogeev, D., Fionda, F., Fiore, E. M.,
 696 Fleck, M. G., Floris, M., Foertsch, S. V., Foka, P., Fokin, S., Fragiacomio, E., Francescon,
 697 A., Frankenfeld, U. M., Fronze, G. G., Fuchs, U., Furget, C., Furs, A., Fusco Girard, M.,
 698 Gaardhoeje, J. J., Gagliardi, M., Gago Medina, A. M., Gallio, M., Gangadharan, D. R.,
 699 Ganoti, P., Gao, C., Garabatos Cuadrado, J., Garcia-Solis, E. J., Gargiulo, C., Gasik, P. J.,
 700 Gauger, E. F., Germain, M., Gheata, M., Ghosh, P., Ghosh, S. K., Gianotti, P., Giubellino,
 701 P., Giubilato, P., Gladysz-Dziadus, E., Glassel, P., Gomez Coral, D. M., Gomez Ramirez,
 702 A., Sanchez Gonzalez, A., Gonzalez, V., Gonzalez Zamora, P., Gorbunov, S., Gorlich,
 703 L. M., Gotovac, S., Grabski, V., Grachov, O. A., Graczykowski, L. K., Graham, K. L.,
 704 Grelli, A., Grigoras, A. G., Grigoras, C., Grigoryev, V., Grigoryan, A., Grigoryan, S.,
 705 Grynyov, B., Grion, N., Gronefeld, J. M., Grosse-Oetringhaus, J. F., Grosso, R., Guber,
 706 F., Guernane, R., Guerzoni, B., Gulbrandsen, K. H., Gunji, T., Gupta, A., Gupta, R.,
 707 Haake, R., Haaland, O. S., Hadjidakis, C. M., Haiduc, M., Hamagaki, H., Hamar, G.,
 708 Hamon, J. C., Harris, J. W., Harton, A. V., Hatzifotiadou, D., Hayashi, S., Heckel, S. T.,
 709 Hellbar, E., Helstrup, H., Herghelegiu, A. I., Herrera Corral, G. A., Hess, B. A., Hetland,
 710 K. F., Hillemanns, H., Hippolyte, B., Horak, D., Hosokawa, R., Hristov, P. Z., Humanic,

711 T., Hussain, N., Hussain, T., Hutter, D., Hwang, D. S., Ilkaev, R., Inaba, M., Incani,
 712 E., Ippolitov, M., Irfan, M., Ivanov, M., Ivanov, V., Izucheev, V., Jacazio, N., Jacobs,
 713 P. M., Jadhav, M. B., Jadlovská, S., Jadlovsky, J., Jahnke, C., Jakubowska, M. J., Jang,
 714 H. J., Janik, M. A., Pahula Hewage, S., Jena, C., Jena, S., Jimenez Bustamante, R. T.,
 715 Jones, P. G., Jusko, A., Kalinak, P., Kalweit, A. P., Kamin, J. A., Kang, J. H., Kaplin,
 716 V., Kar, S., Karasu Uysal, A., Karavichev, O., Karavicheva, T., Karayan, L., Karpechev,
 717 E., Kebschull, U. W., Keidel, R., Keijndener, D. L., Keil, M., Khan, M. M., Khan, P.,
 718 Khan, S. A., Khanzadeev, A., Kharlov, Y., Kileng, B., Kim, D. W., Kim, D. J., Kim,
 719 D., Kim, H., Kim, J., Kim, M., Kim, S. Y., Kim, T., Kirsch, S., Kisel, I., Kiselev,
 720 S., Kisiel, A. R., Kiss, G., Klay, J. L., Klein, C., Klein, J., Klein-Boesing, C., Klewin,
 721 S., Kluge, A., Knichel, M. L., Knospe, A. G., Kobdaj, C., Kofarago, M., Kollegger, T.,
 722 Kolozhvari, A., Kondratev, V., Kondratyeva, N., Kondratyuk, E., Konevskikh, A., Kopcik,
 723 M., Kostarakis, P., Kour, M., Kouzinopoulos, C., Kovalenko, O., Kovalenko, V., Kowalski,
 724 M., Koyithatta Meethalevedu, G., Kralik, I., Kravcakova, A., Krivda, M., Krizek, F.,
 725 Kryshen, E., Krzewicki, M., Kubera, A. M., Kucera, V., Kuhn, C. C., Kuijer, P. G.,
 726 Kumar, A., Kumar, J., Kumar, L., Kumar, S., Kurashvili, P., Kurepin, A., Kurepin, A.,
 727 Kuryakin, A., Kweon, M. J., Kwon, Y., La Pointe, S. L., La Rocca, P., Ladron De Guevara,
 728 P., Lagana Fernandes, C., Lakomov, I., Langoy, R., Lapidus, K., Lara Martinez, C. E.,
 729 Lardeux, A. X., Lattuca, A., Laudi, E., Lea, R., Leardini, L., Lee, G. R., Lee, S., Lehas, F.,
 730 Lemmon, R. C., Lenti, V., Leogrande, E., Leon Monzon, I., Leon Vargas, H., Leoncino, M.,
 731 Levai, P., Li, S., Li, X., Lien, J. A., Lietava, R., Lindal, S., Lindenstruth, V., Lippmann,
 732 C., Lisa, M. A., Ljunggren, H. M., Lodato, D. F., Lonne, P.-I., Loginov, V., Loizides, C.,
 733 Lopez, X. B., Lopez Torres, E., Lowe, A. J., Luettig, P. J., Lunardon, M., Luparello,
 734 G., Lutz, T. H., Maevskaya, A., Mager, M., Mahajan, S., Mahmood, S. M., Maire,
 735 A., Majka, R. D., Malaev, M., Maldonado Cervantes, I. A., Malinina, L., Mal'Kevich,
 736 D., Malzacher, P., Mamonov, A., Manko, V., Manso, F., Manzari, V., Marchisone, M.,
 737 Mares, J., Margagliotti, G. V., Margotti, A., Margutti, J., Marin, A. M., Markert, C.,
 738 Marquard, M., Martin, N. A., Martin Blanco, J., Martinengo, P., Martinez Hernandez,
 739 M. I., Martinez-Garcia, G., Martinez Pedreira, M., Mas, A. J.-M., Masciocchi, S., Masera,
 740 M., Masoni, A., Mastroserio, A., Matyja, A. T., Mayer, C., Mazer, J. A., Mazzoni,

741 A. M., Mcdonald, D., Meddi, F., Melikyan, Y., Menchaca-Rocha, A. A., Meninno, E.,
 742 Mercado-Perez, J., Meres, M., Miake, Y., Mieskolainen, M. M., Mikhaylov, K., Milano,
 743 L., Milosevic, J., Mischke, A., Mishra, A. N., Miskowiec, D. C., Mitra, J., Mitu, C. M.,
 744 Mohammadi, N., Mohanty, B., Molnar, L., Montano Zetina, L. M., Montes Prado, E.,
 745 Moreira De Godoy, D. A., Perez Moreno, L. A., Moretto, S., Morreale, A., Morsch, A.,
 746 Muccifora, V., Mudnic, E., Muhlheim, D. M., Muhuri, S., Mukherjee, M., Mulligan, J. D.,
 747 Gameiro Munhoz, M., Munzer, R. H., Murakami, H., Murray, S., Musa, L., Musinsky,
 748 J., Naik, B., Nair, R., Nandi, B. K., Nania, R., Nappi, E., Naru, M. U., Ferreira Natal
 749 Da Luz, P. H., Nattrass, C., Rosado Navarro, S., Nayak, K., Nayak, R., Nayak, T. K.,
 750 Nazarenko, S., Nedosekin, A., Nellen, L., Ng, F., Nicassio, M., Niculescu, M., Niedziela,
 751 J., Nielsen, B. S., Nikolaev, S., Nikulin, S., Nikulin, V., Noferini, F., Nomokonov, P.,
 752 Nooren, G., Cabanillas Noris, J. C., Norman, J., Nyanin, A., Nystrand, J. I., Oeschler,
 753 H. O., Oh, S., Oh, S. K., Ohlson, A. E., Okatan, A., Okubo, T., Olah, L., Oleniacz,
 754 J., Oliveira Da Silva, A. C., Oliver, M. H., Onderwaater, J., Oppedisano, C., Orava, R.,
 755 Oravec, M., Ortiz Velasquez, A., Oskarsson, A. N. E., Otwinowski, J. T., Oyama, K.,
 756 Ozdemir, M., Pachmayer, Y. C., Pagano, D., Pagano, P., Paic, G., Pal, S. K., Pan, J.,
 757 Pandey, A. K., Papikyan, V., Pappalardo, G., Pareek, P., Park, W., Parmar, S., Passfeld,
 758 A., Paticchio, V., Patra, R. N., Paul, B., Pei, H., Peitzmann, T., Pereira Da Costa, H.
 759 D. A., Peresunko, D. Y., Perez Lara, C. E., Perez Lezama, E., Peskov, V., Pestov, Y.,
 760 Petracek, V., Petrov, V., Petrovici, M., Petta, C., Piano, S., Pikna, M., Pillot, P., Ozelin
 761 De Lima Pimentel, L., Pinazza, O., Pinsky, L., Piyaathna, D., Ploskon, M. A., Planinic,
 762 M., Pluta, J. M., Pochybova, S., Podesta Lerma, P. L. M., Poghosyan, M., Polishchuk,
 763 B., Poljak, N., Poonsawat, W., Pop, A., Porteboeuf, S. J., Porter, R. J., Pospisil, J.,
 764 Prasad, S. K., Preghenella, R., Prino, F., Pruneau, C. A., Pshenichnov, I., Puccio, M.,
 765 Puddu, G., Pujahari, P. R., Punin, V., Putschke, J. H., Qvigstad, H., Rachevski, A., Raha,
 766 S., Rajput, S., Rak, J., Rakotozafindrabe, A. M., Ramello, L., Rami, F., Raniwala, R.,
 767 Raniwala, S., Rasanen, S. S., Rascanu, B. T., Rathee, D., Read, K. F., Redlich, K., Reed,
 768 R. J., Rehman, A. U., Reichelt, P. S., Reidt, F., Ren, X., Renfordt, R. A. E., Reolon, A. R.,
 769 Reshetin, A., Reygers, K. J., Riabov, V., Ricci, R. A., Richert, T. O. H., Richter, M. R.,
 770 Riedler, P., Riegler, W., Riggi, F., Ristea, C.-L., Rocco, E., Rodriguez Cahuantzi, M.,

771 Rodriguez Manso, A., Roeed, K., Rogochaya, E., Rohr, D. M., Roehrich, D., Ronchetti,
 772 F., Ronflette, L., Rosnet, P., Rossi, A., Roukoutakis, F., Roy, A., Roy, C. S., Roy, P. K.,
 773 Rubio Montero, A. J., Rui, R., Russo, R., Di Ruzza, B., Ryabinkin, E., Ryabov, Y.,
 774 Rybicki, A., Saarinen, S., Sadhu, S., Sadovskiy, S., Safarik, K., Sahlmuller, B., Sahoo, P.,
 775 Sahoo, R., Sahoo, S., Sahu, P. K., Saini, J., Sakai, S., Saleh, M. A., Salzwedel, J. S. N.,
 776 Sambyal, S. S., Samsonov, V., Sandor, L., Sandoval, A., Sano, M., Sarkar, D., Sarkar, N.,
 777 Sarma, P., Scapparone, E., Scarlassara, F., Schiaua, C. C., Schicker, R. M., Schmidt, C. J.,
 778 Schmidt, H. R., Schuchmann, S., Schukraft, J., Schulc, M., Schutz, Y. R., Schwarz, K. E.,
 779 Schweda, K. O., Scioli, G., Scomparin, E., Scott, R. M., Sefcik, M., Seger, J. E., Sekiguchi,
 780 Y., Sekihata, D., Selyuzhenkov, I., Senosi, K., Senyukov, S., Serradilla Rodriguez, E.,
 781 Sevcenco, A., Shabanov, A., Shabetai, A., Shadura, O., Shahoyan, R., Shahzad, M. I.,
 782 Shangaraev, A., Sharma, A., Sharma, M., Sharma, M., Sharma, N., Sheikh, A. I., Shigaki,
 783 K., Shou, Q., Shtejer Diaz, K., Sibiryak, Y., Siddhanta, S., Sielewicz, K. M., Siemiarczuk,
 784 T., Silvermyr, D. O. R., Silvestre, C. M., Simatovic, G., Simonetti, G., Singaraju, R. N.,
 785 Singh, R., Singha, S., Singhal, V., Sinha, B., Sarkar Sinha, T., Sitar, B., Sitta, M., Skaali,
 786 B., Slupecki, M., Smirnov, N., Snellings, R., Snellman, T. W., Song, J., Song, M., Song,
 787 Z., Soramel, F., Sorensen, S. P., Derradi De Souza, R., Sozzi, F., Spacek, M., Spiriti, E.,
 788 Sputowska, I. A., Spyropoulou-Stassinaki, M., Stachel, J., Stan, I., Stankus, P., Stenlund,
 789 E. A., Steyn, G. F., Stiller, J. H., Stocco, D., Strmen, P., Alarcon Do Passo Suaide, A.,
 790 Sugitate, T., Suire, C. P., Suleymanov, M. K. O., Suljic, M., Sultanov, R., Sumbera,
 791 M., Sumowidagdo, S., Szabo, A., Szanto De Toledo, A., Szarka, I., Szczepankiewicz, A.,
 792 Szymanski, M. P., Tabassam, U., Takahashi, J., Tambave, G. J., Tanaka, N., Tarhini,
 793 M., Tariq, M., Tarzila, M.-G., Tauro, A., Tejeda Munoz, G., Telesca, A., Terasaki, K.,
 794 Terrevoli, C., Teyssier, B., Thaeder, J. M., Thakur, D., Thomas, D., Tieulent, R. N.,
 795 Tikhonov, A., Timmins, A. R., Toia, A., Trogolo, S., Trombetta, G., Trubnikov, V.,
 796 Trzaska, W. H., Tsuji, T., Tumkin, A., Turrisi, R., Tveter, T. S., Ullaland, K., Uras, A.,
 797 Usai, G., Utrobicic, A., Vala, M., Valencia Palomo, L., Vallero, S., Van Der Maarel, J.,
 798 Van Hoorne, J. W., Van Leeuwen, M., Vanat, T., Vande Vyvre, P., Varga, D., Diozcora
 799 Vargas Trevino, A., Vargyas, M., Varma, R., Vasileiou, M., Vasiliev, A., Vauthier, A.,
 800 Vazquez Doce, O., Vechernin, V., Veen, A. M., Veldhoen, M., Velure, A., Vercellin, E.,

Vergara Limon, S., Vernet, R., Verweij, M., Vickovic, L., Viinikainen, J. S., Vilakazi, Z.,
Villalobos Baillie, O., Villatoro Tello, A., Vinogradov, A., Vinogradov, L., Vinogradov,
Y., Virgili, T., Vislavicius, V., Viyogi, Y., Vodopyanov, A., Volkl, M. A., Voloshin, K.,
Voloshin, S., Volpe, G., Von Haller, B., Vorobyev, I., Vranic, D., Vrlakova, J., Vulpescu,
B., Wagner, B., Wagner, J., Wang, H., Wang, M., Watanabe, D., Watanabe, Y., Weber,
M., Weber, S. G., Weiser, D. F., Wessels, J. P., Westerhoff, U., Whitehead, A. M.,
Wiechula, J., Wikne, J., Wilk, G. A., Wilkinson, J. J., Williams, C., Windelband, B. S.,
Winn, M. A., Yang, P., Yano, S., Yasin, Z., Yin, Z., Yokoyama, H., Yoo, I.-K., Yoon,
J. H., Yurchenko, V., Yushmanov, I., Zaborowska, A., Zaccolo, V., Zaman, A., Zampolli,
C., Correia Zanolini, H. J., Zaporozhets, S., Zardoshti, N., Zarochentsev, A., Zavada, P.,
Zavalyov, N., Zbroszczyk, H. P., Zgura, S. I., Zhalov, M., Zhang, H., Zhang, X., Zhang,
Y., Chunhui, Z., Zhang, Z., Zhao, C., Zhigareva, N., Zhou, D., Zhou, Y., Zhou, Z.,
Zhu, H., Zhu, J., Zichichi, A., Zimmermann, A., Zimmermann, M. B., Zinovjev, G., and
Zyzak, M. (2016). Measurement of transverse energy at midrapidity in Pb-Pb collisions at
 $\sqrt{s_{NN}} = 2.76$ TeV. *Phys. Rev. C*, 94(CERN-EP-2016-071. CERN-EP-2016-071):034903.
30 p. 30 pages, 14 captioned figures, 2 tables, authors from page 25, published version,
figures at <http://aliceinfo.cern.ch/ArtSubmission/node/2400>. 6, 15

[2] Adamczyk, L., Adkins, J. K., Agakishiev, G., Aggarwal, M. M., Ahammed, Z., Ajitanand,
N. N., Alekseev, I., Anderson, D. M., Aoyama, R., Aparin, A., Arkhipkin, D., Aschenauer,
E. C., Ashraf, M. U., Attri, A., Averichev, G. S., Bai, X., Bairathi, V., Behera, A.,
Bellwied, R., Bhasin, A., Bhati, A. K., Bhattarai, P., Bielcik, J., Bielcikova, J., Bland,
L. C., Bordyuzhin, I. G., Bouchet, J., Brandenburg, J. D., Brandin, A. V., Brown, D.,
Bunzarov, I., Butterworth, J., Caines, H., Calderón de la Barca Sánchez, M., Campbell,
J. M., Cebra, D., Chakaberia, I., Chaloupka, P., Chang, Z., Chankova-Bunzarova, N.,
Chatterjee, A., Chattopadhyay, S., Chen, X., Chen, J. H., Chen, X., Cheng, J., Cherney,
M., Christie, W., Contin, G., Crawford, H. J., Das, S., De Silva, L. C., Debbe, R. R.,
Dedovich, T. G., Deng, J., Derevschikov, A. A., Didenko, L., Dilks, C., Dong, X.,
Drachenberg, J. L., Draper, J. E., Dunkelberger, L. E., Dunlop, J. C., Efimov, L. G.,
Elsley, N., Engelage, J., Eppley, G., Esha, R., Esumi, S., Evdokimov, O., Ewigleben,

830 J., Eyser, O., Fatemi, R., Fazio, S., Federic, P., Federicova, P., Fedorisin, J., Feng, Z.,
 831 Filip, P., Finch, E., Fisyak, Y., Flores, C. E., Fulek, L., Gagliardi, C. A., Garand, D.,
 832 Geurts, F., Gibson, A., Girard, M., Grosnick, D., Gunarathne, D. S., Guo, Y., Gupta, A.,
 833 Gupta, S., Guryn, W., Hamad, A. I., Hamed, A., Harlenderova, A., Harris, J. W., He, L.,
 834 Heppelmann, S., Heppelmann, S., Hirsch, A., Hoffmann, G. W., Horvat, S., Huang, T.,
 835 Huang, B., Huang, X., Huang, H. Z., Humanic, T. J., Huo, P., Igo, G., Jacobs, W. W.,
 836 Jentsch, A., Jia, J., Jiang, K., Jowzaee, S., Judd, E. G., Kabana, S., Kalinkin, D., Kang,
 837 K., Kauder, K., Ke, H. W., Keane, D., Kechechyan, A., Khan, Z., Kikoła, D. P., Kisel,
 838 I., Kisiel, A., Kochenda, L., Kocmanek, M., Kollegger, T., Kosarzewski, L. K., Kraishan,
 839 A. F., Kravtsov, P., Krueger, K., Kulathunga, N., Kumar, L., Kvapil, J., Kwasizur, J. H.,
 840 Lacey, R., Landgraf, J. M., Landry, K. D., Lauret, J., Lebedev, A., Lednický, R., Lee,
 841 J. H., Li, X., Li, C., Li, W., Li, Y., Lidrych, J., Lin, T., Lisa, M. A., Liu, H., Liu,
 842 P., Liu, Y., Liu, F., Ljubicic, T., Llope, W. J., Lomnitz, M., Longacre, R. S., Luo, S.,
 843 Luo, X., Ma, G. L., Ma, L., Ma, Y. G., Ma, R., Magdy, N., Majka, R., Mallick, D.,
 844 Margetis, S., Markert, C., Matis, H. S., Meehan, K., Mei, J. C., Miller, Z. W., Minaev,
 845 N. G., Mioduszewski, S., Mishra, D., Mizuno, S., Mohanty, B., Mondal, M. M., Morozov,
 846 D. A., Mustafa, M. K., Nasim, M., Nayak, T. K., Nelson, J. M., Nie, M., Nigmatkulov,
 847 G., Niida, T., Nogach, L. V., Nonaka, T., Nurushev, S. B., Odyniec, G., Ogawa, A.,
 848 Oh, K., Okorokov, V. A., Olvitt, D., Page, B. S., Pak, R., Pandit, Y., Panebratsev, Y.,
 849 Pawlik, B., Pei, H., Perkins, C., Pile, P., Pluta, J., Poniatowska, K., Porter, J., Posik,
 850 M., Poskanzer, A. M., Pruthi, N. K., Przybycien, M., Putschke, J., Qiu, H., Quintero, A.,
 851 Ramachandran, S., Ray, R. L., Reed, R., Rehbein, M. J., Ritter, H. G., Roberts, J. B.,
 852 Rogachevskiy, O. V., Romero, J. L., Roth, J. D., Ruan, L., Rusnak, J., Rusnakova, O.,
 853 Sahoo, N. R., Sahu, P. K., Salur, S., Sandweiss, J., Saur, M., Schambach, J., Schmäh,
 854 A. M., Schmidke, W. B., Schmitz, N., Schweid, B. R., Seger, J., Sergeeva, M., Seyboth, P.,
 855 Shah, N., Shahaliev, E., Shanmuganathan, P. V., Shao, M., Sharma, A., Sharma, M. K.,
 856 Shen, W. Q., Shi, Z., Shi, S. S., Shou, Q. Y., Sichtermann, E. P., Sikora, R., Simko,
 857 M., Singha, S., Skoby, M. J., Smirnov, N., Smirnov, D., Solyst, W., Song, L., Sorensen,
 858 P., Spinka, H. M., Srivastava, B., Stanislaus, T. D. S., Strikhanov, M., Stringfellow, B.,
 859 Sugiura, T., Sumbera, M., Summa, B., Sun, Y., Sun, X. M., Sun, X., Surrow, B., Svirida,

D. N., Tang, A. H., Tang, Z., Taranenko, A., Tarnowsky, T., Tawfik, A., Thäder, J., Thomas, J. H., Timmins, A. R., Tlusty, D., Todoroki, T., Tokarev, M., Trentalange, S., Tribble, R. E., Tribedy, P., Tripathy, S. K., Trzeciak, B. A., Tsai, O. D., Ullrich, T., Underwood, D. G., Upsal, I., Van Buren, G., van Nieuwenhuizen, G., Vasiliev, A. N., Videbæk, F., Vokal, S., Voloshin, S. A., Vossen, A., Wang, G., Wang, Y., Wang, F., Wang, Y., Webb, J. C., Webb, G., Wen, L., Westfall, G. D., Wieman, H., Wissink, S. W., Witt, R., Wu, Y., Xiao, Z. G., Xie, W., Xie, G., Xu, J., Xu, N., Xu, Q. H., Xu, Y. F., Xu, Z., Yang, Y., Yang, Q., Yang, C., Yang, S., Ye, Z., Ye, Z., Yi, L., Yip, K., Yoo, I.-K., Yu, N., Zbroszczyk, H., Zha, W., Zhang, Z., Zhang, X. P., Zhang, J. B., Zhang, S., Zhang, J., Zhang, Y., Zhang, J., Zhang, S., Zhao, J., Zhong, C., Zhou, L., Zhou, C., Zhu, X., Zhu, Z., and Zyzak, M. (2017). Bulk properties of the medium produced in relativistic heavy-ion collisions from the beam energy scan program. *Phys. Rev. C*, 96:044904. viii, 24, 28, 29

[3] Adare, A., Afanasiev, S., Aidala, C., Ajitanand, N. N., Akiba, Y., Akimoto, R., Al-Bataineh, H., Alexander, J., Alfred, M., Al-Jamel, A., Al-Ta'ani, H., Angerami, A., Aoki, K., Apadula, N., Aphecetche, L., Aramaki, Y., Armendariz, R., Aronson, S. H., Asai, J., Asano, H., Aschenauer, E. C., Atomssa, E. T., Auerbeck, R., Awes, T. C., Azmoun, B., Babintsev, V., Bai, M., Bai, X., Baksay, G., Baksay, L., Baldisseri, A., Bandara, N. S., Bannier, B., Barish, K. N., Barnes, P. D., Bassalleck, B., Basye, A. T., Bathe, S., Batsouli, S., Baublis, V., Bauer, F., Baumann, C., Baumgart, S., Bazilevsky, A., Beaumier, M., Beckman, S., Belikov, S., Belmont, R., Bennett, R., Berdnikov, A., Berdnikov, Y., Bhom, J. H., Bickley, A. A., Bjorndal, M. T., Black, D., Blau, D. S., Boissevain, J. G., Bok, J. S., Borel, H., Boyle, K., Brooks, M. L., Brown, D. S., Bryslawskyj, J., Bucher, D., Buesching, H., Bumazhnov, V., Bunce, G., Burward-Hoy, J. M., Butsyk, S., Campbell, S., Caringi, A., Castera, P., Chai, J.-S., Chang, B. S., Charvet, J.-L., Chen, C.-H., Chernichenko, S., Chi, C. Y., Chiba, J., Chiu, M., Choi, I. J., Choi, J. B., Choi, S., Choudhury, R. K., Christiansen, P., Chujo, T., Chung, P., Churn, A., Chvala, O., Cianciolo, V., Citron, Z., Cleven, C. R., Cobigo, Y., Cole, B. A., Comets, M. P., Conesa del Valle, Z., Connors, M., Constantin, P., Cronin, N., Crossette, N., Csanád, M., Csörgő, T., Dahms,

889 T., Dairaku, S., Danchev, I., Danley, T. W., Das, K., Datta, A., Daugherty, M. S.,
 890 David, G., Dayananda, M. K., Deaton, M. B., DeBlasio, K., Dehmelt, K., Delagrange,
 891 H., Denisov, A., d'Enterria, D., Deshpande, A., Desmond, E. J., Dharmawardane, K. V.,
 892 Dietzsch, O., Ding, L., Dion, A., Diss, P. B., Do, J. H., Donadelli, M., D'Orazio, L.,
 893 Drachenberg, J. L., Drapier, O., Drees, A., Drees, K. A., Dubey, A. K., Durham, J. M.,
 894 Durum, A., Dutta, D., Dzhordzhadze, V., Edwards, S., Efremenko, Y. V., Egdemir, J.,
 895 Ellinghaus, F., Emam, W. S., Engelmores, T., Enokizono, A., En'yo, H., Espagnon, B.,
 896 Esumi, S., Eyser, K. O., Fadem, B., Feege, N., Fields, D. E., Finger, M., Finger, M.,
 897 Fleuret, F., Fokin, S. L., Forestier, B., Fraenkel, Z., Frantz, J. E., Franz, A., Frawley,
 898 A. D., Fujiwara, K., Fukao, Y., Fung, S.-Y., Fusayasu, T., Gadrat, S., Gainey, K., Gal,
 899 C., Gallus, P., Garg, P., Garishvili, A., Garishvili, I., Gastineau, F., Ge, H., Germain, M.,
 900 Giordano, F., Glenn, A., Gong, H., Gong, X., Gonin, M., Gosset, J., Goto, Y., Granier de
 901 Cassagnac, R., Grau, N., Greene, S. V., Grim, G., Grosse Perdekamp, M., Gu, Y., Gunji,
 902 T., Guo, L., Guragain, H., Gustafsson, H.-A., Hachiya, T., Hadj Henni, A., Haegemann,
 903 C., Haggerty, J. S., Hagiwara, M. N., Hahn, K. I., Hamagaki, H., Hamblen, J., Hamilton,
 904 H. F., Han, R., Han, S. Y., Hanks, J., Harada, H., Hartouni, E. P., Haruna, K., Harvey,
 905 M., Hasegawa, S., Haseler, T. O. S., Hashimoto, K., Haslum, E., Hasuko, K., Hayano, R.,
 906 Hayashi, S., He, X., Heffner, M., Hemmick, T. K., Hester, T., Heuser, J. M., Hiejima, H.,
 907 Hill, J. C., Hobbs, R., Hohlmann, M., Hollis, R. S., Holmes, M., Holzmann, W., Homma,
 908 K., Hong, B., Horaguchi, T., Hori, Y., Hornback, D., Hoshino, T., Hotvedt, N., Huang, J.,
 909 Huang, S., Hur, M. G., Ichihara, T., Ichimiya, R., Iinuma, H., Ikeda, Y., Imai, K., Imazu,
 910 Y., Imrek, J., Inaba, M., Inoue, Y., Iordanova, A., Isenhowe, D., Isenhowe, L., Ishihara,
 911 M., Isinhue, A., Isobe, T., Issah, M., Isupov, A., Ivanishchev, D., Iwanaga, Y., Jacak,
 912 B. V., Javani, M., Jeon, S. J., Jezghani, M., Jia, J., Jiang, X., Jin, J., Jinnouchi, O.,
 913 Johnson, B. M., Jones, T., Joo, K. S., Jouan, D., Jumper, D. S., Kajihara, F., Kametani,
 914 S., Kamihara, N., Kamin, J., Kanda, S., Kaneta, M., Kaneti, S., Kang, B. H., Kang, J. H.,
 915 Kang, J. S., Kanou, H., Kapustinsky, J., Karatsu, K., Kasai, M., Kawagishi, T., Kawall,
 916 D., Kawashima, M., Kazantsev, A. V., Kelly, S., Kempel, T., Key, J. A., Khachatryan, V.,
 917 Khandai, P. K., Khanzadeev, A., Kijima, K. M., Kikuchi, J., Kim, A., Kim, B. I., Kim, C.,
 918 Kim, D. H., Kim, D. J., Kim, E., Kim, E.-J., Kim, G. W., Kim, H. J., Kim, K.-B., Kim,

919 M., Kim, Y.-J., Kim, Y. K., Kim, Y.-S., Kimelman, B., Kinney, E., Kiss, A., Kistenev, E.,
 920 Kitamura, R., Kiyomichi, A., Klatsky, J., Klay, J., Klein-Boeing, C., Kleinjan, D., Kline,
 921 P., Koblesky, T., Kochenda, L., Kochetkov, V., Kofarago, M., Komatsu, Y., Komkov,
 922 B., Konno, M., Koster, J., Kotchetkov, D., Kotov, D., Kozlov, A., Král, A., Kravitz, A.,
 923 Krizek, F., Kroon, P. J., Kubart, J., Kunde, G. J., Kurihara, N., Kurita, K., Kurosawa,
 924 M., Kweon, M. J., Kwon, Y., Kyle, G. S., Lacey, R., Lai, Y. S., Lajoie, J. G., Lebedev,
 925 A., Le Bornec, Y., Leckey, S., Lee, B., Lee, D. M., Lee, G. H., Lee, J., Lee, K. B.,
 926 Lee, K. S., Lee, M. K., Lee, S., Lee, S. H., Lee, S. R., Lee, T., Leitch, M. J., Leite, M.
 927 A. L., Leitgab, M., Lenzi, B., Lewis, B., Li, X., Li, X. H., Lichtenwalner, P., Liebing, P.,
 928 Lim, H., Lim, S. H., Linden Levy, L. A., Liška, T., Litvinenko, A., Liu, H., Liu, M. X.,
 929 Love, B., Lynch, D., Maguire, C. F., Makdisi, Y. I., Makek, M., Malakhov, A., Malik,
 930 M. D., Manion, A., Manko, V. I., Mannel, E., Mao, Y., Maruyama, T., Mašek, L., Masui,
 931 H., Masumoto, S., Matathias, F., McCain, M. C., McCumber, M., McGaughey, P. L.,
 932 McGlinchey, D., McKinney, C., Means, N., Meles, A., Mendoza, M., Meredith, B., Miake,
 933 Y., Mibe, T., Midori, J., Mignerey, A. C., Mikeš, P., Miki, K., Miller, T. E., Milov, A.,
 934 Mioduszewski, S., Mishra, D. K., Mishra, G. C., Mishra, M., Mitchell, J. T., Mitrovski,
 935 M., Miyachi, Y., Miyasaka, S., Mizuno, S., Mohanty, A. K., Mohapatra, S., Montuenga,
 936 P., Moon, H. J., Moon, T., Morino, Y., Morreale, A., Morrison, D. P., Moskowitz, M.,
 937 Moss, J. M., Motschwiller, S., Moukhanova, T. V., Mukhopadhyay, D., Murakami, T.,
 938 Murata, J., Mwai, A., Nagae, T., Nagamiya, S., Nagashima, K., Nagata, Y., Nagle, J. L.,
 939 Naglis, M., Nagy, M. I., Nakagawa, I., Nakagomi, H., Nakamiya, Y., Nakamura, K. R.,
 940 Nakamura, T., Nakano, K., Nam, S., Natrass, C., Nederlof, A., Netrakanti, P. K., Newby,
 941 J., Nguyen, M., Nihashi, M., Niida, T., Nishimura, S., Norman, B. E., Nouicer, R., Novák,
 942 T., Novitzky, N., Nukariya, A., Nyanin, A. S., Nystrand, J., Oakley, C., Obayashi, H.,
 943 O'Brien, E., Oda, S. X., Ogilvie, C. A., Ohnishi, H., Oide, H., Ojha, I. D., Oka, M.,
 944 Okada, K., Omiwade, O. O., Onuki, Y., Orjuela Koop, J. D., Osborn, J. D., Oskarsson,
 945 A., Otterlund, I., Ouchida, M., Ozawa, K., Pak, R., Pal, D., Palounek, A. P. T., Pantuev,
 946 V., Papavassiliou, V., Park, B. H., Park, I. H., Park, J., Park, J. S., Park, S., Park, S. K.,
 947 Park, W. J., Pate, S. F., Patel, L., Patel, M., Pei, H., Peng, J.-C., Pereira, H., Perepelitsa,
 948 D. V., Perera, G. D. N., Peresedov, V., Peressounko, D., Perry, J., Petti, R., Pinkenburg,

949 C., Pinson, R., Pisani, R. P., Proissl, M., Purschke, M. L., Purwar, A. K., Qu, H., Rak,
 950 J., Rakotozafindrabe, A., Ramson, B. J., Ravinovich, I., Read, K. F., Rembeczki, S.,
 951 Reuter, M., Reygers, K., Reynolds, D., Riabov, V., Riabov, Y., Richardson, E., Rinn, T.,
 952 Riveli, N., Roach, D., Roche, G., Rolnick, S. D., Romana, A., Rosati, M., Rosen, C. A.,
 953 Rosendahl, S. S. E., Rosnet, P., Rowan, Z., Rubin, J. G., Rukoyatkin, P., Ružička, P.,
 954 Rykov, V. L., Ryu, M. S., Ryu, S. S., Sahlmueller, B., Saito, N., Sakaguchi, T., Sakai, S.,
 955 Sakashita, K., Sakata, H., Sako, H., Samsonov, V., Sano, M., Sano, S., Sarsour, M., Sato,
 956 H. D., Sato, S., Sato, T., Sawada, S., Schaefer, B., Schmoll, B. K., Sedgwick, K., Seele,
 957 J., Seidl, R., Sekiguchi, Y., Semenov, V., Sen, A., Seto, R., Sett, P., Sexton, A., Sharma,
 958 D., Shaver, A., Shea, T. K., Shein, I., Shevel, A., Shibata, T.-A., Shigaki, K., Shimomura,
 959 M., Shohjoh, T., Shoji, K., Shukla, P., Sickles, A., Silva, C. L., Silvermyr, D., Silvestre,
 960 C., Sim, K. S., Singh, B. K., Singh, C. P., Singh, V., Skolnik, M., Skutnik, S., Slunečka,
 961 M., Smith, W. C., Snowball, M., Solano, S., Soldatov, A., Soltz, R. A., Sondheim, W. E.,
 962 Sorensen, S. P., Sourikova, I. V., Staley, F., Stankus, P. W., Steinberg, P., Stenlund, E.,
 963 Stepanov, M., Ster, A., Stoll, S. P., Stone, M. R., Sugitate, T., Suire, C., Sukhanov, A.,
 964 Sullivan, J. P., Sumita, T., Sun, J., Sziklai, J., Tabaru, T., Takagi, S., Takagui, E. M.,
 965 Takahara, A., Taketani, A., Tanabe, R., Tanaka, K. H., Tanaka, Y., Taneja, S., Tanida, K.,
 966 Tannenbaum, M. J., Tarafdar, S., Taranenko, A., Tarján, P., Tennant, E., Themann, H.,
 967 Thomas, D., Thomas, T. L., Tieulent, R., Timilsina, A., Todoroki, T., Togawa, M., Toia,
 968 A., Tojo, J., Tomášek, L., Tomášek, M., Torii, H., Towell, C. L., Towell, R., Towell, R. S.,
 969 Tram, V.-N., Tserruya, I., Tsuchimoto, Y., Tsuji, T., Tuli, S. K., Tydesjö, H., Tyurin,
 970 N., Vale, C., Valle, H., van Hecke, H. W., Vargyas, M., Vazquez-Zambrano, E., Veicht,
 971 A., Velkovska, J., Vértési, R., Vinogradov, A. A., Virius, M., Voas, B., Vossen, A., Vrba,
 972 V., Vznuzdaev, E., Wagner, M., Walker, D., Wang, X. R., Watanabe, D., Watanabe, K.,
 973 Watanabe, Y., Watanabe, Y. S., Wei, F., Wei, R., Wessels, J., Whitaker, S., White, A. S.,
 974 White, S. N., Willis, N., Winter, D., Wolin, S., Woody, C. L., Wright, R. M., Wysocki, M.,
 975 Xia, B., Xie, W., Xue, L., Yalcin, S., Yamaguchi, Y. L., Yamaura, K., Yang, R., Yanovich,
 976 A., Yasin, Z., Ying, J., Yokkaichi, S., Yoo, J. H., Yoon, I., You, Z., Young, G. R., Younus,
 977 I., Yu, H., Yushmanov, I. E., Zajc, W. A., Zaudtke, O., Zelenski, A., Zhang, C., Zhou, S.,

Zimanyi, J., Zolin, L., and Zou, L. (2016). Transverse energy production and charged-particle multiplicity at midrapidity in various systems from $\sqrt{s_{NN}} = 7.7$ to 200 gev. *Phys. Rev. C*, 93:024901. ix, 5, 23, 38, 40

[4] Adare, A., Afanasiev, S., Aidala, C., Ajitanand, N. N., Akiba, Y., Al-Bataineh, H., Alexander, J., Al-Jamel, A., Aoki, K., Aphecetche, L., and et al. (2007). Scaling Properties of Azimuthal Anisotropy in Au+Au and Cu+Cu Collisions at $s_{NN}=200\text{GeV}$. *Physical Review Letters*, 98(16):162301. vii, 16, 17, 18

[5] Adler, S. S., Afanasiev, S., Aidala, C., Ajitanand, N. N., Akiba, Y., Al-Jamel, A., Alexander, J., Aoki, K., Aphecetche, L., Armendariz, R., Aronson, S. H., Auerbeck, R., Awes, T. C., Azmoun, B., Babintsev, V., Baldisseri, A., Barish, K. N., Barnes, P. D., Bassalleck, B., Bathe, S., Batsouli, S., Baublis, V., Bauer, F., Bazilevsky, A., Belikov, S., Bennett, R., Berdnikov, Y., Bjorndal, M. T., Boissevain, J. G., Borel, H., Boyle, K., Brooks, M. L., Brown, D. S., Bruner, N., Bucher, D., Buesching, H., Bumazhnov, V., Bunce, G., Burward-Hoy, J. M., Butsyk, S., Camard, X., Campbell, S., Chai, J.-S., Chand, P., Chang, W. C., Chernichenko, S., Chi, C. Y., Chiba, J., Chiu, M., Choi, I. J., Choudhury, R. K., Chujo, T., Cianciolo, V., Cleven, C. R., Cobigo, Y., Cole, B. A., Comets, M. P., Constantin, P., Csanád, M., Csörgő, T., Cussonneau, J. P., Dahms, T., Das, K., David, G., Deák, F., Delagrange, H., Denisov, A., d'Enterria, D., Deshpande, A., Desmond, E. J., Devismes, A., Dietzsch, O., Dion, A., Drachenberg, J. L., Drapier, O., Drees, A., Dubey, A. K., Durum, A., Dutta, D., Dzhordzhadze, V., Efremenko, Y. V., Egdemir, J., Enokizono, A., En'yo, H., Espagnon, B., Esumi, S., Fields, D. E., Finck, C., Fleuret, F., Fokin, S. L., Forestier, B., Fox, B. D., Fraenkel, Z., Frantz, J. E., Franz, A., Frawley, A. D., Fukao, Y., Fung, S.-Y., Gadrat, S., Gastineau, F., Germain, M., Glenn, A., Gonin, M., Gosset, J., Goto, Y., Granier de Cassagnac, R., Grau, N., Greene, S. V., Grosse Perdekamp, M., Gunji, T., Gustafsson, H.-A., Hachiya, T., Hadj Henni, A., Haggerty, J. S., Hagiwara, M. N., Hamagaki, H., Hansen, A. G., Harada, H., Hartouni, E. P., Haruna, K., Harvey, M., Haslum, E., Hasuko, K., Hayano, R., He, X., Heffner, M., Hemmick, T. K., Heuser, J. M., Hidas, P., Hiejima, H., Hill, J. C., Hobbs, R., Holmes, M., Holzmann, W., Homma, K., Hong, B., Hoover, A., Horaguchi, T., Hur, M. G., Ichihara, T.,

1007 Iinuma, H., Ikonnikov, V. V., Imai, K., Inaba, M., Inuzuka, M., Isenhowe, D., Isenhowe,
 1008 L., Ishihara, M., Isobe, T., Issah, M., Isupov, A., Jacak, B. V., Jia, J., Jin, J., Jinnouchi,
 1009 O., Johnson, B. M., Johnson, S. C., Joo, K. S., Jouan, D., Kajihara, F., Kametani,
 1010 S., Kamihara, N., Kaneta, M., Kang, J. H., Katou, K., Kawabata, T., Kawagishi, T.,
 1011 Kazantsev, A. V., Kelly, S., Khachaturov, B., Khanzadeev, A., Kikuchi, J., Kim, D. J.,
 1012 Kim, E., Kim, E. J., Kim, G.-B., Kim, H. J., Kim, Y.-S., Kinney, E., Kiss, A., Kistenev, E.,
 1013 Kiyomichi, A., Klein-Boesing, C., Kobayashi, H., Kochenda, L., Kochetkov, V., Kohara,
 1014 R., Komkov, B., Konno, M., Kotchetkov, D., Kozlov, A., Kroon, P. J., Kuberg, C. H.,
 1015 Kunde, G. J., Kurihara, N., Kurita, K., Kweon, M. J., Kwon, Y., Kyle, G. S., Lacey, R.,
 1016 Lajoie, J. G., Lebedev, A., Le Bornec, Y., Leckey, S., Lee, D. M., Lee, M. K., Leitch,
 1017 M. J., Leite, M. A. L., Li, X. H., Lim, H., Litvinenko, A., Liu, M. X., Maguire, C. F.,
 1018 Makdisi, Y. I., Malakhov, A., Malik, M. D., Manko, V. I., Mao, Y., Martinez, G., Masui,
 1019 H., Matathias, F., Matsumoto, T., McCain, M. C., McGaughey, P. L., Miake, Y., Miller,
 1020 T. E., Milov, A., Mioduszewski, S., Mishra, G. C., Mitchell, J. T., Mohanty, A. K.,
 1021 Morrison, D. P., Moss, J. M., Moukhanova, T. V., Mukhopadhyay, D., Muniruzzaman,
 1022 M., Murata, J., Nagamiya, S., Nagata, Y., Nagle, J. L., Naglis, M., Nakamura, T., Newby,
 1023 J., Nguyen, M., Norman, B. E., Nyanin, A. S., Nystrand, J., O'Brien, E., Ogilvie, C. A.,
 1024 Ohnishi, H., Ojha, I. D., Okada, K., Omiwade, O. O., Oskarsson, A., Otterlund, I., Oyama,
 1025 K., Ozawa, K., Pal, D., Palounek, A. P. T., Pantuev, V., Papavassiliou, V., Park, J., Park,
 1026 W. J., Pate, S. F., Pei, H., Penev, V., Peng, J.-C., Pereira, H., Peresedov, V., Peressounko,
 1027 D., Pierson, A., Pinkenburg, C., Pisani, R. P., Purschke, M. L., Purwar, A. K., Qu, H.,
 1028 Qualls, J. M., Rak, J., Ravinovich, I., Read, K. F., Reuter, M., Reygers, K., Riabov,
 1029 V., Riabov, Y., Roche, G., Romana, A., Rosati, M., Rosendahl, S. S. E., Rosnet, P.,
 1030 Rukoyatkin, P., Rykov, V. L., Ryu, S. S., Sahlmueller, B., Saito, N., Sakaguchi, T., Sakai,
 1031 S., Samsonov, V., Sanfratello, L., Santo, R., Sarsour, M., Sato, H. D., Sato, S., Sawada,
 1032 S., Schutz, Y., Semenov, V., Seto, R., Sharma, D., Shea, T. K., Shein, I., Shibata, T.-A.,
 1033 Shigaki, K., Shimomura, M., Shohjoh, T., Shoji, K., Sickles, A., Silva, C. L., Silvermyr, D.,
 1034 Sim, K. S., Singh, C. P., Singh, V., Skutnik, S., Smith, W. C., Soldatov, A., Soltz, R. A.,
 1035 Sondheim, W. E., Sorensen, S. P., Sourikova, I. V., Staley, F., Stankus, P. W., Stenlund,
 1036 E., Stepanov, M., Ster, A., Stoll, S. P., Sugitate, T., Suire, C., Sullivan, J. P., Sziklai, J.,

Tabaru, T., Takagi, S., Takagui, E. M., Taketani, A., Tanaka, K. H., Tanaka, Y., Tanida, K., Tannenbaum, M. J., Taranenko, A., Tarján, P., Thomas, T. L., Togawa, M., Tojo, J., Torii, H., Towell, R. S., Tram, V.-N., Tserruya, I., Tsuchimoto, Y., Tuli, S. K., Tydesjö, H., Tyurin, N., Uam, T. J., Vale, C., Valle, H., van Hecke, H. W., Velkovska, J., Velkovsky, M., Vértesi, R., Veszprémi, V., Vinogradov, A. A., Volkov, M. A., Vznuzdaev, E., Wagner, M., Wang, X. R., Watanabe, Y., Wessels, J., White, S. N., Willis, N., Winter, D., Wohn, F. K., Woody, C. L., Wysocki, M., Xie, W., Yanovich, A., Yokkaichi, S., Young, G. R., Younus, I., Yushmanov, I. E., Zajc, W. A., Zaudtke, O., Zhang, C., Zhou, S., Zimányi, J., Zolin, L., and Zong, X. (2014). Transverse-energy distributions at midrapidity in $p + p$, $d + \text{Au}$, and $\text{Au} + \text{Au}$ collisions at $\sqrt{s_{\text{NN}}} = 62.4 \sim 200$ gev and implications for particle-production models. *Phys. Rev. C*, 89:044905. 22

[6] Adler, S. S., Afanasiev, S., Aidala, C., Ajitanand, N. N., Akiba, Y., Alexander, J., Amirikas, R., Aphecetche, L., Aronson, S. H., Auerbeck, R., Awes, T. C., Azmoun, R., Babintsev, V., Baldissieri, A., Barish, K. N., Barnes, P. D., Bassalleck, B., Bathe, S., Batsouli, S., Baublis, V., Bazilevsky, A., Belikov, S., Berdnikov, Y., Bhagavatula, S., Boissevain, J. G., Borel, H., Borenstein, S., Brooks, M. L., Brown, D. S., Bruner, N., Bucher, D., Buesching, H., Bumazhnov, V., Bunce, G., Burward-Hoy, J. M., Butsyk, S., Camard, X., Chai, J.-S., Chand, P., Chang, W. C., Chernichenko, S., Chi, C. Y., Chiba, J., Chiu, M., Choi, I. J., Choi, J., Choudhury, R. K., Chujo, T., Cianciolo, V., Cobigo, Y., Cole, B. A., Constantin, P., d’Enterria, D. G., David, G., Delagrange, H., Denisov, A., Deshpande, A., Desmond, E. J., Dietzsch, O., Drapier, O., Drees, A., Rietz, R. d., Durum, A., Dutta, D., Efremenko, Y. V., Chenawi, K. E., Enokizono, A., En’yo, H., Esumi, S., Ewell, L., Fields, D. E., Fleuret, F., Fokin, S. L., Fox, B. D., Fraenkel, Z., Frantz, J. E., Franz, A., Frawley, A. D., Fung, S.-Y., Garpman, S., Ghosh, T. K., Glenn, A., Gogiberidze, G., Gonin, M., Gosset, J., Goto, Y., Cassagnac, R. G. d., Grau, N., Greene, S. V., Perdekamp, M. G., Guryn, W., Gustafsson, H.-A., Hachiya, T., Haggerty, J. S., Hamagaki, H., Hansen, A. G., Hartouni, E. P., Harvey, M., Hayano, R., He, X., Heffner, M., Hemmick, T. K., Heuser, J. M., Hibino, M., Hill, J. C., Holzmann, W., Homma, K., Hong, B., Hoover, A., Ichihara, T., Ikonnikov, V. V., Imai, K., Isenhower, D., Ishihara,

1066 M., Issah, M., Isupov, A., Jacak, B. V., Jang, W. Y., Jeong, Y., Jia, J., Jinnouchi, O.,
 1067 Johnson, B. M., Johnson, S. C., Joo, K. S., Jouan, D., Kametani, S., Kamihara, N.,
 1068 Kang, J. H., Kapoor, S. S., Katou, K., Kelly, S., Khachaturov, B., Khanzadeev, A.,
 1069 Kikuchi, J., Kim, D. H., Kim, D. J., Kim, D. W., Kim, E., Kim, G.-B., Kim, H. J.,
 1070 Kistenev, E., Kiyomichi, A., Kiyoyama, K., Klein-Boesing, C., Kobayashi, H., Kochenda,
 1071 L., Kochetkov, V., Koehler, D., Kohama, T., Kopytine, M., Kotchetkov, D., Kozlov, A.,
 1072 Kroon, P. J., Kuberg, C. H., Kurita, K., Kuroki, Y., Kweon, M. J., Kwon, Y., Kyle,
 1073 G. S., Lacey, R., Ladygin, V., Lajoie, J. G., Lebedev, A., Leckey, S., Lee, D. M., Lee, S.,
 1074 Leitch, M. J., Li, X. H., Lim, H., Litvinenko, A., Liu, M. X., Liu, Y., Maguire, C. F.,
 1075 Makdisi, Y. I., Malakhov, A., Manko, V. I., Mao, Y., Martinez, G., Marx, M. D., Masui,
 1076 H., Matathias, F., Matsumoto, T., McGaughey, P. L., Melnikov, E., Mendenhall, M.,
 1077 Messer, F., Miake, Y., Milan, J., Miller, T. E., Milov, A., Mioduszewski, S., Mischke,
 1078 R. E., Mishra, G. C., Mitchell, J. T., Mohanty, A. K., Morrison, D. P., Moss, J. M.,
 1079 Mühlbacher, F., Mukhopadhyay, D., Muniruzzaman, M., Murata, J., Nagamiya, S., Nagle,
 1080 J. L., Nakamura, T., Nandi, B. K., Nara, M., Newby, J., Nilsson, P., Nyanin, A. S.,
 1081 Nystrand, J., O'Brien, E., Ogilvie, C. A., Ohnishi, H., Ojha, I. D., Okada, K., Ono, M.,
 1082 Onuchin, V., Oskarsson, A., Otterlund, I., Oyama, K., Ozawa, K., Pal, D., Palounek, A.
 1083 P. T., Pantuev, V. S., Papavassiliou, V., Park, J., Parmar, A., Pate, S. F., Peitzmann,
 1084 T., Peng, J.-C., Peresedov, V., Pinkenburg, C., Pisani, R. P., Plasil, F., Purschke, M. L.,
 1085 Purwar, A. K., Rak, J., Ravinovich, I., Read, K. F., Reuter, M., Reygers, K., Riabov, V.,
 1086 Riabov, Y., Roche, G., Romana, A., Rosati, M., Rosnet, P., Ryu, S. S., Sadler, M. E.,
 1087 Saito, N., Sakaguchi, T., Sakai, M., Sakai, S., Samsonov, V., Sanfratello, L., Santo, R.,
 1088 Sato, H. D., Sato, S., Sawada, S., Schutz, Y., Semenov, V., Seto, R., Shaw, M. R., Shea,
 1089 T. K., Shibata, T.-A., Shigaki, K., Shiina, T., Silva, C. L., Silvermyr, D., Sim, K. S., Singh,
 1090 C. P., Singh, V., Sivertz, M., Soldatov, A., Soltz, R. A., Sondheim, W. E., Sorensen, S. P.,
 1091 Sourikova, I. V., Staley, F., Stankus, P. W., Stenlund, E., Stepanov, M., Ster, A., Stoll,
 1092 S. P., Sugitate, T., Sullivan, J. P., Takagui, E. M., Taketani, A., Tamai, M., Tanaka, K. H.,
 1093 Tanaka, Y., Tanida, K., Tannenbaum, M. J., Tarján, P., Tepe, J. D., Thomas, T. L., Tojo,
 1094 J., Torii, H., Towell, R. S., Tserruya, I., Tsuruoka, H., Tuli, S. K., Tydesjö, H., Tyurin,
 1095 N., Hecke, H. W. v., Velkovska, J., Velkovsky, M., Villatte, L., Vinogradov, A. A., Volkov,

1096 M. A., Vznuzdaev, E., Wang, X. R., Watanabe, Y., White, S. N., Wohn, F. K., Woody,
1097 C. L., Xie, W., Yang, Y., Yanovich, A., Yokkaichi, S., Young, G. R., Yushmanov, I. E.,
1098 Zajc, W. A., Zhang, C., Zhou, S., Zhou, S. J., and Zolin, L. (2005). Systematic studies of
1099 the centrality and $\sqrt{s_{NN}}$ dependence of the $de_T/d\eta$ and $dn_{ch}/d\eta$ in heavy ion collisions at
1100 midrapidity. *Phys. Rev. C*, 71:034908. 23

1101 [7] Anderson, M. et al. (2003). The Star time projection chamber: A Unique tool for studying
1102 high multiplicity events at RHIC. *Nucl. Instrum. Meth.*, A499:659–678. 27

1103 [8] Ayala, A. (2016). Hadronic matter at the edge: A survey of some theoretical approaches
1104 to the physics of the qcd phase diagram. *Journal of Physics: Conference Series*,
1105 761(1):012066. vii, 5, 6

1106 [9] Bethe, H. A. and Ashkin, J. (1953). Passage of radiations through matter experimental
1107 nuclear physics vol 1 ed e segre. 25

1108 [10] Bjorken, J. D. (1983). Highly relativistic nucleus-nucleus collisions: The central rapidity
1109 region. *Phys. Rev. D*, 27:140–151. 15

1110 [11] Chatrchyan, S., Khachatryan, V., Sirunyan, A. M., Tumasyan, A., Adam, W., Bergauer,
1111 T., Dragicevic, M., Erö, J., Fabjan, C., Friedl, M., Frühwirth, R., Ghete, V. M., Hammer,
1112 J., Hörmann, N., Hrubec, J., Jeitler, M., Kiesenhofer, W., Knünz, V., Krammer, M., Liko,
1113 D., Mikulec, I., Pernicka, M., Rahbaran, B., Rohringer, C., Rohringer, H., Schöfbeck, R.,
1114 Strauss, J., Taurok, A., Wagner, P., Waltenberger, W., Walzel, G., Widl, E., Wulz, C.-E.,
1115 Mossolov, V., Shumeiko, N., Suarez Gonzalez, J., Bansal, S., Cornelis, T., De Wolf, E. A.,
1116 Janssen, X., Luyckx, S., Maes, T., Mucibello, L., Ochesanu, S., Roland, B., Rougny,
1117 R., Selvaggi, M., Staykova, Z., Van Haevermaet, H., Van Mechelen, P., Van Remortel,
1118 N., Van Spilbeeck, A., Blekman, F., Blyweert, S., D’Hondt, J., Gonzalez Suarez, R.,
1119 Kalogeropoulos, A., Maes, M., Olbrechts, A., Van Doninck, W., Van Mulders, P.,
1120 Van Onsem, G. P., Vilella, I., Clerbaux, B., De Lentdecker, G., Dero, V., Gay, A. P. R.,
1121 Hreus, T., Léonard, A., Marage, P. E., Reis, T., Thomas, L., Vander Velde, C., Vanlaer, P.,
1122 Wang, J., Adler, V., Beernaert, K., Cimmino, A., Costantini, S., Garcia, G., Grunewald,
1123 M., Klein, B., Lellouch, J., Marinov, A., McCartin, J., Ocampo Rios, A. A., Ryckbosch, D.,

1124 Strobbe, N., Thyssen, F., Tytgat, M., Verwilligen, P., Walsh, S., Yazgan, E., Zaganidis,
1125 N., Basegmez, S., Bruno, G., Castello, R., Ceard, L., Delaere, C., du Pree, T., Favart, D.,
1126 Forthomme, L., Giammanco, A., Hollar, J., Lemaitre, V., Liao, J., Militaru, O., Nuttens,
1127 C., Pagano, D., Pin, A., Piotrkowski, K., Schul, N., Vizan Garcia, J. M., Beliy, N.,
1128 Caebergs, T., Daubie, E., Hammad, G. H., Alves, G. A., Correa Martins Junior, M.,
1129 De Jesus Damiao, D., Martins, T., Pol, M. E., Souza, M. H. G., Aldá Júnior, W. L.,
1130 Carvalho, W., Custódio, A., Da Costa, E. M., De Oliveira Martins, C., Fonseca De Souza,
1131 S., Matos Figueiredo, D., Mundim, L., Nogima, H., Oguri, V., Prado Da Silva, W. L.,
1132 Santoro, A., Soares Jorge, L., Sznajder, A., Bernardes, C. A., Dias, F. A., Fernandez
1133 Perez Tomei, T. R., Gregores, E. M., Lagana, C., Marinho, F., Mercadante, P. G., Novaes,
1134 S. F., Padula, S. S., Genchev, V., Iaydjiev, P., Piperov, S., Rodozov, M., Stoykova, S.,
1135 Sultanov, G., Tcholakov, V., Trayanov, R., Vutova, M., Dimitrov, A., Hadjiiska, R.,
1136 Kozhuharov, V., Litov, L., Pavlov, B., Petkov, P., Bian, J. G., Chen, G. M., Chen, H. S.,
1137 Jiang, C. H., Liang, D., Liang, S., Meng, X., Tao, J., Wang, J., Wang, X., Wang, Z.,
1138 Xiao, H., Xu, M., Zang, J., Zhang, Z., Asawatangtrakuldee, C., Ban, Y., Guo, S., Guo,
1139 Y., Li, W., Liu, S., Mao, Y., Qian, S. J., Teng, H., Wang, S., Zhu, B., Zou, W., Avila,
1140 C., Gomez, J. P., Gomez Moreno, B., Osorio Oliveros, A. F., Sanabria, J. C., Godinovic,
1141 N., Lelas, D., Plestina, R., Polic, D., Puljak, I., Antunovic, Z., Kovac, M., Brigljevic, V.,
1142 Duric, S., Kadija, K., Luetic, J., Morovic, S., Attikis, A., Galanti, M., Mavromanolakis,
1143 G., Mousa, J., Nicolaou, C., Ptochos, F., Razis, P. A., Finger, M., Finger, M., Assran,
1144 Y., Elgammal, S., Ellithi Kamel, A., Khalil, S., Mahmoud, M. A., Radi, A., Kadastik,
1145 M., Müntel, M., Raidal, M., Rebane, L., Tiko, A., Azzolini, V., Eerola, P., Fedi, G.,
1146 Voutilainen, M., Härkönen, J., Heikkinen, A., Karimäki, V., Kinnunen, R., Kortelainen,
1147 M. J., Lampén, T., Lassila-Perini, K., Lehti, S., Lindén, T., Luukka, P., Mäenpää, T.,
1148 Peltola, T., Tuominen, E., Tuominiemi, J., Tuovinen, E., Ungaro, D., Wendland, L.,
1149 Banzuzi, K., Karjalainen, A., Korpela, A., Tuuva, T., Besancon, M., Choudhury, S.,
1150 Dejardin, M., Denegri, D., Fabbro, B., Faure, J. L., Ferri, F., Ganjour, S., Givernaud,
1151 A., Gras, P., Hamel de Monchenault, G., Jarry, P., Locci, E., Malcles, J., Millischer, L.,
1152 Nayak, A., Rander, J., Rosowsky, A., Shreyber, I., Titov, M., Baffioni, S., Beaudette,
1153 F., Benhabib, L., Bianchini, L., Bluj, M., Broutin, C., Busson, P., Charlot, C., Daci,

1154 N., Dahms, T., Dobrzynski, L., Granier de Cassagnac, R., Haguenauer, M., Miné, P.,
 1155 Mironov, C., Nguyen, M., Ochando, C., Paganini, P., Sabes, D., Salerno, R., Sirois, Y.,
 1156 Veelken, C., Zabi, A., Agram, J.-L., Andrea, J., Bloch, D., Bodin, D., Brom, J.-M.,
 1157 Cardaci, M., Chabert, E. C., Collard, C., Conte, E., Drouhin, F., Ferro, C., Fontaine, J.-
 1158 C., Gelé, D., Goerlach, U., Juillot, P., Le Bihan, A.-C., Van Hove, P., Fassi, F., Mercier,
 1159 D., Beauceron, S., Beaupere, N., Bondu, O., Boudoul, G., Chasserat, J., Chierici, R.,
 1160 Contardo, D., Depasse, P., El Mamouni, H., Fay, J., Gascon, S., Gouzevitch, M., Ille,
 1161 B., Kurca, T., Lethuillier, M., Mirabito, L., Perries, S., Sordini, V., Tosi, S., Tschudi,
 1162 Y., Verdier, P., Viret, S., Tsamalaidze, Z., Anagnostou, G., Beranek, S., Edelhoff, M.,
 1163 Feld, L., Heracleous, N., Hindrichs, O., Jussen, R., Klein, K., Merz, J., Ostapchuk, A.,
 1164 Perieanu, A., Raupach, F., Sammet, J., Schael, S., Sprenger, D., Weber, H., Wittmer,
 1165 B., Zhukov, V., Ata, M., Caudron, J., Dietz-Laursonn, E., Erdmann, M., Güth, A.,
 1166 Hebbeker, T., Heidemann, C., Hoepfner, K., Klingebiel, D., Kreuzer, P., Lingemann,
 1167 J., Magass, C., Merschmeyer, M., Meyer, A., Olschewski, M., Papacz, P., Pieta, H.,
 1168 Reithler, H., Schmitz, S. A., Sonnenschein, L., Steggemann, J., Teyssier, D., Weber, M.,
 1169 Bontenackels, M., Cherepanov, V., Flügge, G., Geenen, H., Geisler, M., Haj Ahmad, W.,
 1170 Hoehle, F., Kargoll, B., Kress, T., Kuessel, Y., Nowack, A., Perchalla, L., Pooth, O.,
 1171 Rennefeld, J., Sauerland, P., Stahl, A., Aldaya Martin, M., Behr, J., Behrenhoff, W.,
 1172 Behrens, U., Bergholz, M., Bethani, A., Borrás, K., Burgmeier, A., Cakir, A., Calligaris,
 1173 L., Campbell, A., Castro, E., Costanza, F., Dammann, D., Diez Pardos, C., Eckerlin, G.,
 1174 Eckstein, D., Flucke, G., Geiser, A., Glushkov, I., Gunnellini, P., Habib, S., Hauk, J.,
 1175 Jung, H., Kasemann, M., Katsas, P., Kleinwort, C., Kluge, H., Knutsson, A., Krämer, M.,
 1176 Krücker, D., Kuznetsova, E., Lange, W., Lohmann, W., Lutz, B., Mankel, R., Marfin, I.,
 1177 Marienfeld, M., Melzer-Pellmann, I.-A., Meyer, A. B., Mnich, J., Mussgiller, A., Naumann-
 1178 Emme, S., Olzem, J., Perrey, H., Petrukhin, A., Pitzl, D., Raspereza, A., Ribeiro Cipriano,
 1179 P. M., Riedl, C., Ron, E., Rosin, M., Salfeld-Nebgen, J., Schmidt, R., Schoerner-Sadenius,
 1180 T., Sen, N., Spiridonov, A., Stein, M., Walsh, R., Wissing, C., Autermann, C., Blobel,
 1181 V., Draeger, J., Enderle, H., Erfle, J., Gebbert, U., Görner, M., Hermanns, T., Höing,
 1182 R. S., Kaschube, K., Kaussen, G., Kirschenmann, H., Klanner, R., Lange, J., Mura, B.,
 1183 Nowak, F., Peiffer, T., Pietsch, N., Sander, C., Schettler, H., Schleper, P., Schlieckau, E.,

1184 Schmidt, A., Schröder, M., Schum, T., Sola, V., Stadie, H., Steinbrück, G., Thomsen,
 1185 J., Vanelderden, L., Barth, C., Berger, J., Chwalek, T., De Boer, W., Dierlamm, A.,
 1186 Feindt, M., Guthoff, M., Hackstein, C., Hartmann, F., Heinrich, M., Held, H., Hoffmann,
 1187 K. H., Honc, S., Katkov, I., Komaragiri, J. R., Lobelle Pardo, P., Martschei, D., Mueller,
 1188 S., Müller, T., Niegel, M., Nürnberg, A., Oberst, O., Oehler, A., Ott, J., Quast, G.,
 1189 Rabbertz, K., Ratnikov, F., Ratnikova, N., Röcker, S., Scheurer, A., Schilling, F.-P.,
 1190 Schott, G., Simonis, H. J., Stober, F. M., Troendle, D., Ulrich, R., Wagner-Kuhr, J.,
 1191 Weiler, T., Zeise, M., Daskalakis, G., Geralis, T., Kesisoglou, S., Kyriakis, A., Loukas,
 1192 D., Manolakos, I., Markou, A., Markou, C., Mavrommatis, C., Ntomari, E., Gouskos, L.,
 1193 Mertzimekis, T. J., Panagiotou, A., Saoulidou, N., Evangelou, I., Foudas, C., Kokkas, P.,
 1194 Manthos, N., Papadopoulos, I., Patras, V., Bencze, G., Hajdu, C., Hidas, P., Horvath, D.,
 1195 Sikler, F., Veszpremi, V., Vesztergombi, G., Beni, N., Czellar, S., Molnar, J., Palinkas, J.,
 1196 Szillasi, Z., Karancsi, J., Raics, P., Trocsanyi, Z. L., Ujvari, B., Beri, S. B., Bhatnagar,
 1197 V., Dhingra, N., Gupta, R., Jindal, M., Kaur, M., Mehta, M. Z., Nishu, N., Saini, L. K.,
 1198 Sharma, A., Singh, J., Ahuja, S., Bhardwaj, A., Choudhary, B. C., Kumar, A., Kumar,
 1199 A., Malhotra, S., Naimuddin, M., Ranjan, K., Sharma, V., Shivpuri, R. K., Banerjee,
 1200 S., Bhattacharya, S., Dutta, S., Gomber, B., Jain, S., Jain, S., Khurana, R., Sarkar,
 1201 S., Sharan, M., Abdulsalam, A., Choudhury, R. K., Dutta, D., Kailas, S., Kumar, V.,
 1202 Mehta, P., Mohanty, A. K., Pant, L. M., Shukla, P., Aziz, T., Ganguly, S., Guchait, M.,
 1203 Maity, M., Majumder, G., Mazumdar, K., Mohanty, G. B., Parida, B., Sudhakar, K.,
 1204 Wickramage, N., Banerjee, S., Dugad, S., Arfaei, H., Bakhshiansohi, H., Etesami, S. M.,
 1205 Fahim, A., Hashemi, M., Hesari, H., Jafari, A., Khakzad, M., Mohammadi Najafabadi,
 1206 M., Paktinat Mehdiabadi, S., Safarzadeh, B., Zeinali, M., Abbrescia, M., Barbone, L.,
 1207 Calabria, C., Chhibra, S. S., Colaleo, A., Creanza, D., De Filippis, N., De Palma, M.,
 1208 Fiore, L., Iaselli, G., Lusito, L., Maggi, G., Maggi, M., Marangelli, B., My, S., Nuzzo,
 1209 S., Pacifico, N., Pompili, A., Pugliese, G., Selvaggi, G., Silvestris, L., Singh, G., Zito,
 1210 G., Abbiendi, G., Benvenuti, A. C., Bonacorsi, D., Braibant-Giacomelli, S., Brigliadori,
 1211 L., Capiluppi, P., Castro, A., Cavallo, F. R., Cuffiani, M., Dallavalle, G. M., Fabbri, F.,
 1212 Fanfani, A., Fasanella, D., Giacomelli, P., Grandi, C., Guiducci, L., Marcellini, S., Masetti,
 1213 G., Meneghelli, M., Montanari, A., Navarria, F. L., Odorici, F., Perrotta, A., Primavera,

1214 F., Rossi, A. M., Rovelli, T., Siroli, G., Travaglini, R., Albergo, S., Cappello, G., Chiorboli,
 1215 M., Costa, S., Potenza, R., Tricomi, A., Tuve, C., Barbagli, G., Ciulli, V., Civinini, C.,
 1216 D'Alessandro, R., Focardi, E., Frosali, S., Gallo, E., Gonzi, S., Meschini, M., Paoletti,
 1217 S., Sguazzoni, G., Tropiano, A., Benussi, L., Bianco, S., Colafranceschi, S., Fabbri, F.,
 1218 Piccolo, D., Fabbricatore, P., Musenich, R., Benaglia, A., De Guio, F., Di Matteo, L.,
 1219 Fiorendi, S., Gennai, S., Ghezzi, A., Malvezzi, S., Manzoni, R. A., Martelli, A., Massironi,
 1220 A., Menasce, D., Moroni, L., Paganoni, M., Pedrini, D., Ragazzi, S., Redaelli, N., Sala,
 1221 S., Tabarelli de Fatis, T., Buontempo, S., Carrillo Montoya, C. A., Cavallo, N., De Cosa,
 1222 A., Dogangun, O., Fabozzi, F., Iorio, A. O. M., Lista, L., Meola, S., Merola, M., Paolucci,
 1223 P., Azzi, P., Bacchetta, N., Bellan, P., Bisello, D., Branca, A., Carlin, R., Checchia, P.,
 1224 Dorigo, T., Dosselli, U., Gasparini, F., Gasparini, U., Gozzelino, A., Kanishchev, K.,
 1225 Lacaprara, S., Lazzizzera, I., Margoni, M., Meneguzzo, A. T., Nespolo, M., Ronchese,
 1226 P., Simonetto, F., Torassa, E., Vanini, S., Zotto, P., Zumerle, G., Gabusi, M., Ratti,
 1227 S. P., Riccardi, C., Torre, P., Vitulo, P., Biasini, M., Bilei, G. M., Fanò, L., Lariccia, P.,
 1228 Lucaroni, A., Mantovani, G., Menichelli, M., Nappi, A., Romeo, F., Saha, A., Santocchia,
 1229 A., Taroni, S., Azzurri, P., Bagliesi, G., Boccali, T., Broccolo, G., Castaldi, R., D'Agnolo,
 1230 R. T., Dell'Orso, R., Fiori, F., Foà, L., Giassi, A., Kraan, A., Ligabue, F., Lomtadze, T.,
 1231 Martini, L., Messineo, A., Palla, F., Rizzi, A., Serban, A. T., Spagnolo, P., Squillacioti, P.,
 1232 Tenchini, R., Tonelli, G., Venturi, A., Verdini, P. G., Barone, L., Cavallari, F., Del Re, D.,
 1233 Diemoz, M., Grassi, M., Longo, E., Meridiani, P., Micheli, F., Nourbakhsh, S., Organtini,
 1234 G., Paramatti, R., Rahatlou, S., Sigamani, M., Soffi, L., Amapane, N., Arcidiacono, R.,
 1235 Argiro, S., Arneodo, M., Biino, C., Cartiglia, N., Costa, M., Demaria, N., Graziano,
 1236 A., Mariotti, C., Maselli, S., Migliore, E., Monaco, V., Musich, M., Obertino, M. M.,
 1237 Pastrone, N., Pelliccioni, M., Potenza, A., Romero, A., Ruspa, M., Sacchi, R., Solano, A.,
 1238 Staiano, A., Vilela Pereira, A., Belforte, S., Candelise, V., Cossutti, F., Della Ricca, G.,
 1239 Gobbo, B., Marone, M., Montanino, D., Penzo, A., Schizzi, A., Heo, S. G., Kim, T. Y.,
 1240 Nam, S. K., Chang, S., Kim, D. H., Kim, G. N., Kong, D. J., Park, H., Ro, S. R., Son,
 1241 D. C., Son, T., Kim, J. Y., Kim, Z. J., Song, S., Choi, S., Gyun, D., Hong, B., Jo, M.,
 1242 Kim, H., Kim, T. J., Lee, K. S., Moon, D. H., Park, S. K., Choi, M., Kim, J. H., Park,
 1243 C., Park, I. C., Park, S., Ryu, G., Cho, Y., Choi, Y., Choi, Y. K., Goh, J., Kim, M. S.,

1244 Kwon, E., Lee, B., Lee, J., Lee, S., Seo, H., Yu, I., Bilinskas, M. J., Grigelionis, I., Janulis,
 1245 M., Juodagalvis, A., Castilla-Valdez, H., De La Cruz-Burelo, E., Heredia-de La Cruz, I.,
 1246 Lopez-Fernandez, R., Magaña Villalba, R., Martínez-Ortega, J., Sánchez-Hernández, A.,
 1247 Villasenor-Cendejas, L. M., Carrillo Moreno, S., Vazquez Valencia, F., Salazar Ibarguen,
 1248 H. A., Casimiro Linares, E., Morelos Pineda, A., Reyes-Santos, M. A., Krofcheck, D.,
 1249 Bell, A. J., Butler, P. H., Doesburg, R., Reucroft, S., Silverwood, H., Ahmad, M.,
 1250 Asghar, M. I., Hoorani, H. R., Khalid, S., Khan, W. A., Khurshid, T., Qazi, S., Shah,
 1251 M. A., Shoaib, M., Bialkowska, H., Boimska, B., Frueboes, T., Gokieli, R., Górski,
 1252 M., Kazana, M., Nawrocki, K., Romanowska-Rybinska, K., Szleper, M., Wrochna, G.,
 1253 Zalewski, P., Brona, G., Bunkowski, K., Cwiok, M., Dominik, W., Doroba, K., Kalinowski,
 1254 A., Konecki, M., Krolkowski, J., Almeida, N., Bargassa, P., David, A., Faccioli, P.,
 1255 Ferreira Parracho, P. G., Gallinaro, M., Seixas, J., Varela, J., Vischia, P., Belotelov,
 1256 I., Bunin, P., Gavrilenko, M., Golutvin, I., Gorbunov, I., Kamenev, A., Karjavin, V.,
 1257 Kozlov, G., Lanev, A., Malakhov, A., Moisenz, P., Palichik, V., Perelygin, V., Shmatov,
 1258 S., Smirnov, V., Volodko, A., Zarubin, A., Evstyukhin, S., Golovtsov, V., Ivanov, Y.,
 1259 Kim, V., Levchenko, P., Murzin, V., Oreshkin, V., Smirnov, I., Sulimov, V., Uvarov,
 1260 L., Vavilov, S., Vorobyev, A., Vorobyev, A., Andreev, Y., Dermenev, A., Gninenko,
 1261 S., Golubev, N., Kirsanov, M., Krasnikov, N., Matveev, V., Pashenkov, A., Tlisov, D.,
 1262 Toropin, A., Epshteyn, V., Erofeeva, M., Gavrilov, V., Kossov, M., Lychkovskaya, N.,
 1263 Popov, V., Safronov, G., Semenov, S., Stolin, V., Vlasov, E., Zhokin, A., Belyaev, A.,
 1264 Boos, E., Ershov, A., Gribushin, A., Klyukhin, V., Kodolova, O., Korotkikh, V., Lokhtin,
 1265 I., Markina, A., Obraztsov, S., Perfilov, M., Petrushanko, S., Popov, A., Sarycheva, L.,
 1266 Savrin, V., Snigirev, A., Vardanyan, I., Andreev, V., Azarkin, M., Dremin, I., Kirakosyan,
 1267 M., Leonidov, A., Mesyats, G., Rusakov, S. V., Vinogradov, A., Azhgirey, I., Bayshev, I.,
 1268 Bitioukov, S., Grishin, V., Kachanov, V., Konstantinov, D., Korablev, A., Krychkine,
 1269 V., Petrov, V., Ryutin, R., Sobol, A., Tourtchanovitch, L., Troshin, S., Tyurin, N.,
 1270 Uzunian, A., Volkov, A., Adzic, P., Djordjevic, M., Ekmedzic, M., Krpic, D., Milosevic, J.,
 1271 Aguilar-Benitez, M., Alcaraz Maestre, J., Arce, P., Battilana, C., Calvo, E., Cerrada, M.,
 1272 Chamizo Llatas, M., Colino, N., De La Cruz, B., Delgado Peris, A., Domínguez Vázquez,
 1273 D., Fernandez Bedoya, C., Fernández Ramos, J. P., Ferrando, A., Flix, J., Fouz, M. C.,

1274 Garcia-Abia, P., Gonzalez Lopez, O., Goy Lopez, S., Hernandez, J. M., Josa, M. I., Merino,
 1275 G., Puerta Pelayo, J., Quintario Olmeda, A., Redondo, I., Romero, L., Santaolalla, J.,
 1276 Soares, M. S., Willmott, C., Albajar, C., Codispoti, G., de Trocóniz, J. F., Brun, H.,
 1277 Cuevas, J., Fernandez Menendez, J., Folgueras, S., Gonzalez Caballero, I., Lloret Iglesias,
 1278 L., Piedra Gomez, J., Brochero Cifuentes, J. A., Cabrillo, I. J., Calderon, A., Chuang,
 1279 S. H., Duarte Campderros, J., Felcini, M., Fernandez, M., Gomez, G., Gonzalez Sanchez,
 1280 J., Jorda, C., Lopez Virto, A., Marco, J., Marco, R., Martinez Rivero, C., Matorras,
 1281 F., Munoz Sanchez, F. J., Rodrigo, T., Rodríguez-Marrero, A. Y., Ruiz-Jimeno, A.,
 1282 Scodellaro, L., Sobron Sanudo, M., Vila, I., Vilar Cortabitarte, R., Abbaneo, D., Auffray,
 1283 E., Auzinger, G., Baillon, P., Ball, A. H., Barney, D., Benitez, J. F., Bernet, C., Bianchi,
 1284 G., Bloch, P., Bocci, A., Bonato, A., Botta, C., Breuker, H., Camporesi, T., Cerminara,
 1285 G., Christiansen, T., Coarasa Perez, J. A., D'Enterria, D., Dabrowski, A., De Roeck,
 1286 A., Di Guida, S., Dobson, M., Dupont-Sagorin, N., Elliott-Peisert, A., Frisch, B., Funk,
 1287 W., Georgiou, G., Giffels, M., Gigi, D., Gill, K., Giordano, D., Giunta, M., Glege, F.,
 1288 Gomez-Reino Garrido, R., Govoni, P., Gowdy, S., Guida, R., Hansen, M., Harris, P.,
 1289 Hartl, C., Harvey, J., Hegner, B., Hinzmann, A., Innocente, V., Janot, P., Kaadze, K.,
 1290 Karavakis, E., Kousouris, K., Lecoq, P., Lee, Y.-J., Lenzi, P., Lourenço, C., Mäki, T.,
 1291 Malberti, M., Malgeri, L., Mannelli, M., Masetti, L., Meijers, F., Mersi, S., Meschi, E.,
 1292 Moser, R., Mozer, M. U., Mulders, M., Musella, P., Nesvold, E., Orimoto, T., Orsini, L.,
 1293 Palencia Cortezon, E., Perez, E., Perrozzi, L., Petrilli, A., Pfeiffer, A., Pierini, M., Pimiä,
 1294 M., Piparo, D., Polese, G., Quertenmont, L., Racz, A., Reece, W., Rodrigues Antunes, J.,
 1295 Rolandi, G., Rommerskirchen, T., Rovelli, C., Rovere, M., Sakulin, H., Santanastasio, F.,
 1296 Schäfer, C., Schwick, C., Segoni, I., Sekmen, S., Sharma, A., Siegrist, P., Silva, P., Simon,
 1297 M., Sphicas, P., Spiga, D., Spiropulu, M., Tsirou, A., Veres, G. I., Vlimant, J. R., Wöhri,
 1298 H. K., Worm, S. D., Zeuner, W. D., Bertl, W., Deiters, K., Erdmann, W., Gabathuler,
 1299 K., Horisberger, R., Ingram, Q., Kaestli, H. C., König, S., Kotlinski, D., Langenegger, U.,
 1300 Meier, F., Renker, D., Rohe, T., Sibille, J., Bäni, L., Bortignon, P., Buchmann, M. A.,
 1301 Casal, B., Chanon, N., Deisher, A., Dissertori, G., Dittmar, M., Dünser, M., Eugster, J.,
 1302 Freudenreich, K., Grab, C., Hits, D., Lecomte, P., Lustermann, W., Martinez Ruiz del
 1303 Arbol, P., Mohr, N., Moortgat, F., Nägeli, C., Nef, P., Nessi-Tedaldi, F., Pandolfi, F.,

1304 Pape, L., Pauss, F., Peruzzi, M., Ronga, F. J., Rossini, M., Sala, L., Sanchez, A. K.,
 1305 Starodumov, A., Stieger, B., Takahashi, M., Tauscher, L., Thea, A., Theofilatos, K.,
 1306 Treille, D., Urscheler, C., Wallny, R., Weber, H. A., Wehrli, L., Aguilo, E., Amsler, C.,
 1307 Chiochia, V., De Visscher, S., Favaro, C., Ivova Rikova, M., Millan Mejias, B., Otiougova,
 1308 P., Robmann, P., Snoek, H., Tupputi, S., Verzetti, M., Chang, Y. H., Chen, K. H., Kuo,
 1309 C. M., Li, S. W., Lin, W., Liu, Z. K., Lu, Y. J., Mekterovic, D., Singh, A. P., Volpe, R., Yu,
 1310 S. S., Bartalini, P., Chang, P., Chang, Y. H., Chang, Y. W., Chao, Y., Chen, K. F., Dietz,
 1311 C., Grundler, U., Hou, W.-S., Hsiung, Y., Kao, K. Y., Lei, Y. J., Lu, R.-S., Majumder, D.,
 1312 Petrakou, E., Shi, X., Shiu, J. G., Tzeng, Y. M., Wan, X., Wang, M., Adiguzel, A., Bakirci,
 1313 M. N., Cerci, S., Dozen, C., Dumanoglu, I., Eskut, E., Girgis, S., Gokbulut, G., Gurpinar,
 1314 E., Hos, I., Kangal, E. E., Karapinar, G., Kayis Topaksu, A., Onengut, G., Ozdemir, K.,
 1315 Ozturk, S., Polatoz, A., Sogut, K., Sunar Cerci, D., Tali, B., Topakli, H., Vergili, L. N.,
 1316 Vergili, M., Akin, I. V., Aliev, T., Bilin, B., Bilmis, S., Deniz, M., Gamsizkan, H., Guler,
 1317 A. M., Ocalan, K., Ozpineci, A., Serin, M., Sever, R., Surat, U. E., Yalvac, M., Yildirim,
 1318 E., Zeyrek, M., Gülmez, E., Isildak, B., Kaya, M., Kaya, O., Ozkorucuklu, S., Sonmez, N.,
 1319 Cankocak, K., Levchuk, L., Bostock, F., Brooke, J. J., Clement, E., Cussans, D., Flacher,
 1320 H., Frazier, R., Goldstein, J., Grimes, M., Heath, G. P., Heath, H. F., Kreczko, L.,
 1321 Metson, S., Newbold, D. M., Nirunpong, K., Poll, A., Senkin, S., Smith, V. J., Williams,
 1322 T., Basso, L., Bell, K. W., Belyaev, A., Brew, C., Brown, R. M., Cockerill, D. J. A.,
 1323 Coughlan, J. A., Harder, K., Harper, S., Jackson, J., Kennedy, B. W., Olaiya, E., Petyt,
 1324 D., Radburn-Smith, B. C., Shepherd-Themistocleous, C. H., Tomalin, I. R., Womersley,
 1325 W. J., Bainbridge, R., Ball, G., Beuselinck, R., Buchmuller, O., Colling, D., Cripps, N.,
 1326 Cutajar, M., Dauncey, P., Davies, G., Della Negra, M., Ferguson, W., Fulcher, J., Futyan,
 1327 D., Gilbert, A., Guneratne Bryer, A., Hall, G., Hatherell, Z., Hays, J., Iles, G., Jarvis,
 1328 M., Karapostoli, G., Lyons, L., Magnan, A.-M., Marrouche, J., Mathias, B., Nandi, R.,
 1329 Nash, J., Nikitenko, A., Papageorgiou, A., Pela, J., Pesaresi, M., Petridis, K., Pioppi,
 1330 M., Raymond, D. M., Rogerson, S., Rose, A., Ryan, M. J., Seez, C., Sharp, P., Sparrow,
 1331 A., Stoye, M., Tapper, A., Vazquez Acosta, M., Virdee, T., Wakefield, S., Wardle, N.,
 1332 Whyntie, T., Chadwick, M., Cole, J. E., Hobson, P. R., Khan, A., Kyberd, P., Leslie, D.,
 1333 Martin, W., Reid, I. D., Symonds, P., Teodorescu, L., Turner, M., Hatakeyama, K., Liu,

H., Scarborough, T., Charaf, O., Henderson, C., Rumerio, P., Avetisyan, A., Bose, T.,
Fantasia, C., Heiste (2012). Measurement of the pseudorapidity and centrality dependence
of the transverse energy density in pb-pb collisions at $\sqrt{s_{\text{NN}}} = 2.76$ TeV. *Phys. Rev. Lett.*,
109:152303. 6, 22

[12] Collaboration, T. A., Aamodt, K., Quintana, A. A., Achenbach, R., Acounis, S.,
Adamov, D., Adler, C., Aggarwal, M., Agnese, F., Rinella, G. A., Ahammed, Z., Ahmad,
A., Ahmad, N., Ahmad, S., Akindinov, A., Akishin, P., Aleksandrov, D., Alessandro,
B., Alfaro, R., Alfarone, G., Alici, A., Alme, J., Alt, T., Altinpinar, S., Amend, W.,
Andrei, C., Andres, Y., Andronic, A., Anelli, G., Anfreville, M., Angelov, V., Anzo, A.,
Anson, C., Antici, T., Antonenko, V., Antonczyk, D., Antinori, F., Antinori, S., Antonioli,
P., Aphecetche, L., Appelshuser, H., Aprodu, V., Arba, M., Arcelli, S., Argentieri, A.,
Armesto, N., Arnaldi, R., Arefiev, A., Arsene, I., Asryan, A., Augustinus, A., Awes, T. C.,
ysto, J., Azmi, M. D., Bablock, S., Badal, A., Badyal, S. K., Baechler, J., Bagnasco, S.,
Bailhache, R., Bala, R., Baldisseri, A., Baldit, A., Bn, J., Barbera, R., Barberis, P.-L.,
Barbet, J. M., Barnfoldi, G., Barret, V., Bartke, J., Bartos, D., Basile, M., Basmanov, V.,
Bastid, N., Batigne, G., Batyunya, B., Baudot, J., Baumann, C., Bearden, I., Becker, B.,
Belikov, J., Bellwied, R., Belmont-Moreno, E., Belogianni, A., Belyaev, S., Benato, A.,
Beney, J. L., Benhabib, L., Benotto, F., Beol, S., Berceanu, I., Bercuci, A., Berdermann,
E., Berdnikov, Y., Bernard, C., Berny, R., Berst, J. D., Bertelsen, H., Betev, L., Bhasin,
A., Baskar, P., Bhati, A., Bianchi, N., Bielik, J., Bielikov, J., Bimbot, L., Blanchard, G.,
Blanco, F., Blanco, F., Blau, D., Blume, C., Blyth, S., Boccioni, M., Bogdanov, A., Bggild,
H., Bogolyubsky, M., Boldizsr, L., Bombara, M., Bombonati, C., Bondila, M., Bonnet,
D., Bonvicini, V., Borel, H., Borotto, F., Borshchov, V., Bortoli, Y., Borysov, O., Bose,
S., Bosisio, L., Botje, M., Bttger, S., Bourdaud, G., Bourrion, O., Bouvier, S., Braem,
A., Braun, M., Braun-Munzinger, P., Bravina, L., Bregant, M., Bruckner, G., Brun, R.,
Bruna, E., Brunasso, O., Bruno, G. E., Bucher, D., Budilov, V., Budnikov, D., Buesching,
H., Buncic, P., Burns, M., Burachas, S., Busch, O., Bushop, J., Cai, X., Caines, H.,
Calaon, F., Caldogno, M., Cali, I., Camerini, P., Campagnolo, R., Campbell, M., Cao,
X., Capitani, G. P., Romeo, G. C., Cardenas-Montes, M., Carduner, H., Carena, F.,

1363 Carena, W., Cariola, P., Carminati, F., Casado, J., Diaz, A. C., Caselle, M., Castellanos,
 1364 J. C., Castor, J., Catanescu, V., Cattaruzza, E., Cavazza, D., Cerello, P., Ceresa, S.,
 1365 ern, V., Chambert, V., Chapeland, S., Charpy, A., Charrier, D., Chartoire, M., Charvet,
 1366 J. L., Chattopadhyay, S., Chattopadhyay, S., Chepurnov, V., Chernenko, S., Cherney,
 1367 M., Cheshkov, C., Cheynis, B., Chochula, P., Chiavassa, E., Barroso, V. C., Choi, J.,
 1368 Christakoglou, P., Christiansen, P., Christensen, C., Chykalov, O. A., Cicalo, C., Cifarelli-
 1369 Strolin, L., Ciobanu, M., Cindolo, F., Cirstoiu, C., Clausse, O., Cleymans, J., Cobanoglu,
 1370 O., Coffin, J.-P., Coli, S., Colla, A., Colledani, C., Combaret, C., Combet, M., Comets,
 1371 M., Balbastre, G. C., del Valle, Z. C., Contin, G., Contreras, J., Cormier, T., Corsi, F.,
 1372 Cortese, P., Costa, F., Crescio, E., Crochet, P., Cuautle, E., Cussonneau, J., Dahlinger,
 1373 M., Dainese, A., Dalsgaard, H. H., Daniel, L., Das, I., Das, T., Dash, A., Silva, R. D.,
 1374 Davenport, M., Daues, H., Caro, A. D., de Cataldo, G., Cuveland, J. D., Falco, A. D.,
 1375 de Gaspari, M., de Girolamo, P., de Groot, J., Gruttola, D. D., Haas, A. D., Marco, N. D.,
 1376 Pasquale, S. D., Remigis, P. D., de Vaux, D., Decock, G., Delagrange, H., Franco, M. D.,
 1377 Dellacasa, G., Dell'Olio, C., Dell'Olio, D., Deloff, A., Demanov, V., Dnes, E., D'Erasmus,
 1378 G., Derkach, D., Devaux, A., Bari, D. D., Bartolomeo, A. D., Giglio, C. D., Liberto,
 1379 S. D., Mauro, A. D., Nezza, P. D., Dialinas, M., Diaz, L., Valdes, R. D., Dietel, T., Dima,
 1380 R., Ding, H., Dinca, C., Divi, R., Dobretsov, V., Dobrin, A., Doenigus, B., Dobrowolski,
 1381 T., Domnguez, I., Dorn, M., Drouet, S., Dubey, A. E., Ducroux, L., Dumitrache, F.,
 1382 Dumonteil, E., Dupieux, P., Duta, V., Majumdar, A. D., Majumdar, M. D., Dyhre,
 1383 T., Efimov, L., Efremov, A., Elia, D., Emschermann, D., Engster, C., Enokizono, A.,
 1384 Espagnon, B., Estienne, M., Evangelista, A., Evans, D., Evrard, S., Fabjan, C. W.,
 1385 Fabris, D., Faivre, J., Falchieri, D., Fantoni, A., Farano, R., Fearick, R., Fedorov, O.,
 1386 Fekete, V., Felea, D., Feofilov, G., Tllez, A. F., Ferretti, A., Fichera, F., Filchagin, S.,
 1387 Filoni, E., Finck, C., Fini, R., Fiore, E. M., Flierl, D., Floris, M., Fodor, Z., Foka, Y.,
 1388 Fokin, S., Force, P., Formenti, F., Fragiaco, E., Fragiadakis, M., Fraissard, D., Franco,
 1389 A., Franco, M., Frankenfeld, U., Fratino, U., Fresneau, S., Frolov, A., Fuchs, U., Fujita, J.,
 1390 Furget, C., Furini, M., Girard, M. F., Gaardhje, J.-J., Gabrielli, A., Gadrat, S., Gagliardi,
 1391 M., Gago, A., Gaido, L., Torreira, A. G., Gallio, M., Gandolfi, E., Ganoti, P., Ganti, M.,
 1392 Garabatos, J., Lopez, A. G., Garizzo, L., Gaudichet, L., Gemme, R., Germain, M., Gheata,

1393 A., Gheata, M., Ghidini, B., Ghosh, P., Giolu, G., Giraudo, G., Giubellino, P., Glasow,
 1394 R., Glssel, P., Ferreira, E. G., Gutierrez, C. G., Gonzales-Trueba, L. H., Gorbunov, S.,
 1395 Gorbunov, Y., Gos, H., Gosset, J., Gotovac, S., Gottschlag, H., Gottschalk, D., Grabski,
 1396 V., Grassi, T., Gray, H., Grebenyuk, O., Grebieszko, K., Gregory, C., Grigoras, C.,
 1397 Grion, N., Grigoriev, V., Grigoryan, A., Grigoryan, C., Grigoryan, S., Grishuk, Y., Gros,
 1398 P., Grosse-Oetringhaus, J., Grossiord, J.-Y., Grosso, R., Grynyov, B., Guarnaccia, C.,
 1399 Guber, F., Guerin, F., Guernane, R., Guerzoni, M., Guichard, A., Guida, M., Guilloux,
 1400 G., Gulkanyan, H., Gulbrandsen, K., Gunji, T., Gupta, A., Gupta, V., Gustafsson, H.-
 1401 A., Gutbrod, H., Hadjidakis, C., Haiduc, M., Hamar, G., Hamagaki, H., Hamblen, J.,
 1402 Hansen, J. C., Hardy, P., Hatzifotiadou, D., Harris, J. W., Hartig, M., Harutyunyan, A.,
 1403 Hayrapetyan, A., Hasch, D., Hasegan, D., Hehner, J., Heine, N., Heinz, M., Helstrup, H.,
 1404 Herghelegiu, A., Herlant, S., Corral, G. H., Herrmann, N., Hetland, K., Hille, P., Hinke,
 1405 H., Hippolyte, B., Hoch, M., Hoebbel, H., Hoedlmoser, H., Horaguchi, T., Horner, M.,
 1406 Hristov, P., Hivnov, I., Hu, S., Guo, C. H., Humanic, T., Hurtado, A., Hwang, D. S.,
 1407 Ianigro, J. C., Idzik, M., Igoekin, S., Ilkaev, R., Ilkiv, I., Imhoff, M., Innocenti, P. G.,
 1408 Ionescu, E., Ippolitov, M., Irfan, M., Insa, C., Inuzuka, M., Ivan, C., Ivanov, A., Ivanov,
 1409 M., Ivanov, V., Jacobs, P., Jacholkowski, A., Janurov, L., Janik, R., Jasper, M., Jena, C.,
 1410 Jirde, L., Johnson, D. P., Jones, G. T., Jorgensen, C., Jouve, F., Jovanovi, P., Junique,
 1411 A., Jusko, A., Jung, H., Jung, W., Kadija, K., Kamal, A., Kamermans, R., Kapusta, S.,
 1412 Kaidalov, A., Kakoyan, V., Kalcher, S., Kang, E., Kapitan, J., Kaplin, V., Karadzhev, K.,
 1413 Karavichev, O., Karavicheva, T., Karpechev, E., Karpio, K., Kazantsev, A., Kebschull,
 1414 U., Keidel, R., Khan, M. M., Khanzadeev, A., Kharlov, Y., Kikola, D., Kileng, B., Kim,
 1415 D., Kim, D. S., Kim, D. W., Kim, H. N., Kim, J. S., Kim, S., Kinson, J. B., Kiprich, S. K.,
 1416 Kisel, I., Kiselev, S., Kisiel, A., Kiss, T., Kiworra, V., Klay, J., Bsing, C. K., Kliemant, M.,
 1417 Klimov, A., Klovning, A., Kluge, A., Kluit, R., Kniege, S., Kolevatov, R., Kollegger, T.,
 1418 Kolojvari, A., Kondratiev, V., Kornas, E., Koshurnikov, E., Kotov, I., Kour, R., Kowalski,
 1419 M., Kox, S., Kozlov, K., Krlik, I., Kramer, F., Kraus, I., Kravkov, A., Krawutschke, T.,
 1420 Krivda, M., Kryshen, E., Kucheriaev, Y., Kugler, A., Kuhn, C., Kuijer, P., Kumar, L.,
 1421 Kumar, N., Kumpumaeki, P., Kurepin, A., Kurepin, A. N., Kushpil, S., Kushpil, V.,
 1422 Kutovsky, M., Kvaerno, H., Kweon, M., Labb, J.-C., Lackner, F., de Guevara, P. L.,

1423 Lafage, V., Rocca, P. L., Lamont, M., Lara, C., Larsen, D. T., Laurenti, G., Lazzeroni,
 1424 C., Bornec, Y. L., Bris, N. L., Gailliard, C. L., Lebedev, V., Lecoq, J., Lee, K. S., Lee, S. C.,
 1425 Lefvre, F., Legrand, I., Lehmann, T., Leistam, L., Lenoir, P., Lenti, V., Leon, H., Monzon,
 1426 I. L., Lvai, P., Li, Q., Li, X., Librizzi, F., Lietava, R., Lindegaard, N., Lindenstruth, V.,
 1427 Lippmann, C., Lisa, M., Listratenko, O. M., Littel, F., Liu, Y., Lo, J., Lobanov, V.,
 1428 Loginov, V., Noriega, M. L., Lpez-Ramrez, R., Torres, E. L., Lorenzo, P. M., Lvhidden,
 1429 G., Lu, S., Ludolphs, W., Lunardon, M., Luquin, L., Lusso, S., Lutz, J.-R., Luvisetto,
 1430 M., Lyapin, V., Maevskaya, A., Magureanu, C., Mahajan, A., Majahan, S., Mahmoud,
 1431 T., Mairani, A., Mahapatra, D., Makarov, A., Makhlyueva, I., Malek, M., Malkiewicz,
 1432 T., Mal'Kevich, D., Malzacher, P., Mamonov, A., Manea, C., Mangotra, L. K., Maniero,
 1433 D., Manko, V., Manso, F., Manzari, V., Mao, Y., Marcel, A., Marchini, S., Mare, J.,
 1434 Margagliotti, G. V., Margotti, A., Marin, A., Marin, J.-C., Marras, D., Martinengo, P.,
 1435 Martnez, M. I., Martinez-Davalos, A., Garcia, G. M., Martini, S., Chiesa, A. M., Marzocca,
 1436 C., Masciocchi, S., Masera, M., Masetti, M., Maslov, N. I., Masoni, A., Massera, F., Mast,
 1437 M., Mastroserio, A., Matthews, Z. L., Mayer, B., Mazza, G., Mazzaro, M. D., Mazzoni,
 1438 A., Meddi, F., Meleshko, E., Menchaca-Rocha, A., Meneghini, S., Meoni, M., Perez, J. M.,
 1439 Mereu, P., Meunier, O., Miake, Y., Michalon, A., Michinelli, R., Miftakhov, N., Mignone,
 1440 M., Mikhailov, K., Milosevic, J., Minaev, Y., Minafra, F., Mischke, A., Mikowiec, D.,
 1441 Mitsyn, V., Mitu, C., Mohanty, B., Moisa, D., Molnar, L., Mondal, M., Mondal, N.,
 1442 Zetina, L. M., Monteno, M., Morando, M., Morel, M., Moretto, S., Morhardt, T., Morsch,
 1443 A., Moukhanova, T., Mucchi, M., Muccifora, V., Mudnic, E., Mller, H., Mller, W., Munoz,
 1444 J., Mura, D., Musa, L., Muraz, J. F., Musso, A., Nania, R., Nandi, B., Nappi, E., Navach,
 1445 F., Navin, S., Nayak, T., Nazarenko, S., Nazarov, G., Nellen, L., Nendaz, F., Nianine,
 1446 A., Nicassio, M., Nielsen, B. S., Nikolaev, S., Nikolic, V., Nikulin, S., Nikulin, V., Nilsen,
 1447 B., Nitti, M., Noferini, F., Nomokonov, P., Nooren, G., Noto, F., Nouais, D., Nyiri,
 1448 A., Nystrand, J., Odyniec, G., Oeschler, H., Oinonen, M., Oldenburg, M., Oleks, I.,
 1449 Olsen, E. K., Onuchin, V., Oppedisano, C., Orsini, F., Ortiz-Velzquez, A., Oskamp, C.,
 1450 Oskarsson, A., Osmic, F., sterman, L., Otterlund, I., Ovrebekk, G., Oyama, K., Pachr,
 1451 M., Pagano, P., Pai, G., Pajares, C., Pal, S., Pal, S., Plla, G., Palmeri, A., Pancaldi,
 1452 G., Panse, R., Pantaleo, A., Pappalardo, G. S., Pastirk, B., Pastore, C., Patarakin, O.,

1453 Paticchio, V., Patimo, G., Pavlinov, A., Pawlak, T., Peitzmann, T., Pnichot, Y., Pepato,
 1454 A., Pereira, H., Peresunko, D., Perez, C., Griffo, J. P., Perini, D., Perrino, D., Peryt, W.,
 1455 Pesci, A., Peskov, V., Pestov, Y., Peters, A. J., Petrek, V., Petridis, A., Petris, M., Petrov,
 1456 V., Petrov, V., Petrovici, M., Peyr, J., Piano, S., Piccotti, A., Pichot, P., Piemonte, C.,
 1457 Pikna, M., Pilastrini, R., Pillot, P., Pinazza, O., Pini, B., Pinsky, L., Morais, V. P.,
 1458 Pismennaya, V., Piuz, F., Platt, R., Ploskon, M., Plumeri, S., Pluta, J., Pocheptsov,
 1459 T., Podesta, P., Poggio, F., Poghosyan, M., Poghosyan, T., Polk, K., Polichtchouk, B.,
 1460 Polozov, P., Polyakov, V., Pommeresch, B., Pompei, F., Pop, A., Popescu, S., Posa, F.,
 1461 Pospil, V., Potukuchi, B., Pouthas, J., Prasad, S., Preghenella, R., Prino, F., Prodan, L.,
 1462 Prono, G., Protsenko, M. A., Pruneau, C. A., Przybyla, A., Pshenichnov, I., Puddu, G.,
 1463 Pujahari, P., Pulvirenti, A., Punin, A., Punin, V., Putschke, J., Quartieri, J., Quercigh,
 1464 E., Rachevskaya, I., Rachevski, A., Rademakers, A., Radomski, S., Radu, A., Rak, J.,
 1465 Ramello, L., Raniwala, R., Raniwala, S., Rasmussen, O. B., Rasson, J., Razin, V., Read,
 1466 K., Real, J., Redlich, K., Reichling, C., Renard, C., Renault, G., Renfordt, R., Reolon,
 1467 A. R., Reshetin, A., Revol, J.-P., Reygers, K., Ricaud, H., Riccati, L., Ricci, R. A., Richter,
 1468 M., Riedler, P., Rigalleau, L. M., Riggi, F., Riegler, W., Rindel, E., Riso, J., Rivetti, A.,
 1469 Rizzi, M., Rizzi, V., Cahuantzi, M. R., Red, K., Rhricht, D., Romn-Lpez, S., Romanato, M.,
 1470 Romita, R., Ronchetti, F., Rosinsky, P., Rosnet, P., Rossegger, S., Rossi, A., Rostchin,
 1471 V., Rotondo, F., Roukoutakis, F., Rousseau, S., Roy, C., Roy, D., Roy, P., Royer, L.,
 1472 Rubin, G., Rubio, A., Rui, R., Rusanov, I., Russo, G., Ruuskanen, V., Ryabinkin, E.,
 1473 Rybicki, A., Sadovsky, S., afak, K., Sahoo, R., Saini, J., Saiz, P., Salur, S., Sambyal,
 1474 S., Samsonov, V., ndor, L., Sandoval, A., Sann, H., Santiard, J.-C., Santo, R., Santoro,
 1475 R., Sargsyan, G., Saturnini, P., Scapparone, E., Scarlassara, F., Schackert, B., Schiaua,
 1476 C., Schicker, R., Schioler, T., Schippers, J. D., Schmidt, C., Schmidt, H., Schneider, R.,
 1477 Schossmaier, K., Schukraft, J., Schutz, Y., Schwarz, K., Schweda, K., Schyns, E., Scioli,
 1478 G., Scomparin, E., Snow, H., Sedykh, S., Segato, G., Sellitto, S., Semeria, F., Senyukov,
 1479 S., Seppnen, H., Serici, S., Serkin, L., Serra, S., Sesselmann, T., Sevcenco, A., Sgura, I.,
 1480 Shabratova, G., Shahoyan, R., Sharkov, E., Sharma, S., Shigaki, K., Shileev, K., Shukla,
 1481 P., Shurygin, A., Shurygina, M., Sibiriak, Y., Siddi, E., Siemiarczuk, T., Sigward, M. H.,
 1482 Silenzi, A., Silvermyr, D., Silvestri, R., Simili, E., Simion, V., Simon, R., Simonetti, L.,

Singaraju, R., Singhal, V., Sinha, B., Sinha, T., Siska, M., Sitz, B., Sitta, M., Skaali,
 B., Skowronski, P., Slodkowski, M., Smirnov, N., Smykov, L., Snellings, R., Snoeys, W.,
 Soegaard, C., Soerensen, J., Sokolov, O., Soldatov, A., Soloviev, A., Soltveit, H., Soltz,
 R., Sommer, W., Soos, C., Soramel, F., Sorensen, S., Soyk, D., Spyropoulou-Stassinaki,
 M., Stachel, J., Staley, F., Stan, I., Stavinskiy, A., Steckert, J., Stefanini, G., Stefanek,
 G., Steinbeck, T., Stelzer, H., Stenlund, E., Stocco, D., Stockmeier, M., Stoicea, G.,
 Stolpovsky, P., Strme, P., Stutzmann, J. S., Su, G., Sugitate, T., umbera, M., Suire, C.,
 Susa, T., Kumar, K. S., Swoboda, D., Symons, J., Szarka, I., Szostak, A., Szuba, M.,
 Szymanski, P., Tadel, M., Tagridis, C., Tan, L., Takaki, D. T., Taureg, H., Tauro, A.,
 Tavlet, M., Munoz, G. T., Thder, J., Tieulent, R., Timmer, P., Tolyhy, T., Topilskaya,
 N., de Matos, C. T., Torii, H., Toscano, L., Tosello, F., Tournaire, A., Traczyk, T., Trger,
 G., Tromeur, W., Truesdale, D., Trzaska, W., Tsileidakis, G., Tsilis, E., Tsvetkov, A.,
 Turcato, M., Turrise, R., Tuveri, M., Tveter, T., Tydesjo, H., Tykarski, L., Tywoniuk, K.,
 Ugolini, E., Ullaland, K., Urbn, J., Urciuoli, G. M., Usai, G. L., Usseglio, M., Vacchi, A.,
 Vala, M., Valiev, F., Vyvre, P. V., Brink, A. V. D., Eijndhoven, N. V., Kolk, N. V. D.,
 van Leeuwen, M., Vannucci, L., Vanzetto, S., Vanuxem, J.-P., Vargas, M. A., Varma,
 R., Vascotto, A., Vasiliev, A., Vassiliou, M., Vasta, P., Vechernin, V., Venaruzzo, M.,
 Vercellin, E., Vergara, S., Verhoeven, W., Veronese, F., Vetlitskiy, I., Vernet, R., Victorov,
 V., Vidak, L., Viesti, G., Vikhlyantsev, O., Vilakazi, Z., Baillie, O. V., Vinogradov, A.,
 Vinogradov, L., Vinogradov, Y., Virgili, T., Viyogi, Y., Vodopianov, A., Volpe, G., Vranic,
 D., Vrlkov, J., Vulpescu, B., Wabnitz, C., Wagner, V., Wallet, L., Wan, R., Wang, Y.,
 Wang, Y., Wheadon, R., Weis, R., Wen, Q., Wessels, J., Westergaard, J., Wiechula, J.,
 Wiesenaecker, A., Wikne, J., Wilk, A., Wilk, G., Williams, C., Willis, N., Windelband, B.,
 Witt, R., Woehri, H., Wyllie, K., Xu, C., Yang, C., Yang, H., Yermia, F., Yin, Z., Yin, Z.,
 Ky, B. Y., Yushmanov, I., Yuting, B., Zabrodin, E., Zagato, S., Zagreev, B., Zaharia, P.,
 Zalite, A., Zampa, G., Zampolli, C., Zanevskiy, Y., Zarochentsev, A., Zaudtke, O., Zvada,
 P., Zbroszczyk, H., Zepeda, A., Zeter, V., Zgura, I., Zhalov, M., Zhou, D., Zhou, S., Zhu,
 G., Zichichi, A., Zinchenko, A., Zinovjev, G., Zoccarato, Y., Zubarev, A., Zucchini, A.,
 and Zuffa, M. (2008). The alice experiment at the cern lhc. *Journal of Instrumentation*,
 3(08):S08002. 25

- [13] Connors, M., Nattrass, C., Reed, R., and Salur, S. (2017). Review of Jet Measurements in Heavy Ion Collisions. vii, 11, 14
- [14] Elia, D. and the ALICE Collaboration (2013). Strangeness production in alice. *Journal of Physics: Conference Series*, 455(1):012005. 18
- [15] Evans, L. and Bryant, P. (2008). Lhc machine. *Journal of Instrumentation*, 3(08):S08001. 9
- [16] Foka, P. and Janik, M. A. (2016). An overview of experimental results from ultra-relativistic heavy-ion collisions at the cern lhc: Bulk properties and dynamical evolution. *Reviews in Physics*, 1:154 – 171. 10
- [17] Gyulassy, M. (2004). The QGP discovered at RHIC. In *Structure and dynamics of elementary matter. Proceedings, NATO Advanced Study Institute, Camyuva-Kemer, Turkey, September 22-October 2, 2003*, pages 159–182. 7
- [18] Hilke, H. J. (2010). Time projection chambers. *Reports on Progress in Physics*, 73(11):116201. viii, 27
- [19] Huovinen, P., Kolb, P. F., Heinz, U., Ruuskanen, P. V., and Voloshin, S. A. (2001). Radial and elliptic flow at RHIC: further predictions. *Physics Letters B*, 503:58–64. 16
- [20] Jacobs, P. and Wang, X.-N. (2005). Matter in extremis: ultrarelativistic nuclear collisions at RHIC. *Progress in Particle and Nuclear Physics*, 54:443–534. 15
- [21] Kapusta, J. I. (1979). Quantum chromodynamics at high temperature. *Nuclear Physics B*, 148(3):461 – 498. 3
- [22] Luo, X. (2016). Exploring the qcd phase structure with beam energy scan in heavy-ion collisions. *Nuclear Physics A*, 956:75 – 82. The XXV International Conference on Ultrarelativistic Nucleus-Nucleus Collisions: Quark Matter 2015. 20
- [23] Martinez, G. (2013). Advances in Quark Gluon Plasma. *ArXiv e-prints*. 6
- [24] Nattrass, C. (2009). System, energy, and flavor dependence of jets through di-hadron correlations in heavy ion collisions. vi, 10, 26

- [25] Odyniec, G. (2013). The rhic beam energy scan program in star and what's next ...
Journal of Physics: Conference Series, 455(1):012037. 20
- [26] Ozaki, S. and Roser, T. (2015). Relativistic heavy ion collider, its construction and
 upgrade. *Progress of Theoretical and Experimental Physics*, 2015(3):03A102. vii, 8
- [27] Preghenella, R. (2011). Transverse momentum spectra of identified charged hadrons
 with the ALICE detector in Pb-Pb collisions at $\sqrt{s_{NN}} = 2.76$ TeV. *PoS, EPS-*
HEP2011:118. 24
- [28] Qin, G.-Y. and Wang, X.-N. (2015). Jet quenching in high-energy heavy-ion collisions.
International Journal of Modern Physics E, 24:1530014–438. 19
- [29] Satz, H. (2006). Colour deconfinement and quarkonium binding. *Journal of Physics G:*
Nuclear and Particle Physics, 32(3):R25. 4, 6
- [30] Schenke, B. (2017). Origins of collectivity in small systems. *Nuclear Physics A*, 967:105
 – 112. The 26th International Conference on Ultra-relativistic Nucleus-Nucleus Collisions:
 Quark Matter 2017. 16
- [31] Shao, M., Barannikova, O. Yu., Dong, X., Fisyak, Y., Ruan, L., Sorensen, P., and Xu,
 Z. (2006). Extensive particle identification with TPC and TOF at the STAR experiment.
Nucl. Instrum. Meth., A558:419–429. 27
- [32] Shuryak, E. V. (1988). The qcd vacuum and quark-gluon plasma. *Zeitschrift für Physik*
C Particles and Fields, 38(1):141–145. 3
- [33] Snellings, R. (2011). Elliptic flow: a brief review. *New Journal of Physics*, 13(5):055008.
 16
- [34] Stock, R. (2004). Ultra-relativistic nucleus-nucleus collisions. Proceedings, 17th
 International Conference, Quark Matter 2004, Oakland, USA, January 11-17, 2004. *J.*
Phys., G30:S633–S648. 7
- [35] Strickland, M. (2014). Anisotropic hydrodynamics: Motivation and methodology.
Nuclear Physics A, 926:92–101. 16

- 1565 [36] Stcker, H. (2005). Collective flow signals the quarkgluon plasma. *Nuclear Physics A*,
1566 750(1):121 – 147. Quark-Gluon Plasma. New Discoveries at RHIC: Case for the Strongly
1567 Interacting Quark-Gluon Plasma. Contributions from the RBRC Workshop held May 14-
1568 15, 2004. viii, 21
- 1569 [37] Vovchenko, V., Anchishkin, D., and Csernai, L. P. (2014). Time dependence of
1570 partition into spectators and participants in relativistic heavy-ion collisions. *Phys. Rev.*
1571 *C*, 90:044907. vii, 12
- 1572 [38] Wilde, M. (2013). Measurement of Direct Photons in pp and Pb-Pb Collisions with
1573 ALICE. *Nucl. Phys.*, A904-905:573c–576c. 18
- 1574 [39] Wong, C.-Y. (1994). *Introduction to high-energy heavy-ion collisions*. World scientific.
1575 vii, 12, 17, 18, 19, 20

Appendices